

BULLETIN OF RUSSIAN STATE MEDICAL UNIVERSITY

BIOMEDICAL JOURNAL OF PIROGOV RUSSIAN NATIONAL
RESEARCH MEDICAL UNIVERSITY

EDITOR-IN-CHIEF Denis Rebrikov, DSc, professor

DEPUTY EDITOR-IN-CHIEF Alexander Oettinger, DSc, professor

EDITORS Valentina Geidebrekht, PhD; Nadezda Tikhomirova

TECHNICAL EDITOR Evgeny Lukyanov

TRANSLATORS Nadezda Tikhomirova, Vyacheslav Vityuk

DESIGN AND LAYOUT Marina Doronina

EDITORIAL BOARD

Averin VI, DSc, professor (Minsk, Belarus)
Alipov NN, DSc, professor (Moscow, Russia)
Belousov VV, DSc, professor (Moscow, Russia)
Bogomilskiy MR, corr. member of RAS, DSc, professor (Moscow, Russia)
Bozhenko VK, DSc, CSc, professor (Moscow, Russia)
Bylova NA, CSc, docent (Moscow, Russia)
Gainetdinov RR, CSc (Saint-Petersburg, Russia)
Gendlin GYe, DSc, professor (Moscow, Russia)
Ginter EK, member of RAS, DSc (Moscow, Russia)
Gorbacheva LR, DSc, professor (Moscow, Russia)
Gordeev IG, DSc, professor (Moscow, Russia)
Gudkov AV, PhD, DSc (Buffalo, USA)
Gulyaeva NV, DSc, professor (Moscow, Russia)
Gusev EI, member of RAS, DSc, professor (Moscow, Russia)
Danilenko VN, DSc, professor (Moscow, Russia)
Zarubina TV, DSc, professor (Moscow, Russia)
Zatevakhin II, member of RAS, DSc, professor (Moscow, Russia)
Kagan VE, professor (Pittsburgh, USA)
Kzyzhkowska YuG, DSc, professor (Heidelberg, Germany)
Kobrinikii BA, DSc, professor (Moscow, Russia)
Kozlov AV, MD PhD (Vienna, Austria)
Kotelevtsev YuV, CSc (Moscow, Russia)
Lebedev MA, PhD (Darem, USA)
Manturova NE, DSc (Moscow, Russia)
Milushkina OYu, DSc, professor (Moscow, Russia)
Mitupov ZB, DSc, professor (Moscow, Russia)
Moshkovskii SA, DSc, professor (Moscow, Russia)
Munblit DB, MSc, PhD (London, Great Britain)

Negrebetsky VV, DSc, professor (Moscow, Russia)
Novikov AA, DSc (Moscow, Russia)
Pivovarov YuP, member of RAS, DSc, professor (Moscow, Russia)
Polunina NV, corr. member of RAS, DSc, professor (Moscow, Russia)
Poryadin GV, corr. member of RAS, DSc, professor (Moscow, Russia)
Razumovskii AYU, corr. member of RAS, DSc, professor (Moscow, Russia)
Rebrova OYu, DSc (Moscow, Russia)
Rudoy AS, DSc, professor (Minsk, Belarus)
Rylova AK, DSc, professor (Moscow, Russia)
Savelieva GM, member of RAS, DSc, professor (Moscow, Russia)
Semiglazov VF, corr. member of RAS, DSc, professor (Saint-Petersburg, Russia)
Skoblina NA, DSc, professor (Moscow, Russia)
Slavyanskaya TA, DSc, professor (Moscow, Russia)
Smirnov VM, DSc, professor (Moscow, Russia)
Spallone A, DSc, professor (Rome, Italy)
Starodubov VI, member of RAS, DSc, professor (Moscow, Russia)
Stepanov VA, corr. member of RAS, DSc, professor (Tomsk, Russia)
Suchkov SV, DSc, professor (Moscow, Russia)
Takhchidi KhP, member of RAS, DSc, professor (Moscow, Russia)
Trufanov GE, DSc, professor (Saint-Petersburg, Russia)
Favorova OO, DSc, professor (Moscow, Russia)
Filipenko ML, CSc, leading researcher (Novosibirsk, Russia)
Khazipov RN, DSc (Marsel, France)
Chundukova MA, DSc, professor (Moscow, Russia)
Shimanovskii NL, corr. member of RAS, DSc, professor (Moscow, Russia)
Shishkina LN, DSc, senior researcher (Novosibirsk, Russia)
Yakubovskaya RI, DSc, professor (Moscow, Russia)

SUBMISSION <http://vestnikrgmu.ru/login?lang=en>

CORRESPONDENCE editor@vestnikrgmu.ru

COLLABORATION manager@vestnikrgmu.ru

ADDRESS ul. Ostrovityanova, d. 1, Moscow, Russia, 117997

Indexed in Scopus. CiteScore 2022: 0.5

Scopus[®]

SCImago Journal & Country Rank 2020: 0.14

SJR

Scimago Journal & Country Rank

Indexed in WoS. JCR 2021: 0.5

WEB OF SCIENCE[™]

Listed in HAC 31.01.2020 (№ 507)



ВЫСШАЯ
АТТЕСТАЦИОННАЯ
КОМИССИЯ (ВАК)

Five-year h-index is 8

Google
scholar

Open access to archive

CYBERLENINKA

Issue DOI: 10.24075/brsmu.2023-02

The mass media registration certificate № 012769 issued on July 29, 1994

Founder and publisher is Pirogov Russian National Research Medical University (Moscow, Russia)

The journal is distributed under the terms of Creative Commons Attribution 4.0 International License www.creativecommons.org



Approved for print 30.04.2023
Circulation: 100 copies. Printed by Print.Formula
www.print-formula.ru

ВЕСТНИК РОССИЙСКОГО ГОСУДАРСТВЕННОГО МЕДИЦИНСКОГО УНИВЕРСИТЕТА

НАУЧНЫЙ МЕДИЦИНСКИЙ ЖУРНАЛ РНИМУ ИМ. Н. И. ПИРОГОВА

ГЛАВНЫЙ РЕДАКТОР Денис Ребриков, д. б. н., профессор

ЗАМЕСТИТЕЛЬ ГЛАВНОГО РЕДАКТОРА Александр Эттингер, д. м. н., профессор

РЕДАКТОРЫ Валентина Гейдебрехт, к. б. н.; Надежда Тихомирова

ТЕХНИЧЕСКИЙ РЕДАКТОР Евгений Лукьянов

ПЕРЕВОДЧИКИ Надежда Тихомирова, Вячеслав Витюк

ДИЗАЙН И ВЕРСТКА Марины Дорониной

РЕДАКЦИОННАЯ КОЛЛЕГИЯ

В. И. Аверин, д. м. н., профессор (Минск, Белоруссия)
Н. Н. Алипов, д. м. н., профессор (Москва, Россия)
В. В. Белоусов, д. б. н., профессор (Москва, Россия)
М. Р. Богомилский, член-корр. РАН, д. м. н., профессор (Москва, Россия)
В. К. Боженко, д. м. н., к. б. н., профессор (Москва, Россия)
Н. А. Былова, к. м. н., доцент (Москва, Россия)
Р. Р. Гайнетдинов, к. м. н. (Санкт-Петербург, Россия)
Г. Е. Гендлин, д. м. н., профессор (Москва, Россия)
Е. К. Гинтер, академик РАН, д. б. н. (Москва, Россия)
Л. Р. Горбачева, д. б. н., профессор (Москва, Россия)
И. Г. Гордеев, д. м. н., профессор (Москва, Россия)
А. В. Гудков, PhD, DSc (Буффало, США)
Н. В. Гуляева, д. б. н., профессор (Москва, Россия)
Е. И. Гусев, академик РАН, д. м. н., профессор (Москва, Россия)
В. Н. Даниленко, д. б. н., профессор (Москва, Россия)
Т. В. Зарубина, д. м. н., профессор (Москва, Россия)
И. И. Затевахин, академик РАН, д. м. н., профессор (Москва, Россия)
В. Е. Каган, профессор (Питтсбург, США)
Ю. Г. Кжышковска, д. б. н., профессор (Гейдельберг, Германия)
Б. А. Кобринский, д. м. н., профессор (Москва, Россия)
А. В. Козлов, MD PhD (Вена, Австрия)
Ю. В. Котелевцев, к. х. н. (Москва, Россия)
М. А. Лебедев, PhD (Дарем, США)
Н. Е. Мантурова, д. м. н. (Москва, Россия)
О. Ю. Милушкина, д. м. н., доцент (Москва, Россия)
З. Б. Митупов, д. м. н., профессор (Москва, Россия)
С. А. Мошковский, д. б. н., профессор (Москва, Россия)
Д. Б. Мунблит, MSc, PhD (Лондон, Великобритания)

В. В. Негребцкий, д. х. н., профессор (Москва, Россия)
А. А. Новиков, д. б. н. (Москва, Россия)
Ю. П. Пивоваров, д. м. н., академик РАН, профессор (Москва, Россия)
Н. В. Полунина, член-корр. РАН, д. м. н., профессор (Москва, Россия)
Г. В. Порядин, член-корр. РАН, д. м. н., профессор (Москва, Россия)
А. Ю. Разумовский, член-корр., профессор (Москва, Россия)
О. Ю. Реброва, д. м. н. (Москва, Россия)
А. С. Рудой, д. м. н., профессор (Минск, Белоруссия)
А. К. Рылова, д. м. н., профессор (Москва, Россия)
Г. М. Савельева, академик РАН, д. м. н., профессор (Москва, Россия)
В. Ф. Семглазов, член-корр. РАН, д. м. н., профессор (Санкт-Петербург, Россия)
Н. А. Скоблина, д. м. н., профессор (Москва, Россия)
Т. А. Славянская, д. м. н., профессор (Москва, Россия)
В. М. Смирнов, д. б. н., профессор (Москва, Россия)
А. Спаллоне, д. м. н., профессор (Рим, Италия)
В. И. Стародубов, академик РАН, д. м. н., профессор (Москва, Россия)
В. А. Степанов, член-корр. РАН, д. б. н., профессор (Томск, Россия)
С. В. Сучков, д. м. н., профессор (Москва, Россия)
Х. П. Тахчиди, академик РАН, д. м. н., профессор (Москва, Россия)
Г. Е. Труфанов, д. м. н., профессор (Санкт-Петербург, Россия)
О. О. Фаворова, д. б. н., профессор (Москва, Россия)
М. Л. Филипенко, к. б. н. (Новосибирск, Россия)
Р. Н. Хазипов, д. м. н. (Марсель, Франция)
М. А. Чундокова, д. м. н., профессор (Москва, Россия)
Н. Л. Шимановский, член-корр. РАН, д. м. н., профессор (Москва, Россия)
Л. Н. Шишкина, д. б. н. (Новосибирск, Россия)
Р. И. Якубовская, д. б. н., профессор (Москва, Россия)

ПОДАЧА РУКОПИСЕЙ <http://vestnikrgmu.ru/login>

ПЕРЕПИСКА С РЕДАКЦИЕЙ editor@vestnikrgmu.ru

СОТРУДНИЧЕСТВО manager@vestnikrgmu.ru

АДРЕС РЕДАКЦИИ ул. Островитянова, д. 1, г. Москва, 117997

Журнал включен в Scopus. CiteScore 2022: 0,5

Журнал включен в WoS. JCR 2021: 0,5

Индекс Хирша (h²) журнала по оценке Google Scholar: 8

Scopus[®]

SCImago Journal & Country Rank 2020: 0,14

SJR
Scimago Journal & Country Rank

WEB OF SCIENCE[™]

Журнал включен в Перечень 31.01.2020 (№ 507)



**ВЫСШАЯ
АТТЕСТАЦИОННАЯ
КОМИССИЯ (ВАК)**

Google
scholar

Здесь находится открытый архив журнала

CYBERLENINKA

DOI выпуска: 10.24075/vrgmu.2023-02

Свидетельство о регистрации средства массовой информации № 012769 от 29 июля 1994 г.

Учредитель и издатель — Российский национальный исследовательский медицинский университет имени Н. И. Пирогова (Москва, Россия)

Журнал распространяется по лицензии Creative Commons Attribution 4.0 International www.creativecommons.org



Подписано в печать 30.04.2023

Тираж 100 экз. Отпечатано в типографии Print.Formula
www.print-formula.ru

ORIGINAL RESEARCH

4

Apoptosis of granulosa cells in women with impaired reproductive function and extragenital pathology

Rogova LN, Lipov DS, Perfilova VN, Kustova MV, Mukhina AV, Churzina DA

Уровень апоптоза гранулезных клеток у женщин с нарушением репродуктивной функции и экстрагенитальной патологией

Л. Н. Рогова, Д. С. Липов, В. Н. Перфилова, М. В. Кустова, А. В. Мухина, Д. А. Чурзина

ORIGINAL RESEARCH

9

Gut microbiota alterations and their association with IL6, IL8 and TNF α levels in patients with external genital endometriosis

Gumenyuk LN, Zemlyanaya IA, Rami Almasoud, Badula ES, Ismailov AR, Seroshtanov NA, Kokareva SS, Cheremisova AA, Kupreichyuk YuR

Изменения микробиоты кишечника и их связь с показателями IL6, IL8 и TNF α у пациенток с наружным генитальным эндометриозом

Л. Н. Гуменюк, И. А. Земляная, Алмасуд Рами, Е. С. Бадула, А. Р. Исмаилов, Н. А. Сероштанов, С. С. Кокарева, А. А. Черемисова, Ю. Р. Купрейчук

CLINICAL CASE

16

A rare case of combination trichorhinophalangeal syndrome and Mayer–Rokitansky–Küster–Hauser syndrome

Batyrova ZK, Bolshakova AS, Kумыkova ZKh, Kruglyak DA, Uvarova EV, Chuprynin VD, Mamedova FSh, Sadelov IO, Trofimov DY

Редкий случай сочетания трихоринофалангеального синдрома и синдрома Майера–Рокитанского–Кюстера–Хаузера

З. К. Батырова, А. С. Большакова, З. Х. Кумыкова, Д. А. Кругляк, Е. В. Уварова, В. Д. Чупрынин, Ф. Ш. Мамедова, И. О. Саделов, Д. Ю. Трофимов

ORIGINAL RESEARCH

21

Detection of *SMN1* loss with PCR-based screening test

Nazarov VD, Cherebillo CC, Lapin SV, Sidorenko DV, Devyatkina YA, Musonova AC, Petrova TV, Nikiforova AI, Ivanova AV

Детекция различных форм потери гена *SMN1* с помощью набора для ПЦР-РВ

В. Д. Назаров, К. К. Черемилло, С. В. Лапин, Д. В. Сидоренко, Е. А. Девяткина, А. К. Мусонова, Т. В. Петрова, А. И. Никифорова, А. В. Иванова

CLINICAL CASE

28

Type 1 diabetes mellitus: features of differential diagnosis

Gantsorn EV, Denisenko OV, Osipenko YaO, Kalmykova DA, Ivanov AV, Gerasyuta SS, Bulguryan GA, Ivanova MH, Saakyan DA

Сахарный диабет 1-го типа: особенности дифференциальной диагностики

Е. В. Гандзорн, О. В. Денисенко, Я. О. Осипенко, Д. А. Калмыкова, А. В. Иванов, С. С. Герасюта, Г. А. Булгурян, М. Х. Иванова, Д. А. Саакян

ORIGINAL RESEARCH

32

The role of Caucasian, Iranian and steppe populations in shaping the diversity of autosomal gene pool of the Eastern Caucasus

Balanovska EV, Gorin IO, Petruschenko VS, Ponomarev GYu, Belov RO, Pocheshkhova EA, Salaev VA, Iskandarov NA, Pylev VYu

Роль кавказского, иранского и степного населения в формировании многообразия аутосомного генофонда Восточного Кавказа

Е. В. Балановская, И. О. Горин, В. С. Петрушенко, Г. Ю. Пономарёв, Р. О. Белов, Э. А. Почешхова, В. А. Салаев, Н. А. Искандаров, В. Ю. Пылёв

ORIGINAL RESEARCH

42

Immunogenicity of full-length and multi-epitope mRNA vaccines for *M. tuberculosis* as demonstrated by the intensity of T-cell response: a comparative study in mice

Vasileva OO, Tereschenko VP, Krapivin BN, Muslimov AR, Kukushkin IS, Pateev II, Rytsov SA, Ivanov RA, Reshetnikov VV

Сравнительное исследование иммуногенности полноразмерной и мультиэпитопной мРНК-вакцин против *M. tuberculosis* по выраженности Т-клеточного ответа у мышей

О. О. Васильева, В. П. Терещенко, Б. Н. Крапивин, А. Р. Муслимов, И. С. Кукушкин, И. И. Патеев, С. А. Рыбцов, Р. А. Иванов, В. В. Решетников

ORIGINAL RESEARCH

49

Activation of microglia in the brain of spontaneously hypertensive rats

Guselnikova VV, Razenkova VA, Sufieva DA, Korzhevskii DE

Активация микроглии в головном мозге спонтанно гипертензивных крыс

В. В. Гусельникова, В. А. Разенкова, Д. А. Суфиева, Д. Э. Коржевский

ORIGINAL RESEARCH

56

Morphological peculiarities of regeneration of oral mucosa associated with use of polymeric piezoelectric membranes

Konjaeva AD, Varakuta EYu, Leiman AE, Rafiev DO, Bolbasov EN, Stankevich KS

Морфологические особенности регенерации слизистой оболочки полости рта при применении полимерных пьезоэлектрических мембран

А. Д. Коняева, Е. Ю. Варакута, А. Е. Лейман, Д. О. Рафиев, Е. Н. Большасов, К. С. Станкевич

APOPTOSIS OF GRANULOSA CELLS IN WOMEN WITH IMPAIRED REPRODUCTIVE FUNCTION AND EXTRAGENITAL PATHOLOGY

Rogova LN¹, Lipov DS¹✉, Perfilova VN², Kustova MV¹, Mukhina AV³, Churzin DA¹

¹ Volgograd State Medical University of the Ministry of Health of the Russian Federation, Volgograd, Russia

² Innovative Medicines R&D and Piloting Center, Volgograd, Russia

³ Department of Assisted Reproductive Technologies. Multidisciplinary Clinic No. 1, Volgograd, Russia

Granulosa cells feed the oocyte during its maturation and protect it. Aberrant apoptosis in these cells is known to ultimately impair oogenesis. The current knowledge of how extragenital inflammation affects apoptosis in granulosa cells is incomprehensive, which is the root of an urgent problem connected to the spread of inflammatory diseases and the growing level of female infertility. This study aimed to assess the intensity of granulosa cell apoptosis in women with impaired reproductive function that suffer from chronic respiratory and/or digestive system diseases of inflammatory origin, and to identify the link, if any, between the studied factor and dysfunction of the reproductive system in the test group. The group included 60 women with a history of respiratory and/or digestive system inflammatory pathology that underwent IVF in 2021–2022. The women were donors of the granulosa cells from the follicular fluid collected through transvaginal puncture of preovulatory follicles. We studied the apoptosis process with the help of flow cytometry. For statistical analysis, we used the Fisher's F-test and the Kruskal–Wallis test. Twenty participants without extragenital pathology in their medical histories, the first subgroup, had the level of apoptosis in granulosa cells at $0.0088 \pm 0.0062\%$, which is significantly lower than in twenty donors with a history of chronic inflammatory digestive system diseases, the second subgroup (granulosa cell apoptosis at $0.0140 \pm 0.0099\%$, $p = 0.015$), and the subgroup of women suffering from inflammatory diseases of the respiratory system (granulosa cell apoptosis at $0.0650 \pm 0.0391\%$, $p = 0.033$); the efficacy of IVF was higher in the first subgroup.

Keywords: apoptosis, granulosa cells, infertility, flow cytometry

Author contribution: LN Rogova — study planning, data analysis and interpretation; DS Lipov — manuscript authoring, analysis of the study data; VN Perfilova, MV Kustova — determination of the level of apoptosis in granulosa cells by flow cytometry; AV Mukhina — collection of the granulosa cell samples from patients; DA Churzin — analysis of the published papers, statistical processing of the obtained data.

Compliance with ethical standards: the study was approved by the Ethics Committee of the Volgograd State Medical University (Minutes № 2021/053 of May 27, 2021) and conducted in compliance with the ethics principles of the WMA Declaration of Helsinki (2000). All donors have voluntarily signed the participant consent forms.

✉ **Correspondence should be addressed:** Danil S. Lipov
Vysokaya, 18a, Volgograd, 400127, Russia; danillipov@yandex.ru

Received: 12.05.2023 **Accepted:** 07.06.2023 **Published online:** 17.06.2023

DOI: 10.24075/brsmu.2023.019

УРОВЕНЬ АПОПТОЗА ГРАНУЛЕЗНЫХ КЛЕТОК У ЖЕНЩИН С НАРУШЕНИЕМ РЕПРОДУКТИВНОЙ ФУНКЦИИ И ЭКСТРАГЕНИТАЛЬНОЙ ПАТОЛОГИЕЙ

Л. Н. Рогова¹, Д. С. Липов¹✉, В. Н. Перфилова², М. В. Кустова¹, А. В. Мухина³, Д. А. Чурзин¹

¹ Волгоградский государственный медицинский университет Министерства здравоохранения Российской Федерации, Волгоград, Россия

² Научный центр инновационных лекарственных средств с опытно-промышленным производством, Волгоград, Россия

³ Отделение вспомогательных репродуктивных технологий. Многопрофильная клиника № 1, Волгоград, Россия

Гранулезные клетки питают и защищают ооцит во время его созревания. Известно, что абберантный апоптоз в этих клетках может привести к нарушению оогенеза. На современном уровне знаний нет исчерпывающей информации о влиянии экстрагенитального воспаления на апоптоз в гранулезных клетках, что становится актуальной проблемой из-за распространения воспалительных заболеваний и роста бесплодия у женщин. Цель исследования — оценить уровень апоптоза гранулезных клеток у женщин с нарушением репродуктивной функции, имеющих в анамнезе хронические заболевания дыхательной и/или пищеварительной систем воспалительного генеза, а также определить наличие взаимосвязи между изучаемым параметром и репродуктивной дисфункцией в исследуемой группе. Исследовали образцы гранулезных клеток 60 женщин, имеющих патологию воспалительного генеза дыхательной и/или пищеварительной систем в анамнезе, проходивших лечение бесплодия методами ЭКО с 2021 по 2022 г. Образцы клеток были собраны из фолликулярной жидкости, полученной во время трансвагинальной пункции преовуляторных фолликулов. Оценку апоптоза проводили методом проточной цитометрии. Для статистического анализа использовали F-критерий Фишера и критерий Краскела–Уоллиса. Установлено, что у женщин без экстрагенитальной патологии в анамнезе ($n = 20$) уровень апоптоза гранулезных клеток составил $0,0088 \pm 0,0062\%$, что достоверно ниже, чем у женщин группы с воспалительными заболеваниями пищеварительной системы в анамнезе ($n = 20$) — $0,0140 \pm 0,0099\%$ ($p = 0,015$) и группы женщин с воспалительными заболеваниями дыхательной системы в анамнезе — $0,0650 \pm 0,0391\%$ ($p = 0,033$), а результативность ЭКО была выше у представительниц первой группы.

Ключевые слова: апоптоз, гранулезные клетки, бесплодие, проточная цитометрия

Вклад авторов: Л. Н. Рогова — планирование исследования, анализ и интерпретация данных; Д. С. Липов — подготовка рукописи, анализ полученных данных; В. Н. Перфилова, М. В. Кустова — определение уровня апоптоза гранулезных клеток методом проточной цитометрии; А. В. Мухина — сбор образцов гранулезных клеток у пациенток; Д. А. Чурзин — анализ литературы, статистическая обработка полученных данных.

Соблюдение этических стандартов: исследование одобрено этическим комитетом ФГБОУ ВО ВолГМУ Минздрава России (протокол № 2021/053 от 27 мая 2021 г.), проведено с соблюдением этических принципов Хельсинкской декларации Всемирной медицинской ассоциации (2000). Все участники исследования подписали добровольное информированное согласие на участие в исследовании.

✉ **Для корреспонденции:** Данил Сергеевич Липов
ул. Высокая, д. 18а, г. Волгоград, 400127, Россия; danillipov@yandex.ru

Статья получена: 12.05.2023 **Статья принята к печати:** 07.06.2023 **Опубликована онлайн:** 17.06.2023

DOI: 10.24075/vrgmu.2023.019

Today, infertility is an urgent and not fully resolved problem affecting both men and women. According to the World Health Organization, there are 50 to 80 million couples in the world suffering from dysfunction of the reproductive system. In our country, the researchers estimate that up to 15% of couples have problems with fertility.

Female infertility is a matter that researchers pay significant attention to because of the structural and physiological complexity of the female reproductive system and the crucial role it plays in human procreation [1]. There are several factors that are typically mentioned as impairing female fertility: age, chronic diseases, lifestyle, environmental toxins, genetic characteristics etc [2]. Lately, scientists have been actively investigating the relationship between chronic inflammatory extragenital pathology and development of infertility. Extragenital pathology is known to significantly affect women's reproductive system and, consequently, lead to fertility disorders [2, 3]. There is a number of diseases, including diabetes mellitus, autoimmune disorders, thyroid diseases, dysfunction of the immune and hypothalamic-pituitary-ovarian axis, that can have a negative effect on the uterus, ovaries and the process of maturation of oocytes [2, 3]. Most researchers believe that violation of the said process is one of the main causes of female infertility [3, 4].

Oogenesis is a complex and multistage process guided by the interactions of various types of cells, hormones, growth factors, and signaling molecules. The quality of the oocyte is of paramount importance for successful conception and pregnancy, therefore, any disruption in this process can lead to a host of problems with fertility [4].

Oocyte maturation largely depends on the interaction of somatic cells surrounding it, including granulosa and cumulus cells [5]. Although histologically similar from the origin viewpoint, these cells have different functions. Granulosa cells, in particular, drive production of estrogen and participate in regulation of the follicle stimulating hormone that is crucial for development of the follicle [6, 7]. Recent studies have shown that granulosa cells directly affect quality of the oocytes, since they produce growth factors and other signaling molecules that shape oocyte maturation [8].

Cumulus cells are specialized cells found next to the maturing oocyte. They support the developing egg physically and biochemically, generate a number of growth factors and other signaling molecules (hyaluronic acid etc) [9, 10].

Some researchers have provided quantitative and qualitative assessments of apoptosis in granulosa and cumulus cells, and evaluated its effect on the processes of oocyte maturation. It was noted that inhibition of apoptosis in granulosa cells promotes growth of follicles and improves quality of the oocytes [8]. Other authors have shown that selective apoptosis of granulosa cells during oocyte maturation is a necessary prerequisite of successful ovulation [11]. The regulation of apoptosis was found to be influenced by the complex interaction of signaling pathways, including the Fas/FasL system and the Bcl-2 protein family [12]. Many experts agree that investigation of the mechanisms behind apoptosis in granulosa and cumulus cells is necessary for the development of targeted treatment regimens for infertility and other reproductive disorders [12, 13].

However, it should be noted that most studies used cells taken from animals (mice, rats, pigs), and human samples were collected only in isolated cases. With this in mind, seeking to analyze the process of oogenesis and its role in female fertility in greater detail, we used granulosa cells donated by the patients whose infertility was treated with the help of assisted reproduction technologies (ART).

This purpose of this study was to assess the intensity of granulosa cell apoptosis in women with impaired reproductive

function that suffer from chronic respiratory and/or digestive system diseases of inflammatory origin, and to identify the link, if any, between the studied factor and the dysfunction of the reproductive system in the test group.

The results of the study can give insight into the mechanisms underlying pathogenesis of infertility, which can help develop new treatments and targeted therapies aimed at improvement of the reproductive outcomes.

METHODS

This work is a multidirectional cohort study; the Figure shows its design. We analyzed samples of granulosa cells collected from 60 patients who underwent ART infertility treatment in Clinic № 1 of the VolgSMU in 2021–2022. The study involved women of reproductive age with a history of inflammatory extragenital pathology of digestive or respiratory system. These systems and this sort of pathology were chosen because of their high prevalence in the population and the results of the earlier studies that point to the negative effect such combinations have on the outcomes of ART-enabled treatments [14].

Having analyzed the medical documentation, we applied the following criteria to select participants of the study: age 20 through 45; confirmed history of a chronic inflammatory disease of the digestive system (gastritis, duodenitis, peptic ulcer of the stomach and (or) duodenum, pancreatitis) or the respiratory system (chronic pathology, like chronic bronchitis, or frequently recurring acute pathology (more than 4 times a year), like ARVI, influenza, bronchitis, laryngitis, tracheitis, pneumonia), with control group including women suffering no such condition; infertile for at least a year; signature on the informed voluntary participant consent form.

The exclusion criteria were as follows: a combined pathology of the respiratory and digestive systems; oncological diseases; patient's refusal to participate and allow processing of her personal data; patient's belonging to a vulnerable social group.

Overall, we selected 60 for the study and divided them into three groups: group 1 ($n = 20$) — women with no history of extragenital pathology; group 2 ($n = 20$) — women with a history of respiratory system inflammatory diseases (chronic pathology, like chronic bronchitis, or frequently recurring acute pathology (over 4 times a year) — ARVI, influenza, bronchitis, laryngitis, tracheitis, pneumonia); group 3 ($n = 20$) — women with a history of chronic digestive system inflammatory diseases (gastritis, duodenitis, peptic ulcer of the stomach and (or) duodenum, pancreatitis). Technical capability to analyze apoptosis in the granulosa cells was the factor limiting the number of participants.

The age of the women ranged from 21 to 43 years, with the mean age at 33.5 ± 4.7 years. The duration of infertility ranged from 4 to 16 years, with the average period being 7.4 ± 1.5 years. The causes of infertility were established with standard clinical and laboratory tests; the features of the extragenital pathology were described in the collected medical history. Stimulation of ovulation in all treatment cycles and all subsequent procedures were performed in strict accordance with the generally accepted clinical guidelines and protocols [15].

Granulosa cell samples were taken from follicular fluid collected via a transvaginal puncture of the preovulatory follicles. The cells were emerged in the buffer solution (heparin 10 IU/ml, 1% human albumin solution, 0.01% recombinant human insulin, gentamicin sulfate 10 μ g/ml) and transported to the laboratory where apoptosis and the level thereof were investigated. Bringing the samples to the laboratory did not take more than 3 hours.

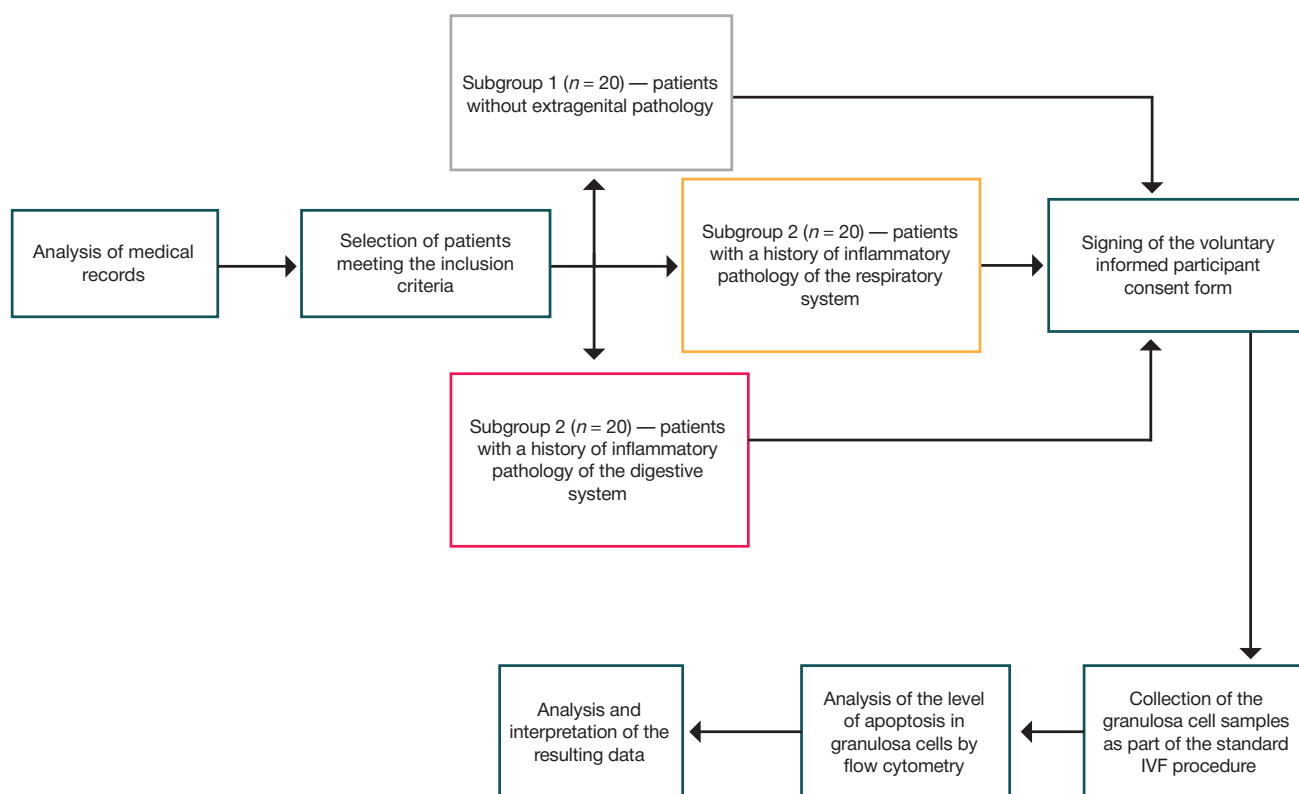


Fig. Research design

The amount of cells with signs of apoptosis was estimated with the help of the dead cell apoptosis kit with annexin V FITC and PI for flow cytometry (Invitrogen, Thermo Fisher Scientific Inc.; USA). The cell suspension was washed with saline. The washed granulosa cells were counted, then resuspended in the annexin-binding buffer to the concentration of 1×10^6 cells per ml, incubated for 15 minutes at room temperature with annexin V FITC and propidium iodide (PI) as per the kit manufacturer's instructions. For the analysis, we used Attune® Acoustic Focusing Cytometer (Thermo Fisher Scientific Inc.; USA) (at least 10 thousand events). For interpretation of the results, we distinguished between living cells that did not fluoresce (Annexin V-FITC-/PI-), cells showing early signs of apoptosis (Annexin V-FITC+/PI-), and cells exhibiting signs of late apoptosis (Annexin V-FITC+/PI+).

Statistical processing of the results was done with StatTech v.2.8.8 software (Stattech, Russia). To assess conformity of the quantitative indicators to the normal distribution patterns we used the Kolmogorov-Smirnov test. The values that did follow the normal distribution patterns, they were described using arithmetic means (M) and standard deviations (SD) with CI at 95%. The values outside normal distribution were described with the help of the median (Me), lower and upper quartiles (Q_1 – Q_3). To compare three or more groups by a quantitative indicator falling within normal distribution, we used one-way ANOVA; for post hoc comparisons, the tests of choice were the Fisher's test (with variances equal) and the Welch's test (with variances unequal). For comparison of three or more groups by the quantitative indicator with distribution outside of the norm we applied the Kruskal–Wallis test.

RESULTS

As shown in Table 1, the analysis of the level of apoptosis in granulosa cells has revealed the respective process to be most active in the women with a history of inflammatory pathology of

the respiratory system, less active in women with inflammatory diseases of the digestive system and least active in the participants that had no pathology at all.

Seeking to understand the relationship between the degree of apoptosis in granulosa cells and oogenesis and fertilization, we counted the number of mature oocytes donated through transvaginal puncture of the preovulatory follicles and the number of eggs fertilized *in vitro*. It was established that no extragenital pathology in the medical history translates into best results of fertilization and the greatest number of mature oocytes, while the worst figures for these two indicators were registered in women that had inflammatory diseases of the respiratory system (Table 2).

DISCUSSION

This study allowed establishing that extragenital inflammatory pathology of the digestive system and the respiratory system affects oogenesis. This is confirmed by the greater number of oocytes in the follicle puncture samples collected from women that did not suffer from these diseases: they had 13.44 ± 2.60 eggs, while women with the considered inflammatory pathologies of respiratory and digestive systems had 4.47 ± 2.00 ($p = 0.001$) and 7.10 ± 1.85 ($p = 0.001$) oocytes, respectively, which is significantly lower. Inflammatory diseases of these systems are known to cause dynamic persistence of various inflammatory mediators in blood (interleukins, tumor necrosis factors etc) [16, 17]. There is published evidence showing that some cytokines, like IL6 and IL8, can negatively affect oogenesis: the higher their level in the blood, the less fertilizable eggs the woman has [18].

The process of maturation of female gametes is quite complex; it is controlled by a number of mechanisms and factors, including interaction of the oocyte with the somatic cells of its microenvironment. Since granulosa cells make the conditions optimal for oogenesis [6], excessive induction of apoptosis in them can increase the possibility of death of the

Table 1. Living granulosa cells and apoptosis in them as registered in the study subgroups. ¹ — F, Fisher's test used for statistical analysis; ² — Kruskal-Wallis test used for statistical analysis

Test group	Live granulosa cell index (%) ¹	Early granulosa cell apoptosis rate (%) ¹	Late granulosa cell apoptosis rate (%) ¹
Subgroup 1 (women with no history of extragenital pathology)	0.2673 ± 0.0151 p_1 (subgroup 1 — subgroup 2) = 0.001 p_2 (subgroup 1 — subgroup 3) = 0.001	0.0088 ± 0.0062 p_1 (subgroup 1 — subgroup 2) = 0.033 p_2 (subgroup 1 — subgroup 3) = 0.015	0.0028 [0.0012–0.0046] p_1 (subgroup 1 — subgroup 2) < 0.001 p_2 (subgroup 1 — subgroup 3) = 0.008
Subgroup 2 (women with a history of inflammatory diseases of the respiratory system)	0.1946 ± 0.0227 p (subgroup 2 — subgroup 3) = 0.008	0.0650 ± 0.0391 p (subgroup 2 — subgroup 3) = 0.026	0.0300 [0.0161–0.0393] p (subgroup 2 — subgroup 3) < 0.001
Subgroup 3 (women with a history of inflammatory diseases of the digestive system)	0.2195 ± 0.0154	0.0140 ± 0.0099	0.0132 [0.0102–0.0206]

Table 2. Results of ART treatment of the study participants. ¹ — F, Fisher's test used for statistical analysis; ² — Kruskal-Wallis test used for statistical analysis

Test group	Number of mature oocytes in the follicle puncture samples ¹	Number of fertilized eggs ²
Subgroup 1 (women with no history of extragenital pathology)	13.44 ± 2.60 p_1 (subgroup 1 — subgroup 2) = 0.001 p_2 (subgroup 1 — subgroup 3) = 0.001	11.00 [9.00–12.00] p_1 (subgroup 1 — subgroup 2) < 0.001 p_2 (subgroup 1 — subgroup 3) = 0.020
Subgroup 2 (women with a history of inflammatory diseases of the respiratory system)	4.47 ± 2.00 p (subgroup 2 — subgroup 3) = 0.013	3.00 [2.50–3.00] p (subgroup 2 — subgroup 3) = 0.038
Subgroup 3 (women with a history of inflammatory diseases of the digestive system)	7.10 ± 1.85	5.50 [4.00–6.75]

egg or disruption of its normal maturation [19]. The growing blood levels of Il2, Il4, TNF α and other factors associated with inflammatory diseases of the respiratory and digestive systems can induce apoptosis by increasing the amount of reactive oxygen species and reducing the transmembrane mitochondrial potential, which can guide cells along the internal pathway of programmed death [20]. A possibly related fact: women without extragenital pathology have significantly more live granulosa cells (0.2673 ± 0.0151%) lower early and late apoptosis rate (0.0088 ± 0.0062% and 0.0028% [0.0012–0.0046%]) than women with chronic inflammatory pathology of the digestive system (number of living cells — 0.2195 ± 0.0154%, early and late apoptosis rate — 0.0140 ± 0.0099% and 0.0132% [0.0102–0.0206%]) and chronic inflammatory pathology of the respiratory system (number of living cells — 0.1946 ± 0.0227%, early and late apoptosis rate — 0.0650 ± 0.0391% and 0.0300% [0.0161–0.0393%]).

It should also be noted that women with diseases of the respiratory system had the lowest number of living cells and the highest rate of early and late apoptosis in granulosa cells,

and, accordingly, compared to the other two subgroups of participants, they had the worst results of oogenesis (lowest number of mature oocytes) and fertilization. This can probably be explained by the possible hypoxia developing against the background of the existing pathology, which can be an additional inducer of apoptosis and disruptor of oogenesis [21].

CONCLUSIONS

Extragenital inflammatory pathology of the respiratory and digestive systems drives up apoptosis in granulosa cells, which affects oogenesis and has an adverse effect on the women's fertility. 2) Extragenital inflammatory pathology of the respiratory system has a greater effect on the spread of apoptosis and viability of granulosa cells. This is why, compared to the control group, women in this subgroup have shown the poorest reaction to ART treatment. 3) The results of this study can be used in the development of new approaches aimed at optimization of preparation for *in vitro* fertilization of women with a history of chronic inflammatory diseases of the respiratory and digestive systems.

References

- Chih HJ, Elias FTS, Gaudet L, Velez MP. Assisted reproductive technology and hypertensive disorders of pregnancy: systematic review and meta-analyses. *BMC Pregnancy and Childbirth*. 2021; 21: 449.
- Sandakova EA, Osipovich OA, Godovalov AP, Karpunina TI. Ehffektivnost' vspomogatel'nykh reproduktivnykh tehnologij u zhenshhin s ginekologicheskimi i ehkstragenital'nymi vospalitel'nymi zabolevaniyami v anamneze. *Medicinskij al'manah*. 2017; 6 (51): 69–72. Russian.
- Anjos JGGD, Carvalho NS, Saab KA, Araujo E, Kulak J. Evaluation of the Seroprevalence of Infectious Diseases in 2,445 *in vitro* Fertilization Cycles. *Revista brasileira de ginecologia e obstetricia: revista da Federacao Brasileira das Sociedades de Ginecologia e Obstetricia*. 2021; 43 (3): 216–9.
- Heber MF, Ptak GE. The effects of assisted reproduction technologies on metabolic health and disease. *Biology of Reproduction*. 2021; 104 (4): 734–44.
- King ML. Molecular control of oogenesis: Progress and perspectives. *Trends in Endocrinology and Metabolism*. 2017; 28 (2): 97–107.
- Sutton-McDowall ML, Gilchrist RB, Thompson JG. The pivotal role of glucose metabolism in determining oocyte developmental competence. *Reproduction, Fertility and Development*. 2010; 22 (5): 393–9.
- Hsueh AJ, Ortega MV. Oocyte development: The role of gonadotropins. *Seminars in Reproductive Medicine*. 2015; 33 (4): 196–206.
- Richards JS, Pangas SA. The ovary: Basic biology and clinical implications. *Journal of Clinical Investigation*. 2010; 120 (4): 963–72.
- El-Hayek S, Demeestere I, Clarke HJ, Scott RT. *In vitro* growth of human follicles: Past, present, and future. *Journal of Assisted Reproduction and Genetics*. 2018; 35 (4): 571–88.
- Turathum B, Gao EM, Chian RC. The function of cumulus cells in oocyte growth and maturation and in subsequent ovulation and fertilization. *Cells*. 2021; 2-10 (9): 2292.
- Jagaramudi K, Adhikari D. Oocyte-somatic cell communication in reproductive health and disease. *Development*. 2010; 137 (18):

- 2927–34.
12. Zheng Y, Ma L, Liu N, Tang X, Guo S, Zhang B, et al. Autophagy and Apoptosis of Porcine Ovarian Granulosa Cells During Follicular Development. *Animals (Basel)*. 2019; 10-9 (12): 1111.
 13. Sun C, Zhang F, Li X, Liu Y, Li Q, Li J, et al. Apoptosis induced by patulin in mouse primary Leydig cells through reactive oxygen species-mediated mitochondrial and endoplasmic reticulum stress signaling pathways. *Oncotarget*. 2010; 7 (29): 44992–5005.
 14. Rogova LN, Lipov DS, Tihayeva KJu, Muhina AV, Kornev AV, Churzina DA. Vliyaniye soputstvuyushhej ehkstragenital'noj patologii na uspeshnost' procedur vspomogatel'nyh reproduktivnyh tehnologij u zhenshhin (po dannym klinik Volgogradskoj oblasti). *Vestnik Volgogradskogo gosudarstvennogo medicinskogo universiteta*. 2023; (1): 92–96. Russian.
 15. Kogan IYu, Gzgzyan AM, Lesik EA. Protokoly stimulyatsii yaichnikov v ciklah EhKO: rukovodstvo dlya vrachej. M.: GEOTAR-Media, 2020; 159 s. Russian.
 16. Fonseca JE, Santos MJ, Canhão H, Choy E. Interleukin-6 as a key player in systemic inflammation and joint destruction. *Autoimmun Rev*. 2009; 8 (7): 538–42.
 17. Mantovani A, Dinarello CA, Molgora M, Garlanda C. Interleukin-1 and Related Cytokines in the Regulation of Inflammation and Immunity. *Immunity*. 2019; 16; 50 (4): 778–95.
 18. Oktay K, Rodriguez-Wallberg KA, Salgado-Moran G. The role of interleukin-8 in the physiology and pathophysiology of the reproductive system. *Human Reproduction Update*. 2019; 25 (4): 411–28.
 19. Zenkina VG. Znachenie apoptoza v yaichnikah pri razvitii nekotoryh zabolevanij reproduktivnoj sistemy. *Fundamental'nye issledovaniya*. 2011; 6: 227–30. Russian.
 20. Chechina OE, Biktasova AK, Sazonova EV, Zhukova OB, Proxorenko TS, Krat IV, i dr. Rol' citokinov v redoks-zavisimoy regulyatsii apoptoza. *Byulleten' sibirskoj mediciny*. 2009; 2: 67–72. Russian.
 21. Yang Z, Hong W, Zheng K, Feng J, Hu C, Tan J, et al. Chitosan oligosaccharides alleviate H2O2-stimulated granulosa cell damage via HIF-1 α signaling pathway. *Oxid Med Cell Longev*. 2022; 2022: 4247042.

Литература

1. Chih HJ, Elias FTS, Gaudet L, Velez MP. Assisted reproductive technology and hypertensive disorders of pregnancy: systematic review and meta-analyses. *BMC Pregnancy and Childbirth*. 2021; 21: 449.
2. Сандакова Е. А., Осипович О. А., Годовалов А. П., Карпунина Т. И. Эффективность вспомогательных репродуктивных технологий у женщин с гинекологическими и экстрагенитальными воспалительными заболеваниями в анамнезе. *Медицинский альманах*. 2017; 6 (51): 69–72.
3. Anjos JGGD, Carvalho NS, Saab KA, Araujo E, Kulak J. Evaluation of the Seroprevalence of Infectious Diseases in 2,445 in vitro Fertilization Cycles. *Revista brasileira de ginecologia e obstetricia: revista da Federacao Brasileira das Sociedades de Ginecologia e Obstetricia*. 2021; 43 (3): 216–9.
4. Heber MF, Ptak GE. The effects of assisted reproduction technologies on metabolic health and disease. *Biology of Reproduction*. 2021; 104 (4): 734–44.
5. King ML. Molecular control of oogenesis: Progress and perspectives. *Trends in Endocrinology and Metabolism*. 2017; 28 (2): 97–107.
6. Sutton-McDowall ML, Gilchrist RB, Thompson JG. The pivotal role of glucose metabolism in determining oocyte developmental competence. *Reproduction, Fertility and Development*. 2010; 22 (5): 393–9.
7. Hsueh AJ, Ortega MV. Oocyte development: The role of gonadotropins. *Seminars in Reproductive Medicine*. 2015; 33 (4): 196–206.
8. Richards JS, Pangas SA. The ovary: Basic biology and clinical implications. *Journal of Clinical Investigation*. 2010; 120 (4): 963–72.
9. El-Hayek S, Demeestere I, Clarke HJ, Scott RT. In vitro growth of human follicles: Past, present, and future. *Journal of Assisted Reproduction and Genetics*. 2018; 35 (4): 571–88.
10. Turathum B, Gao EM, Chian RC. The function of cumulus cells in oocyte growth and maturation and in subsequent ovulation and fertilization. *Cells*. 2021; 2-10 (9): 2292.
11. Jagarlamudi K, Adhikari D. Oocyte-somatic cell communication in reproductive health and disease. *Development*. 2010; 137 (18): 2927–34.
12. Zheng Y, Ma L, Liu N, Tang X, Guo S, Zhang B, et al. Autophagy and Apoptosis of Porcine Ovarian Granulosa Cells During Follicular Development. *Animals (Basel)*. 2019; 10-9 (12): 1111.
13. Sun C, Zhang F, Li X, Liu Y, Li Q, Li J, et al. Apoptosis induced by patulin in mouse primary Leydig cells through reactive oxygen species-mediated mitochondrial and endoplasmic reticulum stress signaling pathways. *Oncotarget*. 2010; 7 (29): 44992–5005.
14. Рогова Л. Н., Липов Д. С., Тихаева К. Ю., Мухина А. В., Корнев А. В., Чурзин Д. А. Влияние сопутствующей экстрагенитальной патологии на успешность процедур вспомогательных репродуктивных технологий у женщин (по данным клиники Волгоградской области). *Вестник Волгоградского государственного медицинского университета*. 2023; (1): 92–96.
15. Коган И. Ю., Гзгзян А. М., Лесик Е. А. Протоколы стимуляции яйчников в циклах ЭКО: руководство для врачей. М.: ГЭОТАР-Медиа, 2020; 159 с.
16. Fonseca JE, Santos MJ, Canhão H, Choy E. Interleukin-6 as a key player in systemic inflammation and joint destruction. *Autoimmun Rev*. 2009; 8 (7): 538–42.
17. Mantovani A, Dinarello CA, Molgora M, Garlanda C. Interleukin-1 and Related Cytokines in the Regulation of Inflammation and Immunity. *Immunity*. 2019; 16; 50 (4): 778–95.
18. Oktay K, Rodriguez-Wallberg KA, Salgado-Moran G. The role of interleukin-8 in the physiology and pathophysiology of the reproductive system. *Human Reproduction Update*. 2019; 25 (4): 411–28.
19. Зенкина В. Г. Значение апоптоза в яйчниках при развитии некоторых заболеваний репродуктивной системы. *Фундаментальные исследования*. 2011; 6: 227–30.
20. Чечина О. Е., Биктасова А. К., Сазонова Е. В., Жукова О. Б., Прохоренко Т. С., Крат И. В., и др. Роль цитокинов в редокс-зависимой регуляции апоптоза. *Бюллетень сибирской медицины*. 2009; 2: 67–72.
21. Yang Z, Hong W, Zheng K, Feng J, Hu C, Tan J, et al. Chitosan oligosaccharides alleviate H2O2-stimulated granulosa cell damage via HIF-1 α signaling pathway. *Oxid Med Cell Longev*. 2022; 2022: 4247042.

GUT MICROBIOTA ALTERATIONS AND THEIR ASSOCIATION WITH IL6, IL8 AND TNF α LEVELS IN PATIENTS WITH EXTERNAL GENITAL ENDOMETRIOSIS

Gumenyuk LN , Zemlyanaya IA, Rami Almasoud, Badula ES, Ismailov AR, Seroshtanov NA, Kokareva SS, Cheremisova AA, Kupreichyuk YuR
SI Georgievsky Medical Academy, VI Vernadsky Crimean Federal University, Simferopol, Russia

Today, the association of gut microbiota with external genital endometriosis (EGE) is of special scientific interest. The study was aimed to assess alterations of the gut microbiota taxonomic composition and explore their correlations with plasma levels of IL6, IL8 and TNF α at the species level in patients with EGE. The cross-sectional comparative study involved 50 patients with EGE (index group) and 50 healthy women (control group). The changes in the gut microbiota taxonomic composition and plasma levels of IL6, IL8 and TNF α were assessed. A significant decrease in the abundance of such species, as *Coprococcus catu* ($p = 0.009$), *Turicibacter sanguinis* ($p = 0.008$) and *Ruminococcus gnavus* ($p < 0.001$), along with the increase in the abundance of *Eubacterium ramulus* ($p = 0.040$), *Bacterioides dorei* ($p = 0.001$), *Prevotella divia* ($p = 0.008$) and *Shigella flexneri* ($p < 0.001$) were found in the gut microbiota taxonomic composition in patients with EGE. Significant correlations between the IL6 levels and the abundance of *Turicibacter sanguinis* ($r = -0.92$; $p = 0.001$), IL8 levels and the abundance of *Shigella flexneri* ($r = 0.72$; $p < 0.001$), TNF α levels and the abundance of *Prevotella divia* ($r = 0.77$; $p = 0.001$) were revealed. The findings add to the available literature data on the features of gut microbiota alterations and their association with some inflammation biomarkers in individuals with EGE, which can justify further research in this area and probably open up new approaches to treatment of the disease.

Keywords: external genital endometriosis, gut microbiota, IL6, IL8, TNF α .

Author contribution: Gumenyuk LN — study concept and design; Zemlyanaya IA, Rami A, Seroshtanov NA — data acquisition, analysis, and interpretation; Badula ES, Ismailov AR — statistical data processing; Kokareva SS, Cheremisova AA, Kupreichyuk YuR — manuscript writing.

Compliance with ethical standards: the study was approved by the Ethics Committee of the SI Georgievsky Medical Academy, VI Vernadsky Crimean Federal University (protocol № 10 of 14 November 2021), planned and conducted in accordance with the Declaration of Helsinki. The informed consent was obtained from all study participants.

 **Correspondence should be addressed:** Lesya N. Gumenyuk
Bulvar Lenina, 5/7295006, Simferopol, Republic of Crimea, Russia; leya.sorokina@mail.ru

Received: 16.05.2023 **Accepted:** 01.06.2023 **Published online:** 15.06.2023

DOI: 10.24075/brsmu.2023.018

ИЗМЕНЕНИЯ МИКРОБИОТЫ КИШЕЧНИКА И ИХ СВЯЗЬ С ПОКАЗАТЕЛЯМИ IL6, IL8 И TNF α У ПАЦИЕНТОК С НАРУЖНЫМ ГЕНИТАЛЬНЫМ ЭНДОМЕТРИОЗОМ

Л. Н. Гуменюк , И. А. Земляная, Алмасуд Рами, Е. С. Бадула, А. Р. Исмаилов, Н. А. Сероштанов, С. С. Кокарева, А. А. Черемисова, Ю. Р. Купрейчук

Медицинская академия имени С. И. Георгиевского (структурное подразделение ФГАОУ ВО «КФУ имени В. И. Вернадского»), Симферополь, Россия

Ассоциация микробиоты кишечника и наружного генитального эндометриоза (НГЭ) на сегодняшний день представляет собой особый научный интерес. Целью исследования было оценить изменения таксономического состава микробиоты кишечника и изучить на уровне видов их взаимосвязь с показателями IL6, IL8 и TNF α в плазме крови у пациенток с НГЭ. В одномоментное сравнительное исследование было включено 50 пациенток с НГЭ (основная группа) и 50 здоровых женщин (контрольная группа). Оценивали изменения таксономического состава микробиоты кишечника и уровни IL6, IL8 и TNF α в плазме крови. У пациенток с НГЭ в таксономическом составе микробиоты кишечника обнаружены статистически значимое снижение представленности видов *Coprococcus catu* ($p = 0,009$), *Turicibacter sanguinis* ($p = 0,008$) и *Ruminococcus gnavus* ($p < 0,001$), повышение представленности видов *Eubacterium ramulus* ($p = 0,040$), *Bacterioides dorei* ($p = 0,001$), *Prevotella divia* ($p = 0,008$) и *Shigella flexneri* ($p < 0,001$). Выявлены статистически значимые корреляции показателя IL6 с представленностью *Turicibacter sanguinis* ($r = -0,92$; $p = 0,001$), IL8 и *Shigella flexneri* ($r = 0,72$; $p < 0,001$), TNF α с представленностью *Prevotella divia* ($r = 0,77$; $p = 0,001$). Полученные результаты дополняют имеющиеся литературные сведения о специфике изменений микробиоты кишечника и их сопряженности с некоторыми биомаркерами воспаления при НГЭ, что может стать обоснованием для продолжения исследований в этом направлении и, возможно, открывает новые подходы к лечению этого заболевания.

Ключевые слова: наружный генитальный эндометриоз, микробиота кишечника, IL6, IL8, TNF α

Вклад авторов: Л. Н. Гуменюк — замысел и дизайн исследования; И. А. Земляная, А. Рами, Н. А. Сероштанов — сбор, анализ и интерпретация данных; Е. С. Бадула, А. Р. Исмаилов — статистическая обработка данных; С. С. Кокарева, А. А. Черемисова, Ю. Р. Купрейчук — подготовка статьи.

Соблюдение этических стандартов: исследование одобрено этическим комитетом Крымской медицинской академии имени С. И. Георгиевского ФГАОУ ВО «Крымский федеральный университет им. В.И. Вернадского» (протокол № 10 от 14 ноября 2021 г.), спланировано и проведено в соответствии с Хельсинской декларацией. Все лица, включенные в исследование, подписали добровольное информированное согласие.

 **Для корреспонденции:** Леся Николаевна Гуменюк
бульвар Ленина, 5/7295006, г. Симферополь, Республика Крым, Россия; leya.sorokina@mail.ru

Статья получена: 16.05.2023 **Статья принята к печати:** 01.06.2023 **Опубликована онлайн:** 15.06.2023

DOI: 10.24075/vrgmu.2023.018

Endometriosis is a significant issue of modern gynecology, it remains under active consideration over the decades. According to the aggregate data, more than 176 million women all over the world have endometriosis [1], and its prevalence rate grows steadily in recent years. It is important to note that endometriosis is associated with infertility in 50–80% of cases and chronic pelvic pain in 50% of cases [1, 2]. These conditions

worsen the patients' mental and physical health, as well as their quality of life [3]. The difficulties in differential diagnosis of endometriosis often result in the diagnosis delay of 4–11 years, and 65% of women are misdiagnosed [3, 4], which results in the disease progression and grave consequences [5]. The today's pharmacological and surgical approaches to treatment of endometriosis are associated with the risk of severe side

effects and show insufficient efficiency. The relapse rate is still high: it reaches 15–21% [3]. That is why the search for new pathophysiological mechanisms underlying external genital endometriosis (EGE), as well as for safe and efficient methods for prevention and treatment of the disease, is still relevant.

EGE, characterized by proliferation of endometrial tissue outside of the uterine cavity, is conventionally considered as a chronic estrogen-dependent immune inflammatory disease that is limited to the pelvis [6]. However, today EGE is more and more often considered as a systemic inflammatory disorder often associated with heterogeneous multiple organ dysfunction [3, 7]. It is believed that aberrant cytokine production accompanied by the immune response dysregulation plays a vital part in pathophysiology of systemic inflammation associated with EGE. In this regard, pro-inflammatory interleukins (IL6, IL8) and tumor necrosis factor alpha (TNF α) are considered to be among the most important. Assessment of the cytokine profile in blood of patients with EGE made it possible to detect the elevated levels of IL6, IL8 and TNF α [8–10]. Furthermore, elevated plasma IL6 levels were associated with the pain severity [11], disease severity [12], and relapse rate [11] in patients with EGE. While plasma levels of IL8 were associated with the size of active lesions [13] and infertility [14], the levels of TNF α were associated with the severity of EGE clinical manifestations, disease activity and depth [15].

Current research suggests that gut microbiota is involved in EGE pathophysiology, which can be explained by its fundamental role in maintaining the immune homeostasis and direct association with the development of numerous inflammatory diseases [16]. The experiments involving the heterologous surgical injection murine model of endometriosis showed that gut microbiota affected the EGE course and progression [17, 18] via modulation of various immune system components [18]. Particularly, administration of normal murine fecal microbiota to mice with experimentally induced endometriosis and gut microbiota depletion was associated with the decline in the endometriotic lesion growth, while administration of fecal microbiota obtained from mice with endometriosis resulted in the disease progression. Furthermore, depletion of intestinal microbiota reduces the severity of inflammatory response associated with endometriosis [17] and modulates the abundance of immune cells in the peritoneum [18]. Finally, the papers provide strong evidence of changes in the intestinal microbiota profile in mice [18–20] and humans [18, 19]. At the same time, clinical data on the gut microbiota species composition in patients with EGE are fragmentary, contradictory and insufficient for unambiguous conclusions. Thus, among 16 studies, focused on assessing the relationship between EGE and microbiome, only six involved the analysis of gut microbiota, and only four involved assessment of human intestinal microbiome [23]. It is also important to note that, among the reviewed papers there are no studies focused on assessing gut microbiota alterations in patients with EGE of Slavic ethnic background. In particular, there is little information on the association between gut microbiota and inflammatory biomarkers in patients with EGE.

The study was aimed to assess alterations of the gut microbiota taxonomic composition and explore their correlations

with plasma levels of IL6, IL8 and TNF α at the species level in patients with EGE.

METHODS

The cross-sectional comparative study was performed in the Saint Luke Multidisciplinary Clinic (Simferopol, Republic of Crimea). The study involved 50 patients aged 18–45 with the confirmed diagnosis of stage I–IV EGE admitted to the Gynecology Department (index group) and 50 age-matched healthy women who underwent preventive medical examination (control group). All EGE patients and healthy women submitted the informed consent to study participation.

Inclusion criteria for the index group: age 18–45 years; the diagnosis of EGE verified by laparoscopy and histological assessment.

Non-inclusion criteria for the index group: age < 18 or > 45 years; body mass index >24.9 kg/m²; pregnancy and lactation; type I or II diabetes mellitus, concomitant chronic systemic and somatic disorders; history of mental and behavioral disorders; verified functional and inflammatory disorders of the gastrointestinal tract, hepatobiliary system; history of inflammatory disorders within a month before the study; history of stool problems (constipation/diarrhea) within a month before the study; taking hormonal oral birth control or anti-inflammatory drugs, antibiotics, probiotics, prebiotics, antiviral drugs, symbiotics or acid-suppression medications within three months before inclusion in the study; taking medications affecting the stool passage within eight weeks before inclusion in the study; refusal to participate in research.

Inclusion criteria for the control group: age 18–45 years; body mass index < 24.9 kg/m²; no somatic disorders or allergy; no infectious or acute disorders within two months before inclusion in the study; no history of mental and behavioral disorders; no stool problems (constipation/diarrhea) within a month before inclusion in the study; taking no hormonal oral birth control or anti-inflammatory drugs, antibiotics, probiotics, prebiotics, antiviral drugs, symbiotics or acid-suppression medications within three months before inclusion in the study; taking no medications affecting the stool passage within eight weeks before inclusion in the study.

Non-inclusion criteria for the control group: body temperature above 36.9 °C.

The characteristics of patients with EGE and controls are provided in Table 1. The groups were matched for age ($p = 0.94$; χ^2) and body mass index ($p = 0.052$; χ^2). A total of 36 patients (70.0%) had stage III–IV EGE.

The diagnosis of endometriosis was verified during surgery in accordance with the criteria of the American Society for Reproductive Medicine (ASRM) classification.

To analyze the taxonomic composition of the gut microbiota of patients with EGE and healthy women, fecal samples were collected in the morning (8 a.m. to 10 a.m.), and in EGE patients sampling was performed on the day of hospital admission. The samples were frozen and stored in disposable plastic containers at a temperature of –80 °C prior to metagenomic analysis. Isolation of total DNA was performed by phenol-based

Table 1. Characteristics of patients with external genital endometriosis and healthy women

Parameter	EGE patients (n = 50)	Control group (n = 50)
Average age, years, median [25%; 75%]	37,0 [32,0; 44,0]	37,7 [32,7; 43,2]
Body mass index, kg/m ² , median [25%; 75%]	23,0 [21,0; 24,3]	22,06 [20,8; 24,1]
Stage I–II EGE, n (%)	14 (28,0%)	–
Stage III–IV EGE, n (%)	36 (70,0%)	–

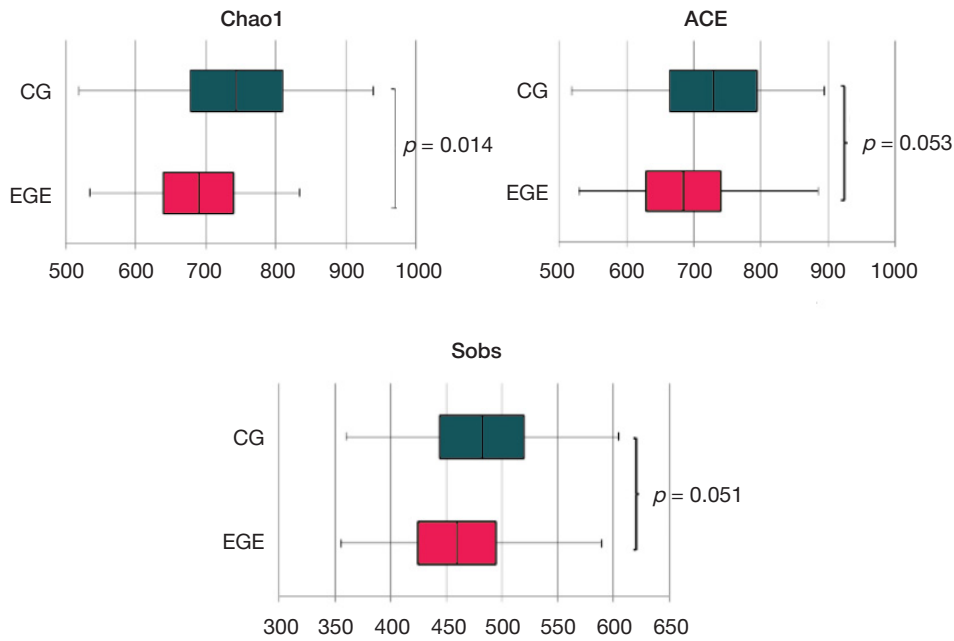


Fig. 1. Phylogenetic composition of gut microbiota in patients with external genital endometriosis (EGE) and healthy women. CG — control group

extraction; the DNA nucleotide sequence was determined by shotgun sequencing using the SOLiD5500 Wildfire high-throughput sequencing system (AppliedBiosystems; USA) [24].

The reads were filtered based on their quality, and the taxonomic classification was performed using the QIIME ver. 1.9.1 software [25]. Taxonomic assignment of the reads was based on the data taken from two taxonomic databases: during the first phase the reference set of bacterial operational taxonomic units (OTUs) was selected based on matching the acquired reads of 16S rRNA genes with the GreenGenes database, ver. 13.5 [26]. During the second phase taxonomic assignment of these OTUs was performed using the RDP algorithm based on the specialized HITdb human intestinal microbiota database [27].

The qualitative and quantitative assessment of gut microbiota composition was performed by identification of

microbial species, genera, and phyla; the microbial community α -diversity was assessed by calculating the Chao1 index, the number of taxa observed (Sobs), and the indicator of species richness (ACE) using the Mothur v.1.22.0 software (<http://www.mothur.org>).

Blood samples of EGE patients and healthy volunteers to be used for immunosorbent assay were collected by venipuncture in the morning in a fasting state at rest (for at least 15 min). Plasma levels of IL6, IL8 and TNF α were assessed by enzyme-linked immunosorbent assay (ELISA) using the test system (Vector-Best; Novosibirsk, Russia). The tubes containing blood serum were frozen and stored at a temperature of -20°C .

Statistical data processing was performed using the STATISTICA 8.0 software package (StatSoft.Inc.; USA). As for quantitative indicators, the distribution type was determined using the Kolmogorov–Smirnov test. Given that the majority of

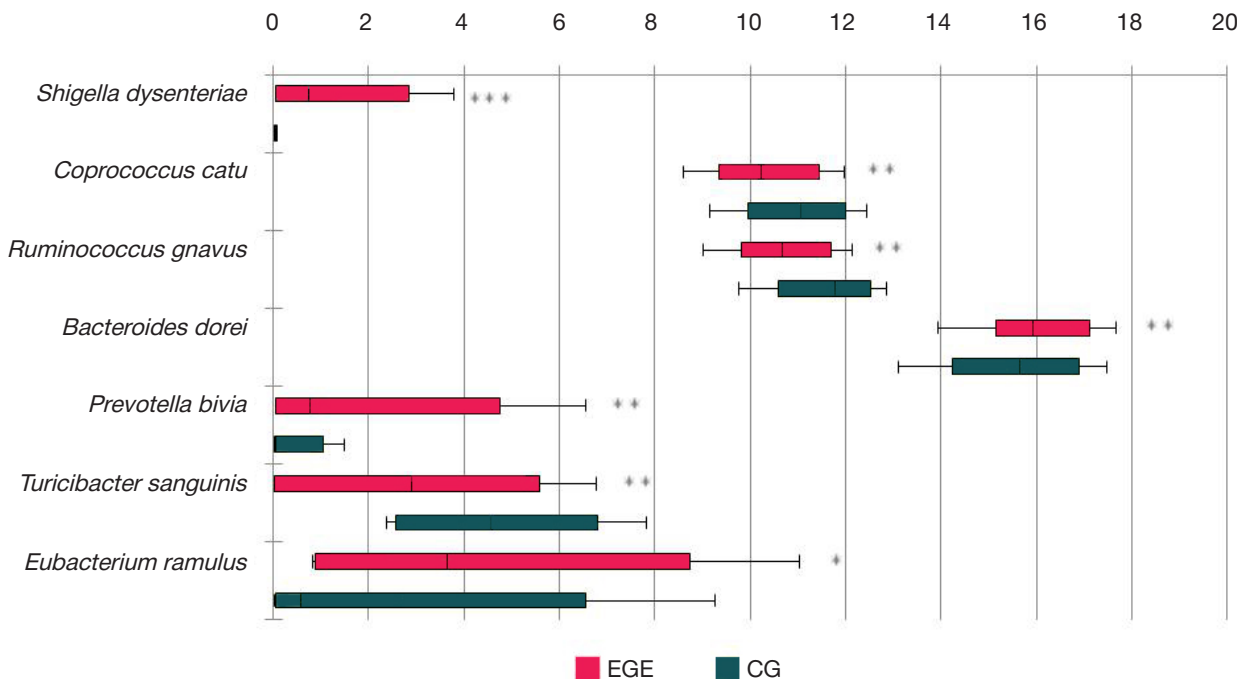


Fig. 2. Species composition of gut microbiota in patients with external genital endometriosis (EGE) and healthy women. CG — control group

Table 2. Comparative analysis of plasma IL6, IL8 and TNF α levels in patients with external genital endometriosis (EGE) and healthy women. CG — control group; p — significance of differences between the values of patients with EGE and the CG

Parameter	EGE patients ($n = 50$)	Control group ($n = 50$)	P
IL6, pg/mL, median [25%; 75%]	14,7 [8,1; 18,3]	3,8 [2,0; 6,6]	< 0,001
IL8, pg/mL, median [25%; 75%]	14,6 [9,6; 28,8]	2,2 [1,4; 6,8]	< 0,001
TNF α , pg/mL, median [25%; 75%]	17,9 [9,3; 26,5]	5,2 [2,8; 7,6]	< 0,001

quantitative indicators were not normally distributed, the median (Me) and interquartile range (25th percentile; 75th percentile) were calculated. As for qualitative traits, the percentage and absolute values were determined. The chi-squared test (χ^2) was used to compare qualitative traits, and quantitative traits were compared using the Mann–Whitney U test. Spearman's rank correlation was applied to assess correlations between the factors. The significance level for comparison of qualitative and quantitative traits, as well as for correlation analysis was set as $p < 0.05$.

RESULTS

Assessment of the gut microbiota taxonomic composition revealed a significant decrease in the bacterial community α -diversity (Chao1 index $p = 0.014$) in patients with EGE compared to healthy women. Furthermore, patients with EGE had lower ACE and Sobs indices than healthy women, however there were no significant differences between groups ($p = 0.053$; $p = 0.051$, respectively) (Fig. 1).

Comparative analysis of the gut microbiota species composition in patients with EGE relative to healthy women revealed a significant decrease in the abundance of *Coprococcus catu* ($p = 0.009$), *Ruminococcus gnavus* ($p < 0.001$) and *Turicibacter sanguinis* ($p = 0.008$) along with the increased abundance of such bacterial species, as *Eubacterium ramulus* ($p = 0.040$), *Bacterioides dorei* ($p = 0.001$), *Prevotella divia* ($p = 0.008$), and *Shigella flexneri* ($p < 0.001$) (Fig. 2).

The IL6, IL8 and TNF α plasma levels of patients with EGE were significantly higher than that of healthy women (Table 2).

At the same time we revealed a strong negative correlation between the abundance of *Turicibacter sanguinis* and the IL6 levels ($r = -0.92$; $p = 0.001$); there was a strong significant positive correlation between the increase in abundance of *Shigella flexneri* bacteria and the levels of IL8 ($r = 0.72$; $p < 0.001$). Furthermore, a strong positive correlation between the TNF α levels and the abundance of *Prevotella divia* ($r = 0.77$; $p = 0.001$) was reported.

DISCUSSION

Gut microbiota is associated with many inflammatory disorders, including EGE [16–19]. However, today there are just a few human studies on the issue, the results of which do not allow any consensus-based conclusions. Given the lack of knowledge of the issue, the primary objective of our study was to refine the gut microbiota taxonomic composition alterations in the group of patients with EGE. Our study has confirmed that gut microbiota composition of EGE patients is quite different from that of healthy women. The findings show that the lower bacterial α -diversity relative to healthy women is typical for patients with EGE, which is a common distinctive feature of chronic inflammatory disorders [28]. Our findings are consistent with the data of the earlier reported study [22], but do not confirm other data [21], according to which patients with EGE are characterized by the decrease in both α - and β -diversity. The results of our study have also shown

that dysbiotic intestinal alterations in patients with EGE are characterized by the decrease in the abundance of bacteria having the potential for immunomodulation: *Coprococcus catu* and *Turicibacter sanguinis* species representatives that are known to produce short-chain fatty acids (SCFAs), i.e. endogenous signaling molecules essential for maintaining the host's immune homeostasis, and *Ruminococcus gnavus*. Moreover, the decrease in the levels of SCFAs results in the increased abundance of Gram-negative bacteria, and therefore lipopolysaccharide (LPS) levels [29]. There is evidence that feces of mice with endometriosis have low levels of SCFAs, specifically butyrate, while butyrate administration inhibits endometriotic cell growth *in vitro* and *in vivo* via inhibition of histone deacetylase activity and activation of expression of the Rap1GAP protein that inactivates the Rap1 intracellular signaling protein [19]. In addition, we have detected the increased abundance of *Eubacterium ramulus*, *Bacterioides dorei*, *Prevotella divia* and *Shigella flexneri*. Among these the presence of *Shigella flexneri* should be noted, since these bacteria have been earlier detected in the fecal samples of patients with stage III–IV EGE in the study [30]. It is suggested that this species plays a role of the trigger that initiates the immune alterations resulting in the development and progression of endometriosis [31]. Our findings are partially in line with the data of the number of other studies. For example, one of the studies has shown that the decrease in the abundance of *Coprococcus* along with the increase in the abundance of *Bacterioides* is typical for patients with EGE [21]. The other study has shown that patients with EGE are characterized by the increase in abundance of *Eubacterium* and *Bacterioides* [22]. The data obtained may be inconsistent due to the fact that, firstly, the studies involved patients of different ethnic groups, and secondly, in contrast to the listed above researchers, we did not enroll overweight patients with EGE (since the effects of this factor on gut microbiota alterations was proven) and the patients taking hormonal, birth control and anti-inflammatory drugs in order to avoid their effects on the study results.

As stated earlier, patients with EGE demonstrate a significant increase in plasma levels of IL6, IL8 and TNF α , the role of which in the disease development and progression to severe forms has been proven [8–10]. Our study has also revealed significantly higher levels of IL6, IL8 and TNF α compared to healthy women in patients with EGE. Meanwhile, intestinal dysbiosis, that is more and more often considered to be a factor of inflammation, autoimmune and immune-mediated disorders, can trigger the inflammatory immune response associated with elevation of pro-inflammatory cytokine levels at the whole-body level [32]. That is why the second objective of the study was to assess the association of gut microbiota composition at the species level with plasma levels of IL6, IL8 and TNF α in the group of patients with EGE. We have found that some intestinal microbial species of patients with EGE are associated with plasma levels of the studied cytokines, which can indicate the association of gut microbiota composition with EGE. In particular, a negative correlation between the elevated IL6 levels and the abundance of *Turicibacter sanguinis* bacteria has been revealed. We have found a probable explanation for

this correlation in the literature. As is well known, the *Turicibacter* bacteria are involved in production of metabolites having a protective effect on the intestinal epithelium and reproductive system, specifically such SCFAs, as acetic, valeric and butyric acids. The decrease in the levels of the latter leads to activation of histone deacetylase and the related NF- κ B nuclear transcription factor, as well as to inhibition of the GPR41, GPR43 and GPR109A G protein-coupled receptors, thereby inducing expression of the genes responsible for synthesis of pro-inflammatory cytokines, including IL6 [33], and promoting the development of chronic inflammation [16]. The earlier reported [34] association of the IL8 levels with the abundance of bacteria of genus *Subdoligranulum* in patients with EGE has not been confirmed in our study. According to our findings, a positive correlation of the IL8 levels with the abundance of *Shigella flexneri* bacteria is typical for patients with EGE, which can be mediated by the ability of the latter to induce persistent NF- κ B inhibitory kinase complex (IKK) activation and subsequent I- κ B degradation via initiation of the pattern recognition receptors TLR4. This, in turn, promotes the release of NF- κ B with subsequent translocation into the nucleus and triggering the IL8 transcription [35]. The literature reports such associations in patients with confirmed *Shigella* infection (*shigellosis*) that have been confirmed by strong positive correlations between the abundance of *Shigella flexneri* and the levels of IL8 in blood plasma [36]. As we have already stated, the contrast between our findings and the results of the study these are compared with may be due to the differences in design, specifically to the fact of selective enrollment of normal-weight EGE patients having no extragenital comorbidities in our study, while in the other study [34] these characteristics were not considered as exclusion criteria. Furthermore, the differences may result from the fact that we enrolled patients with stage I–IV EGE, while

the study [34] involved patients with stage III–IV EGE. This fact could also affect the differences between the associations of IL8 with gut microbiota representatives in EGE patients and the associations reported in the literature. The small sample size (12 patients) used in the earlier reported study should be also noted [34]. Moreover, our study revealed a strong positive correlation between the TNF α blood levels and the abundance of *Prevotella divia*. We have found no reports of the research focused on studying this subject in patients with EGE. However, it has been previously shown that treatment of monocytic cell line with LPS from *Prevotella* results in simultaneous activation of three basic signaling pathways of mitogen-activated protein kinase (MAPK) (extracellular signaling kinase 1/2 (ERK1/2), c-Jun N-terminal kinase 1/2 (JNK1/2), and p38) with subsequent induction of the TNF α mRNA expression and TNF α secretion stimulation [37].

Our findings suggest that gut microbiota plays a vital part in EGE immunogenesis. Apparently, the causal relationships between gut microbiota and blood levels of pro-inflammatory cytokines in individuals with EGE require a more detailed study and further research in this area.

CONCLUSIONS

Significant alterations in the gut microbiota abundance and taxonomic composition have been found in patients with EGE. Furthermore, the significant correlations of some bacterial species with plasma levels of IL6, IL8 and TNF α we have revealed suggest the association of the gut microbiota abundance and composition with the EGE immunopathogenesis. Further research is required to confirm the role of gut microbiota in the EGE pathophysiology. The targeted effects on gut microbiota may contribute to the efficiency of approaches to treatment of EGE.

References

- Zondervan KT, Becker CM, Koga K, Missmer SA, Taylor RN, Viganò P. Endometriosis. *Nat Rev Dis Primers*. 2018; 4: 9.
- Saunders PTK, Horne AW. Endometriosis: Etiology, pathobiology, and therapeutic prospects. *Cell*. 2021; 184 (11): 2807–24.
- Bao C, Wang H, Fang H. Genomic Evidence Supports the Recognition of Endometriosis as an Inflammatory Systemic Disease and Reveals Disease-Specific Therapeutic Potentials of Targeting Neutrophil Degranulation. *Front Immunol*. 2022; 23 (13): 758440.
- Greene R, Stratton P, Cleary SD, Ballweg ML, Sinai N. Diagnostic experience among 4,334 women reporting surgically diagnosed endometriosis. *Fertility and sterility*. 2009; 91 (1): 32–39.
- Greenbaum H, Bat-El L, Galper BEL, Decter DH, Eisenberg VH. Endometriosis and autoimmunity: Can autoantibodies be used as a non-invasive early diagnostic tool? *Autoimmun Rev*. 2021; 20 (5): 102795.
- Clement Philip B. The Pathology of Endometriosis: A Survey of the Many Faces of a Common Disease Emphasizing Diagnostic Pitfalls and Unusual and Newly Appreciated Aspects. *Advances in Anatomic Pathology*. 2007; 14 (4): 241–60.
- Taylor HS, Kotlyar AM, Flores VA. Endometriosis is a chronic systemic disease: clinical challenges and novel innovations. *Lancet*. 2021; 27: 839–52.
- Yarmolinskaya MI. Citokinoviy profil' peritoneal'noy zhidkosti i perifericheskoy krovi bol'nyh s naruzhnym genital'nym ehndometriozom. *Zhurnal akusherstva i zhenskikh bolezney*. 2008; 57 (3): 30–34. Russian.
- Sikora J, Smycz-Kubańska M, Mielczarek-Palacz A, Kondera-Anasz Z. Abnormal peritoneal regulation of chemokine activation — the role of IL8 in pathogenesis of endometriosis. *American Journal of Reproductive Immunology*. 2017; 77 (4).
- Cameron MJ, Kelvin DJ. Cytokines and chemokines — their receptors and their genes: an overview. *Advances in Experimental Medicine and Biology*. 2003; 520: 8–32.
- Somigliana E, Viganò P, Tirelli AS, Felicetta I, Torresani E, Vignali M, et al. Use of the concomitant serum dosage of CA 125, CA 19-9 and interleukin-6 to detect the presence of endometriosis. Results from a series of reproductive age women undergoing laparoscopic surgery for benign gynaecological conditions. *Human Reproduction*. 2004; 19 (8): 1871–6.
- Dong Hao Lu, Song H, Shi G. Anti-TNF α treatment for pelvic pain associated with endometriosis. *Cochrane database of systematic reviews*. 2010; 3 (3): CD008088.
- Li A, Dubey S, Varney ML, Dave BJ, Singh RK. IL8 directly enhanced endothelial cell survival, proliferation, and matrix metalloproteinases production and regulated angiogenesis. *Journal of Immunology*. 2003; 170 (6): 3369–76.
- Malvezzi H, Hernandez C, Piccinato CA, Podgaec S. Interleukin in endometriosis-associated infertility-pelvic pain: systematic review and meta-analysis. *Reproduction*. 2019; 158 (1): 1–12.
- Scholl B, Bersinger NA, Kuhn A. Correlation between symptoms of pain and peritoneal fluid inflammatory cytokine concentrations in endometriosis. *Gynecol Endocrinol*. 2009; 25 (11): 701–6.
- Wu HJ, Wu E. The role of gut microbiota in immune homeostasis and autoimmunity. *Gut Microbes*. 2012; 3 (1): 4–14.
- Chadchan SB, Cheng M, Parnell LA, Yin Y, Schriefer A, Mysorekar IU, et al. Antibiotic therapy with metronidazole reduces endometriosis disease progression in mice: a potential role for gut microbiota. *Hum Reprod*. 2019; 34: 1106–16.
- Chadchan SB, Naik SK, Popli P, et al. Gut microbiota and microbiota-derived metabolites promotes endometriosis. *Cell*

- Death Discov. 2023; 9: 28.
19. Chadchan SB, Popli P, Ambati CR, Tycksen E, Han SJ, Bulun SE, et al. Gut microbiota-derived short-chain fatty acids protect against the progression of endometriosis. *Life Sci Alliance*. 2021; 30; 4 (12): e202101224.
 20. Ni Z, Sun S, Bi Y, Ding J, Cheng W, Yu J, et al. Correlation of fecal metabolomics and gut microbiota in mice with endometriosis. *Am J Reprod Immunol*. 2020; 84: e13307.
 21. Svensson A, Brunkwall L, Roth B, Orho-Melander M, Ohlsson B. Associations Between Endometriosis and Gut Microbiota. *Reprod Sci*. 2021; 28 (8): 2367–77.
 22. Chen S, Gu Z, Zhang W, Jia S, Wu Y, Zheng P, et al. The study of endometriosis and adenomyosis related microbiota in female lower genital tract in Northern Chinese population. *Gynecology and Obstetrics Clinical Medicine*. 2021; 1 (3): 119–29.
 23. Ser H-L, Au Yong S-J, Shafiee MN, Mokhtar NM, Ali RAR. Current updates on the role of microbiome in endometriosis: a narrative review. *Microorganisms*. 2023; 11 (2): 360.
 24. Mitra S, Förster-Fromme K, Damms-Machado A, Scheurenbrand T, Biskup S, Huson, DH, et al. Analysis of the intestinal microbiota using SOLiD16S rRNA gene sequencing and SOLiD shotgun sequencing. *BMC Genomics*. 2013; 14 (5): 16.
 25. Caporaso JG, Kuczynski J, Stombaugh J, Bittinger K, Bushman FD, Costello EK, et al. QIIME allows analysis of high-throughput community sequencing data. *Nat Methods*. 2010; 7 (5): 335–6.
 26. DeSantis TZ, Hugenholtz P, Larsen N. Greengenes, a chimerachecked 16S rRNA gene database and workbench compatible with ARB. *Appl Environ Microbiol*. 2006; 72: 5069–72.
 27. Ritar J, Salojärvi J, Lahti L, de Vos WM. Improved taxonomic assignment of human intestinal 16S rRNA sequences by a dedicated reference database. *BMC Genomics*. 2015; 16 (1): 1056.
 28. Vallejo V, Ilagan JG. A Postpartum Death Due to Coronavirus Disease 2019 (COVID-19) in the United States. *ObstetGynecol*. 2020; 136 (1): 52–55.
 29. Kumari R, Ahuja V, Jaishree P. Fluctuations in butyrate-producing bacteria in ulcerative colitis patients of North India. *World J Gastroenterol*. 2013; 19: 3404–14.
 30. Ata B, Yildiz S, Turkgeldi E, Brocal VP, Dinleyici EC, Moya A, et al. The Endobiota Study: Comparison of Vaginal, Cervical and Gut Microbiota Between Women with Stage 3/4 Endometriosis and Healthy Controls. *Sci Rep*. 2019; 9 (1): 2204.
 31. Kodati VL, Govindan S, Movva S, Ponnala S, Hasan Q. Role of Shigella infection in endometriosis: a novel hypothesis. *Med Hypotheses*. 2008; 70 (2): 239–43.
 32. Gumenyuk LN, Golod MV, Silaeva NV, Sorokina LE, Ilyasov SS, Androschuk NA, et al. Gut microbiota alterations and their relationship to the disease severity and some cytokine profile indicators in patients with COVID-19. *Bulletin of RSMU*. 2022; 1: 22–9.
 33. Liu P, Gao M, Liu Z, Zhang Y, Tu H, Lei L, et al. Gut microbiome composition linked to inflammatory factors and cognitive functions in first-episode, drug-naive major depressive disorder patients. *Front Neurosci*. 2022; 28 (15): 800764.
 34. Shan J, Ni Z, Cheng W, Zhou L, Zhai D, Sun S, et al. Gut microbiota imbalance and its correlations with hormone and inflammatory factors in patients with stage 3/4 endometriosis. *Arch Gynecol Obstet*. 2021; 304: 1363–73.
 35. Philpott DJ, Yamaoka S, Israël A, Sansonetti PJ. Invasive Shigella flexneri activates NF-kappa B through a lipopolysaccharide-dependent innate intracellular response and leads to IL8 expression in epithelial cells. *J Immunol*. 2000; 165 (2): 903–14.
 36. Raqib R, Wretling B, Andersson J, Lindberg AA. Cytokine secretion in acute shigellosis is correlated to disease activity and directed more to stool than to plasma. *J Infect Dis*. 1995; 171: 376–384.
 37. Kim SJ, Choi EY, Kim EG, Shin SH, Lee JY, Choi JI, et al. *Prevotella intermedia* lipopolysaccharide stimulates release of tumor necrosis factor-alpha through mitogen-activated protein kinase signaling pathways in monocyte-derived macrophages. *FEMS Immunol Med Microbiol*. 2007; 51 (2): 407–13.

Литература

1. Zondervan KT, Becker CM, Koga K, Missmer SA, Taylor RN, Viganò P. Endometriosis. *Nat Rev Dis Primers*. 2018; 4: 9.
2. Saunders PTK, Horne AW. Endometriosis: Etiology, pathobiology, and therapeutic prospects. *Cell*. 2021; 184 (11): 2807–24.
3. Bao C, Wang H, Fang H. Genomic Evidence Supports the Recognition of Endometriosis as an Inflammatory Systemic Disease and Reveals Disease-Specific Therapeutic Potentials of Targeting Neutrophil Degranulation. *Front Immunol*. 2022; 23 (13): 758440.
4. Greene R, Stratton P, Cleary SD, Ballweg ML, Sinaii N. Diagnostic experience among 4,334 women reporting surgically diagnosed endometriosis. *Fertility and sterility*. 2009; 91 (1): 32–39.
5. Greenbaum H, Bat-El L, Galper BEL, Decter DH, Eisenberg VH. Endometriosis and autoimmunity: Can autoantibodies be used as a non-invasive early diagnostic tool? *Autoimmun Rev*. 2021; 20 (5): 102795.
6. Clement Philip B. The Pathology of Endometriosis: A Survey of the Many Faces of a Common Disease Emphasizing Diagnostic Pitfalls and Unusual and Newly Appreciated Aspects. *Advances in Anatomic Pathology*. 2007; 14 (4): 241–60.
7. Taylor HS, Kotlyar AM, Flores VA. Endometriosis is a chronic systemic disease: clinical challenges and novel innovations. *Lancet*. 2021; 27: 839–52.
8. Ярмолинская М. И. Цитокиновый профиль перитонеальной жидкости и периферической крови больных с наружным генитальным эндометриозом. *Журнал акушерства и женских болезней*. 2008; 57 (3): 30–34.
9. Sikora J, Smycz-Kubańska M, Mielczarek-Palacz A, Kondera-Anasz Z. Abnormal peritoneal regulation of chemokine activation — the role of IL8 in pathogenesis of endometriosis. *American Journal of Reproductive Immunology*. 2017; 77 (4).
10. Cameron MJ, Kelvin DJ. Cytokines and chemokines — their receptors and their genes: an overview. *Advances in Experimental Medicine and Biology*. 2003; 520: 8–32.
11. Somigliana E, Viganò P, Tirelli AS, Felicetta I, Torresani E, Vignali M, et al. Use of the concomitant serum dosage of CA 125, CA 19-9 and interleukin-6 to detect the presence of endometriosis. Results from a series of reproductive age women undergoing laparoscopic surgery for benign gynaecological conditions. *Human Reproduction*. 2004; 19 (8): 1871–6.
12. Dong Hao Lu, Song H, Shi G. Anti-TNF α treatment for pelvic pain associated with endometriosis. *Cochrane database of systematic reviews*. 2010; 3 (3): CD008088.
13. Li A, Dubey S, Varney ML, Dave BJ, Singh RK. IL8 directly enhanced endothelial cell survival, proliferation, and matrix metalloproteinases production and regulated angiogenesis. *Journal of Immunology*. 2003; 170 (6): 3369–76.
14. Malvezzi H, Hernandez C, Piccinato CA, Podgaec S. Interleukin in endometriosis-associated infertility-pelvic pain: systematic review and meta-analysis. *Reproduction*. 2019; 158 (1): 1–12.
15. Scholl B, Bersinger NA, Kuhn A. Correlation between symptoms of pain and peritoneal fluid inflammatory cytokine concentrations in endometriosis. *Gynecol Endocrinol*. 2009; 25 (11): 701–6.
16. Wu HJ, Wu E. The role of gut microbiota in immune homeostasis and autoimmunity. *Gut Microbes*. 2012; 3 (1): 4–14.
17. Chadchan SB, Cheng M, Parnell LA, Yin Y, Schriefer A, Mysorekar IU, et al. Antibiotic therapy with metronidazole reduces endometriosis disease progression in mice: a potential role for gut microbiota. *Hum Reprod*. 2019; 34: 1106–16.
18. Chadchan SB, Naik SK, Popli P, et al. Gut microbiota and microbiota-derived metabolites promotes endometriosis. *Cell Death Discov*. 2023; 9: 28.
19. Chadchan SB, Popli P, Ambati CR, Tycksen E, Han SJ, Bulun SE, et al. Gut microbiota-derived short-chain fatty acids protect against the progression of endometriosis. *Life Sci Alliance*. 2021; 30; 4 (12): e202101224.
20. Ni Z, Sun S, Bi Y, Ding J, Cheng W, Yu J, et al. Correlation of fecal metabolomics and gut microbiota in mice with endometriosis. *Am*

- J Reprod Immunol. 2020; 84: e13307.
21. Svensson A, Brunkwall L, Roth B, Orho-Melander M, Ohlsson B. Associations Between Endometriosis and Gut Microbiota. *Reprod Sci.* 2021; 28 (8): 2367–77.
 22. Chen S, Gu Z, Zhang W, Jia S, Wu Y, Zheng P, et al. The study of endometriosis and adenomyosis related microbiota in female lower genital tract in Northern Chinese population. *Gynecology and Obstetrics Clinical Medicine.* 2021; 1 (3): 119–29.
 23. Ser H-L, Au Yong S-J, Shafiee MN, Mokhtar NM, Ali RAR. Current updates on the role of microbiome in endometriosis: a narrative review. *Microorganisms.* 2023; 11 (2): 360.
 24. Mitra S, Förster-Fromme K, Damms-Machado A, Scheurenbrand T, Biskup S, Huson, DH, et al. Analysis of the intestinal microbiota using SOLiD16S rRNA gene sequencing and SOLiD shotgun sequencing. *BMC Genomics.* 2013; 14 (5): 16.
 25. Caporaso JG, Kuczynski J, Stombaugh J, Bittinger K, Bushman FD, Costello EK, et al. QIIME allows analysis of high-throughput community sequencing data. *Nat Methods.* 2010; 7 (5): 335–6.
 26. DeSantis TZ, Hugenholtz P, Larsen N. Greengenes, a chimerachecked 16S rRNA gene database and workbench compatible with ARB. *Appl Environ Microbiol.* 2006; 72: 5069–72.
 27. Ritari J, Salojärvi J, Lahti L, de Vos WM. Improved taxonomic assignment of human intestinal 16S rRNA sequences by a dedicated reference database. *BMC Genomics.* 2015; 16 (1): 1056.
 28. Vallejo V, Ilagan JG. A Postpartum Death Due to Coronavirus Disease 2019 (COVID-19) in the United States. *ObstetGynecol.* 2020; 136 (1): 52–55.
 29. Kumari R, Ahuja V, Jaishree P. Fluctuations in butyrate-producing bacteria in ulcerative colitis patients of North India. *World J Gastroenterol.* 2013; 19: 3404–14.
 30. Ata B, Yildiz S, Turkgeldi E, Brocal VP, Dinleyici EC, Moya A, et al. The Endobiota Study: Comparison of Vaginal, Cervical and Gut Microbiota Between Women with Stage 3/4 Endometriosis and Healthy Controls. *Sci Rep.* 2019; 9 (1): 2204.
 31. Kodati VL, Govindan S, Movva S, Ponnala S, Hasan Q. Role of Shigella infection in endometriosis: a novel hypothesis. *Med Hypotheses.* 2008; 70 (2): 239–43.
 32. Гуменюк Л. Н., Голод М. В., Силаева Н. В., Сорокина Л. Е., Ильясов С. С., Андрощук Н. А. и др. Изменения микробиоты кишечника и их связь с тяжестью заболевания и некоторыми показателями цитокинового профиля у пациентов с COVID-19. *Вестник РГМУ.* 2022; 1: 23–30.
 33. Liu P, Gao M, Liu Z, Zhang Y, Tu H, Lei L, et al. Gut microbiome composition linked to inflammatory factors and cognitive functions in first-episode, drug-naive major depressive disorder patients. *Front Neurosci.* 2022; 28 (15): 800764.
 34. Shan J, Ni Z, Cheng W, Zhou L, Zhai D, Sun S, et al. Gut microbiota imbalance and its correlations with hormone and inflammatory factors in patients with stage 3/4 endometriosis. *Arch Gynecol Obstet.* 2021; 304: 1363–73.
 35. Philpott DJ, Yamaoka S, Israël A, Sansonetti PJ. Invasive Shigella flexneri activates NF-kappa B through a lipopolysaccharide-dependent innate intracellular response and leads to IL8 expression in epithelial cells. *J Immunol.* 2000; 165 (2): 903–14.
 36. Raqib R, Wretling B, Andersson J, Lindberg AA. Cytokine secretion in acute shigellosis is correlated to disease activity and directed more to stool than to plasma. *J Infect Dis.* 1995; 171: 376–384.
 37. Kim SJ, Choi EY, Kim EG, Shin SH, Lee JY, Choi JI, et al. Prevotella intermedia lipopolysaccharide stimulates release of tumor necrosis factor-alpha through mitogen-activated protein kinase signaling pathways in monocyte-derived macrophages. *FEMS Immunol Med Microbiol.* 2007; 51 (2): 407–13.

A RARE CASE OF COMBINATION TRICHORINOPHALANGEAL SYNDROME AND MAYER–ROKITANSKY–KÜSTER–HAUSER SYNDROME

Batyrova ZK [✉], Bolshakova AS, Kumykova ZKh, Kruglyak DA, Uvarova EV, Chuprynin VD, Mamedova FSh, Sadelov IO, Trofimov DY

Kulakov National Medical Research Center for Obstetrics, Gynecology and Perinatology, Moscow, Russia

Two forms of Mayer–Rokitansky–Kuster–Hauser (MRKH) syndrome are recognized: isolated uterovaginal agenesis and associated with extragenital malformations, including several well-recognized syndromes. Trichorhinophalangeal syndrome (TRPS) is a rare autosomal dominant condition characterized by facial dysmorphism, ectodermal and skeletal features. TRPS comprises TRPSI (caused by a heterozygous pathogenic variant in TRPS1), TRPSII (caused by contiguous gene deletion of TRPS1, RAD21, and EXT1). Genital anomalies occur particularly in TRPSII. We present a case of rare combination TRPSII with MRKH syndrome. Delayed diagnosis resulted to prolonged pain syndrome and repeated surgery. Recognition of genital anomalies in TRPS allows timely referral diagnosis and appropriate care by paediatrician and adolescent gynaecologists.

Keywords: trichorhinophalangeal syndrome, urogenital anomaly, MRKH syndrome

Acknowledgments: SR Grover from Murdoch Children's Research Institute, Royal Children's Hospital for advices in formulating the concept of the manuscript, AV Asaturova head of the 1st pathoanatomical department of the Kulakov Federal State Budgetary Institution NMICAGP for help in editing the manuscript.

Author contribution: Batyrova ZK, Bolshakova AS — concept; Batyrova ZK, Kruglyak DA, Uvarova EV, Chuprynin VD, Mamedova FSh — collection and processing of material; Batyrova ZK, Bolshakova AS, Kumykova ZKh — text writing; Kumykova ZKh, Sadelov IO, Trofimov DY — editing. All authors approved the final manuscript. All authors were involved in the clinical management of the patient and contributed to the final diagnosis.

✉ **Correspondence should be addressed:** Zalina K. Batyrova
Tolbuhina, 3/2, k. 59, Moscow, 121596, Russia; linadoctor@mail.ru

Received: 17.06.2023 **Accepted:** 26.06.2023 **Published online:** 27.06.2023

DOI: 10.24075/brsmu.2023.022

РЕДКИЙ СЛУЧАЙ СОЧЕТАНИЯ ТРИХОРИНОФАЛАНГЕАЛЬНОГО СИНДРОМА И СИНДРОМА МАЙЕРА–РОКИТАНСКОГО–КЮСТЕРА–ХАУЗЕРА

З. К. Батырова [✉], А. С. Большакова, З. Х. Кумыкова, Д. А. Кругляк, Е. В. Уварова, В. Д. Чупрынин, Ф. Ш. Мамедова, И. О. Саделов, Д. Ю. Трофимов

Национальный медицинский исследовательский центр акушерства, гинекологии и перинатологии имени В. И. Кулакова Минздрава России, Москва, Россия

Выделяют два варианта синдрома Майера–Рокитанского–Кюстера–Хаузера (МРКХ): тип I, при котором наблюдается изолированная аплазия матки и влагалища, и тип II, при котором имеют место сопутствующие экстрагенитальные пороки развития, в рамках некоторых синдромальных состояний. Синдром Лангера–Гидеона или трихоринофалангеальный синдром (TRPS) — редкое аутосомно-доминантное заболевание, характеризующееся лицевым дисморфизмом и аномалиями кожи, ногтей и волос. Выделяют два типа трихоринофалангеального синдрома: TRPSI, обусловленный патогенным вариантом гена TRPS1, и TRPSII, обусловленный делецией с вовлечением генов TRPS1, RAD21 и EXT. Как правило, пороки развития половых органов встречаются при типе II. Представлено клиническое наблюдение TRPSII в сочетании с МРКХ. Отсроченная диагностика порока развития половых органов привела к длительному болевому синдрому у пациентки с крайне отягощенным анамнезом и проведению неоднократных хирургических вмешательств. Своевременное обнаружение сочетания аномалий половых органов у девочек с TRPS позволяет не только установить диагноз, но и оказать квалифицированную помощь с участием гинеколога детей и подростков, с целью минимизации возможных осложнений.

Ключевые слова: трихоринофалангеальный синдром, аномалия мочеполювых органов, МРКХ-синдром

Благодарности: Sonia R. Grover из Murdoch Children's Research Institute, Royal Children's Hospital за помощь в формулировке концепции рукописи, А. В. Асатурову, заведующему 1-м патологоанатомическим отделением ФГБУ НМИЦАГП им. В. И. Кулакова, за помощь в редактировании рукописи.

Вклад авторов: З. К. Батырова, А. С. Большакова — концепция; З. К. Батырова, Д. А. Кругляк, Е. В. Уварова, В. Д. Чупрынин, Ф. Ш. Мамедова — сбор и обработка материала; З. К. Батырова, А. С. Большакова, З. Х. Кумыкова — написание текста; З. Х. Кумыкова, И. О. Саделов, Д. Ю. Трофимов — редактирование.

✉ **Для корреспонденции:** Залина Кимовна Батырова
ул. Толбухина, д. 3/2, к. 59, г. Москва, 121596, Россия; linadoctor@mail.ru

Статья получена: 17.06.2023 **Статья принята к печати:** 26.06.2023 **Опубликована онлайн:** 27.06.2023

DOI: 10.24075/vrgmu.2023.022

The MRKH syndrome (OMIM 277000) is a rare condition with prevalence of about 1 in 5,000 women. It is characterized by the absence or hypoplasia of the uterus and the upper two thirds of the vagina in 46,XX females [1–3]. This malformation can occur isolated or with various anomalies, with a relatively common subset of these comprising Müllerian, renal, and cervicothoracic abnormalities (MURCS association) [2].

Occasionally, MRKH was combined with situs viscerum inversus, Dandy–Walker malformation, Meckel–Gruber syndrome, Bardet–Biedl syndrome, Cornelia de Lange syndrome, Holt–Oram syndrome or McKusick–Kaufman syndrome [1, 2]. However, it can probably be explained by simple coincidence. To our knowledge, the genetic causes of MRKH remains unknown.

Trichorhinophalangeal syndrome was first reported by A. Giedion in 1966, described in more detail by L.O. Langer in 1969 [3, 4]. The population frequency is less than 1 : 1,000,000. It is characterized by severe craniofacial and skeletal abnormalities. Patients with trichorhinophalangeal syndrome usually have a specific skull structure with sparse and slowly growing hair on the head, protruding ears, sparse eyebrows, a convex pear-shaped nose, thin lips, elongated chin, and bone anomalies, including mild to severe brachydactyly, hip dysplasia and short stature [3–8]. Additionally, female patients may have urogenital anomalies [3, 4, 8].

TRPSII or Langer–Giedion syndrome (OMIM 150230) associated with contiguous 8q23.3q24.11 deletion that spans

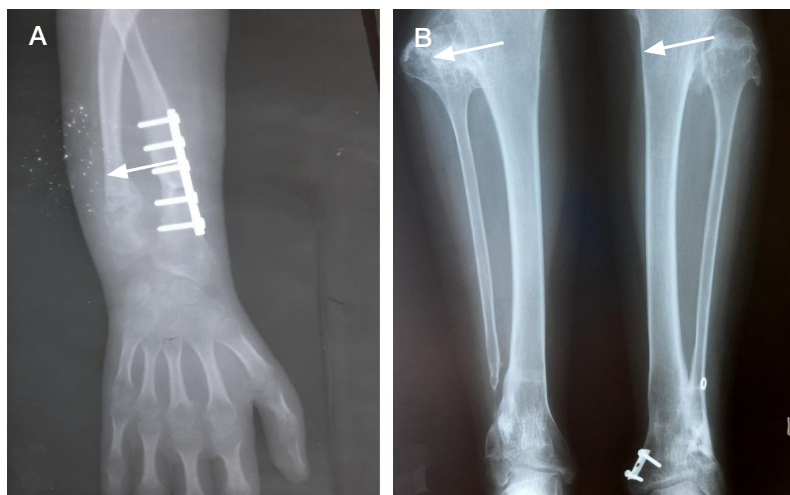


Fig. 1. X-ray picture of the bones of the upper (A) and lower (B) extremities with multiple exostoses (shown by arrows) and metal structures after surgery

the TRPS1-EXT1 interval [2–7], more often diagnosed using chromosomal microarray.

Chromosomal microarray analysis (CMA) is designed to detect microscopic and submicroscopic copy number variations (CNVs) across the genome [9, 10]. Recent guidelines and publications have recommended CMA for the evaluation of children with autism spectrum disorders, developmental delay/intellectual impairment, and/or multiple congenital anomalies [11–15]. CNVs are observed in up to 20% of cases with genital tract malformations [16]. Nik-Zainal et al. reported 14% prevalence of CNVs in a cohort of patients with isolated and syndromic Müllerian aplasia [15].

Unfortunately, limited publications, describing a combination of TRPS and Müllerian anomalies, complicate early diagnosis [8].

Clinical case description

A 14-year-old girl with a known medical history of TRPSII was referred to the National Medical Research Center for Obstetrics, Gynecology and Perinatology for primary amenorrhea and progressively increasing cyclic lower abdominal pain.

The girl was the first child of a non-consanguineous couple and had a younger healthy brother. Her medical history, obtained from her parents, included spontaneous delivery of

first uneventful pregnancy, with a birthweight of 3,600 g, and length 52 cm. At 2 days of age, she was transferred to neonatal intensive care unit due to the lack of sucking and absent swallow reflexes. Subsequently, the girl presented with a delay in physical and mental development, she was characterized by dysplastic body shape, pronounced facial characteristics and shortening of the hands and feet. At the age of 3 years, the TRPSII was diagnosed, but the genetic result was lost.

Since 4 years of age, the girl presented with tumor-like formations in the proximal sections of both humerus, distal forearm, femur, and articular ends of both tibiae. The patient underwent 27 surgical interventions due to deformations of the extremities, associated with multiple exostoses (Fig. 1).

In December 2018, she was hospitalized with severe abdominal pain. The laparoscopic cystectomy of the left ovary and appendectomy were performed. No abnormalities of the genital tract were observed. After discharge from the hospital, the patient suffered cyclic, progressively increased, lower abdominal pain. The parents sought care from our department of pediatric and adolescent gynecology, as there was no improvement under the conservative therapy (non-steroidal anti-inflammatory drugs, gestagens).

The condition of the girl upon admission was stable, with height 144 cm and weight 40 kg. Sexual development was described

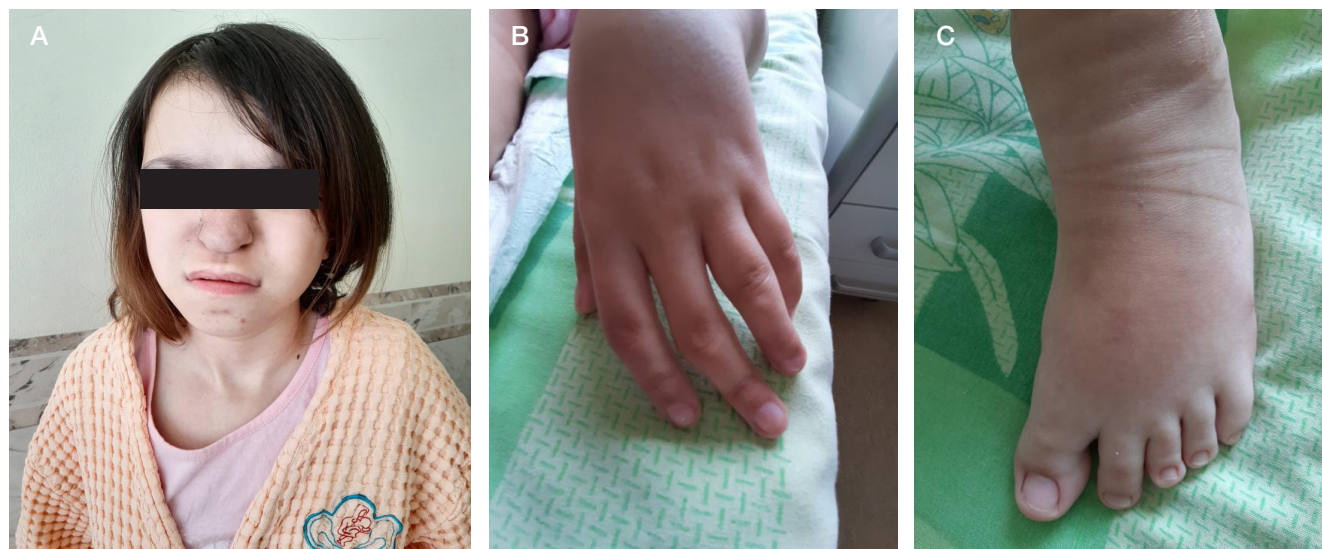


Fig. 2. Typical dysmorphic features of the patient: slowly growing hair, a long pear-shaped nose with a bulbous tip (A) shortening of the hands with enlargement of interphalangeal joints (B) and feet (C)

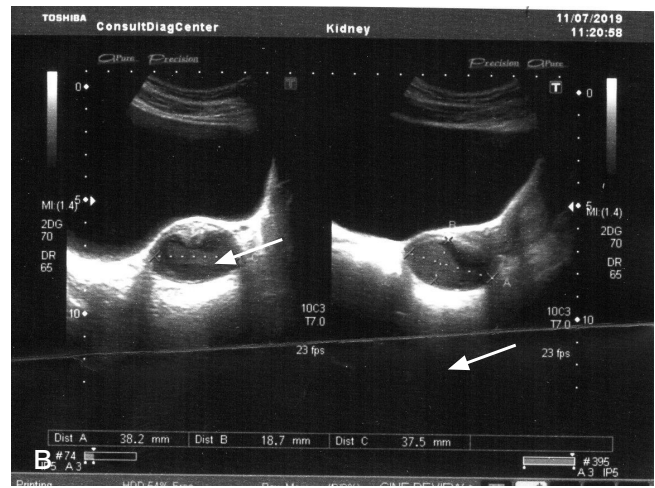


Fig. 3. Transabdominal ultrasound examination: **A** — rudimentary uterine rudiment (transverse scanning); **B** — the same structure in longitudinal scanning

as Tanner 3. She had a dysplastic physique characterized with multiple deformities of the upper and lower extremities, a long pear-shaped nose, lower jaw hyperplasia, large protruding ears and multiple cartilaginous exostoses (Fig. 2).

The gynecological examination revealed normal external female genitalia, hymen fringed, behind the hymen there was a blind ending vaginal fossa to 1.0 cm. During recto-abdominal examination, the uterus was characterized by spherical shape, tender to the palpation. Laboratory parameters of the patient, including hormonal status, were all within normal values.

Following genetic counseling, CMA determined a pathogenic 6,9 Mb deletion at chromosome 8q23.3-q24.12 (115,524,782–122,445,687 bp, GRCh37) with the involvement *TRPS1*, *EXT1*, and *RAD21* genes, and a duplication on the long arm of chromosome 18 (18q12.3) over 2.8 Mb of unknown clinical significance. The genetic results confirmed TRPS II syndrome.

Study of both parents revealed that the patient's deletion was «*de novo*» in origin. The father carried the 18q12.3 duplication; therefore, its contribution to the girl's phenotype is unlikely, and it was considered to be likely benign.

An MRI of the pelvic organs was not possible due to the presence of multiple metal structures. Ultrasound examination of the pelvic organs in our center revealed a spherical structure consistent with a uterus, displaced to the left and upwards with dimensions 38 × 27 × 29 mm, and 3 mm endometrium, the ovaries were located high in the pelvic cavity but there was no identifiable cervix and vagina (Fig. 3).

Due to the cyclic pain syndrome, combined with the ultrasound findings, an obstructive anomaly of the Müllerian

tract was suspected. The laparoscopy revealed two uterine rudiments, each located at the sidewalls of the pelvis, connected by a cord over the bladder. The left rudiment had signs of functioning; the right rudiment recognized as a small muscle nubbin, connected with the round ligament of the uterus and fallopian tube. The cervix and vagina were absent (Fig. 4).

Despite of the size, the left uterine rudiment was a structure without cervix. In this case, a surgical creation of the utero-vaginal anastomosis was considered impractical due to high-risk complications and other patient's health problems. Multidisciplinary team, including ethics specialists, decided to remove the uterine rudiments. The parental consent was obtained. Postoperative period was uneventful and the girl was discharged home in a satisfactory condition. At the one-month and three-month follow-up visits, her parents reported complete resolution of the pain syndrome.

Clinical case discussion

LGS includes the clinical features of TRPS type I, caused by the haploinsufficiency of *TRPS1*, and multiple hereditary exostoses due to deletion *EXT1* [16–18]. Some reported patients have been also characterized with the clinical features of Cornelia de Lange syndrome, type 4 [19,20]. In addition to findings of TRPSII, Müllerian aplasia was ascertained in our proband. Syndromic Müllerian aplasia may be linked to 17q12 microdeletion [21], 1q21.1 microduplication, Xq21.31 microdeletion [22]. Furthermore, several cases of Müllerian



Fig. 4. Laparoscopic view of the internal genital organs: left uterine rudiment with signs of functioning (**A**); right uterine rudiment (muscle nubbin) (**B**)

aplasia in patients with 16p11.2 microdeletion are described in the literature [23]. Mullerian duct remnants are also occasionally associated with TRPS [24].

Other genital abnormalities in patients with TRPS II were reported in previous studies. One reported a woman with vaginal atresia and hematometra with 8q24.11–q24.12 deletion [19]. Another showed a girl with persistent cloaca and prune belly sequence and 8q24.11–q24.13 deletion [20]. Fryns et al. reported hydrometrocolpos in three children with 8q24.11–q24.13 deletion [21]. Plaza-Benhumea et al. described a 19-year-old female with imperforate hymen, severe vaginal stenosis and hematometra with 8q23.3–q24.12 deletion [25].

In our patient 8q23.3q24.12 deletion, approximately 6.9 Mb, affects *TRPS1*, *EIF3H*, *RAD21*, *SLC30A8*, *MED30*, *EXT1*, *TNFRSF11B*, *COLEC10*, *MAL2*, *NOV*, *ENPP2*, *TAF2*,

DSCC1, *DEPTOR*, *COL14A1*, *MRPL13*, *MTBP*, and *SNTB1* genes. It is interesting, that pathogenic variants in *RAD21* have been associated with Cornelia de Lange syndrome type 4, which characterized with variable congenital anomalies, including genitourinary malformations, intellectual disability, distinctive facial features [26–28]. So, in our opinion, *RAD21* can be a good candidate for MRKH syndrome, which requires further research.

CONCLUSION

Female patients with TRPS II would benefit from a multidisciplinary approach with geneticist, pediatrician and adolescent gynecologists in order to allow early detection of Müllerian anomalies.

References

- Ledig S, Wieacker. Clinical and Genetic Aspects of Mayer-Rokitansky-Küster-Hauser Syndrome. *Med Genet.* 2018; 30: 3–11. DOI: 10.1007/s11825-018-0173-7. Epub 2018 Feb 21.
- Williams LS, Demir Eksi D, Shen Y, Lossie AC, Chorich LP, Sullivan ME, et al. Genetic analysis of Mayer-Rokitansky-Kuster-Hauser syndrome in a large cohort of families. *Fertil Steril.* 2017; 108 (1): 145–51. DOI: 10.1016/j.fertnstert.2017.05.017. Epub 2017 Jun 7. PMID: 28600106; PMCID: PMC5770980.
- For Backhouse B, Hanna, Robevska G, et al. Identification of Candidate Genes for Mayer-Rokitansky-Küster-Hauser Syndrome Using Genomic Approaches. *Sex Dev.* 2019; 13: 26–34. DOI: 10.1159/000494896. Epub 2018 Dec 1. DOI: 10.1159/000494896.
- Lüdecke HJ, Johnson C, Wagner MJ, Wells DE, Turleau C, Tommerup N, et al. Molecular definition of the shortest region of deletion overlap in the Langer-Giedion syndrome. *Am J Hum Genet.* 1991; 49: 1197–206.
- Giedon A. Das tricho-rhino-phalangeale syndrome. *Helv Paediatr Acta.* 1966; 21: 475–85.
- Maas S, Shaw A, Bikker H, et al. Trichorhinophalangeal Syndrome. 2017 Apr 20. In: Adam MP, Ardinger HH, Pagon RA, et al., editors. *GeneReviews*® [Internet]. Seattle (WA): University of Washington, Seattle; 1993–2020.
- Trippella G, Lionetti P, Naldini S, et al. An early diagnosis of trichorhinophalangeal syndrome type 1: a case report and a review of literature. *Ital J Pediatr.* 2018; 44: 138. DOI: 10.1186/s13052-018-0580-z.
- Su W, Shi X, Lin M, et al. Non-ossifying fibroma with a pathologic fracture in a 12-year-old girl with tricho-rhino-phalangeal syndrome: a case report. *BMC Med Genet.* 2018; 19: 211. DOI: 10.1186/s12881-018-0732-4.
- Faucett WA, Savage MS. Chromosomal microarray testing. *JAAPA.* 2012; 25 (1): 65–6. DOI: 10.1097/01720610-201201000-00016. PMID: 22384761.
- United Healthcare Medical Policy. Chromosome microarray testing. 10/1/2015. Available from: https://www.unitedhealthcareonline.com/ccmcontent/Provider/UHC/en-US/Assets/ProviderStaticFiles/ProviderStaticFilesPdf/ToolsandResources/PoliciesandProtocols/MedicalPolicies/MedicalPolicies/Chromosome_Microarray_Testing.pdf. Accessed June 26, 2016.
- Riggs ER, Wain KE, Riethmaier D, Smith-Packard B, Faucett WA, Hoppman N, et al. Chromosomal microarray impacts clinical management. *Clin Genet.* 2014; 85 (2): 147–53. DOI: 10.1111/cge.12107. Epub 2013 Feb 21. PMID: 23347240.
- Miller DT, Adam MP, Aradhya S, et al. Consensus statement: chromosomal microarray is a first-tier clinical diagnostic test for individuals with developmental disabilities or congenital anomalies. *Am J Hum Genet.* 2010; 86: 749–64. DOI: 10.1016/j.ajhg.2010.04.006. PMID: 20466091. PMCID: PMC2869000.
- South ST, Lee C, Lamb AN, Higgins AW, Kearney HM. ACMG Standards and Guidelines for constitutional cytogenomic microarray analysis, including postnatal and prenatal applications: revision. 2013. DOI: 10.1038/gim.2013.129. PMID: 24071793.
- Josifova DJ. Genetics of gynaecological disorders. *Best Pract Res Clin Obstet Gynaecol.* 2017; 42: 100–13. DOI: 10.1016/j.bpobgyn.2017.05.001. Epub 2017 May 10. PMID: 28684328.
- Nik-Zainal S, Strick R, Storer M, Huang N, Rad R, Willatt L, et al. High incidence of recurrent copy number variants in patients with isolated and syndromic Müllerian aplasia. *Med Genet.* 2011; 48 (3): 197–204.
- Cappuccio G, Genesio R, Ronga V, Casertano A, Izzo A, Riccio MP, et al. Complex chromosomal rearrangements causing Langer-Giedion syndrome atypical phenotype: genotype-phenotype correlation and literature review. *Am J Med Genet A.* 2014; 164A (3): 753–9. DOI: 10.1002/ajmg.a.36326. Epub 2013 Dec 19. PMID: 24357330.
- Plaza-Benhumea L, Valdes-Miranda JM, Toral-López J, et al. Trichorhinophalangeal syndrome type II due to a novel 8q23.3–q24.12 deletion associated with imperforate hymen and vaginal stenosis. *Br J Dermatol.* 2014; 171: 1581–3. DOI: 10.1111/bjd.13177. Epub 2014 Oct 30.
- Selenti N, Tzetis M, Braoudaki M, Gianikou K, Kitsiou-Tzeli S, Fryssira H. An interstitial deletion at 8q23.1–q24.12 associated with Langer-Giedion syndrome / Trichorhinophalangeal syndrome (TRPS) type II and Cornelia de Lange syndrome 4. DOI: 10.1186/s13039-015-0169-9. PMID: 26269715. PMCID: PMC4534011.
- Partington MW, Rae J, Payne MJ. Haematometra in the Langer-Giedion syndrome. *J Med Genet.* 1991; 28: 644–5. DOI: 10.1136/jmg.28.9.644-b.
- Ramos FJ, McDonald-McGinn DM, Emanuel BS, Zackai EH. Tricho-rhinophalangeal syndrome type II (Langer-Giedion) with persistent cloaca and prune belly sequence in a girl with 8q interstitial deletion. *Am J Med Genet.* 1992; 44: 790–4. DOI: 10.1002/ajmg.1320440614. PMID: 1481848.
- Bernardini L, Gimelli S, Gervasini C, Carella M, Baban A, Frontino G, et al. Recurrent microdeletion at 17q12 as a cause of Mayer-Rokitansky-Kuster-Hauser (MRKH) syndrome: two case reports. *Orphanet J Rare Dis.* 2009; 4: 25. PubMed: 19889212.
- Cheroki C, Krepschi-Santos AC, Szuhai K, Brenner V, Kim CA, Otto PA, Rosenberg C. Genomic imbalances associated with mullerian aplasia. *J Med Genet.* 2008; 45: 228–32. PubMed: 18039948.
- Nik-Zainal S, Strick R, Storer M, et al: High incidence of recurrent copy number variants in patients with isolated and syndromic Müllerian aplasia. *J Med Genet* 2011; 3: 197–204.
- Gericke GS, Fialkov J: The Langer-Giedion phenotype associated with a unique skeletal finding in a mentally retarded adolescent male. *S Afr Med J.* 1980; 57: 548.
- Fryns JP. Trichorhinophalangeal syndrome type 2: another syndromic form of hydrometrocolpos. *Am J Med Genet.* 1997;

- 73: 233. DOI: 10.1002/(sici)1096--8628(1997)73:2<233::aid-ajmg23>3.0.co;2-u. PMID: 9409879.
26. Plaza-Benhumea L, Valdes-Miranda JM, Toral-López J, Pérez-Cabrera A, Cuevas-Covarrubias S. Trichorhinophalangeal syndrome type II due to a novel 8q23.3-q24.12 deletion associated with imperforate hymen and vaginal stenosis. DOI: 10.1111/bjd.13177. PMID: 24909397.
27. Plaza-Benhumea L, Valdes-Miranda JM, Toral-López J, et

- al. Trichorhinophalangeal syndrome type II due to a novel 8q23.3-q24.12 deletion associated with imperforate hymen and vaginal stenosis. *Br J Dermatol*. 2014; 171: 1581–3. DOI: 10.1111/bjd.13177. Epub 2014 Oct 30.
28. Boyle MI, Jespersgaard C, Brøndum-Nielsen K, Bisgaard AM, Tümer Z. Cornelia de Lange syndrome. *Clin Genet*. 2015; 88 (1): 1–12. DOI: 10.1111/cge.12499. Epub 2014 Oct 28. PMID: 25209348.

Литература

- Ledig S, Wieacker. Clinical and Genetic Aspects of Mayer-Rokitansky-Küster-Hauser Syndrome. *Med Genet*. 2018; 30: 3–11. DOI: 10.1007/s11825-018-0173-7. Epub 2018 Feb 21.
- Williams LS, Demir Eksi D, Shen Y, Lossie AC, Chorch LP, Sullivan ME, et al. Genetic analysis of Mayer-Rokitansky-Kuster-Hauser syndrome in a large cohort of families. *Fertil Steril*. 2017; 108 (1): 145–51. DOI: 10.1016/j.fertnstert.2017.05.017. Epub 2017 Jun 7. PMID: 28600106; PMCID: PMC5770980.
- For Backhouse B, Hanna, Robevska G, et al. Identification of Candidate Genes for Mayer-Rokitansky-Küster-Hauser Syndrome Using Genomic Approaches. *Sex Dev*. 2019; 13: 26–34. DOI: 10.1159/000494896. Epub 2018 Dec 1. DOI: 10.1159/000494896.
- Lüdecke HJ, Johnson C, Wagner MJ, Wells DE, Turleau C, Tommerup N, et al. Molecular definition of the shortest region of deletion overlap in the Langer-Giedion syndrome. *Am J Hum Genet*. 1991; 49: 1197–206.
- Giedon A. Das tricho-rhino-phalangeale syndrome. *Helv Paediatr Acta*. 1966; 21: 475–85.
- Maas S, Shaw A, Bikker H, et al. Trichorhinophalangeal Syndrome. 2017 Apr 20. In: Adam MP, Ardinger HH, Pagon RA, et al., editors. *GeneReviews® [Internet]*. Seattle (WA): University of Washington, Seattle; 1993–2020.
- Trippella G, Lionetti P, Naldini S, et al. An early diagnosis of trichorhinophalangeal syndrome type 1: a case report and a review of literature. *Ital J Pediatr*. 2018; 44: 138. DOI: 10.1186/s13052-018-0580-z.
- Su W, Shi X, Lin M, et al. Non-ossifying fibroma with a pathologic fracture in a 12-year-old girl with tricho-rhino-phalangeal syndrome: a case report. *BMC Med Genet*. 2018; 19: 211. DOI: 10.1186/s12881-018-0732-4.
- Faucett WA, Savage MS. Chromosomal microarray testing. *JAAPA*. 2012; 25 (1): 65–6. DOI: 10.1097/01720610-201201000-00016. PMID: 22384761.
- United Healthcare Medical Policy. Chromosome microarray testing. 10/1/2015. Available from: https://www.unitedhealthcareonline.com/ccmcontent/Provider/UHC/en-US/Assets/ProviderStaticFiles/ProviderStaticFilesPdf/ToolsandResources/PoliciesandProtocols/MedicalPolicies/MedicalPolicies/Chromosome_Microarray_Testing.pdf. Accessed June 26, 2016.
- Riggs ER, Wain KE, Riethmaier D, Smith-Packard B, Faucett WA, Hoppman N, et al. Chromosomal microarray impacts clinical management. *Clin Genet*. 2014; 85 (2): 147–53. DOI: 10.1111/cge.12107. Epub 2013 Feb 21. PMID: 23347240.
- Miller DT, Adam MP, Aradhya S, et al. Consensus statement: chromosomal microarray is a first-tier clinical diagnostic test for individuals with developmental disabilities or congenital anomalies. *Am J Hum Genet*. 2010; 86: 749–64. DOI: 10.1016/j.ajhg.2010.04.006. PMID: 20466091. PMCID: PMC2869000.
- South ST, Lee C, Lamb AN, Higgins AW, Kearney HM. ACMG Standards and Guidelines for constitutional cytogenomic microarray analysis, including postnatal and prenatal applications: revision. 2013. DOI: 10.1038/gim.2013.129. PMID: 24071793.
- Josifova DJ. Genetics of gynaecological disorders. *Best Pract Res Clin Obstet Gynaecol*. 2017; 42: 100–13. DOI: 10.1016/j.bpobgyn.2017.05.001. Epub 2017 May 10. PMID: 28684328.
- Nik-Zainal S, Strick R, Storer M, Huang N, Rad R, Willatt L, et al. High incidence of recurrent copy number variants in patients with isolated and syndromic Müllerian aplasia. *Med Genet*. 2011; 48 (3): 197–204.
- Cappuccio G, Genesio R, Ronga V, Casertano A, Izzo A, Riccio MP, et al. Complex chromosomal rearrangements causing Langer-Giedion syndrome atypical phenotype: genotype-phenotype correlation and literature review. *Am J Med Genet A*. 2014; 164A (3): 753–9. DOI: 10.1002/ajmg.a.36326. Epub 2013 Dec 19. PMID: 24357330.
- Plaza-Benhumea L, Valdes-Miranda JM, Toral-López J, et al. Trichorhinophalangeal syndrome type II due to a novel 8q23.3-q24.12 deletion associated with imperforate hymen and vaginal stenosis. *Br J Dermatol*. 2014; 171: 1581–3. DOI: 10.1111/bjd.13177. Epub 2014 Oct 30.
- Selenti N, Tzetis M, Braoudaki M, Gianikou K, Kitsiou-Tzeli S, Fryssira H. An interstitial deletion at 8q23.1-q24.12 associated with Langer-Giedion syndrome / Trichorhinophalangeal syndrome (TRPS) type II and Cornelia de Lange syndrome 4. DOI: 10.1186/s13039-015-0169-9. PMID: 26269715. PMCID: PMC4534011.
- Partington MW, Rae J, Payne MJ. Haematometra in the Langer-Giedion syndrome. *J Med Genet*. 1991; 28: 644–5. DOI: 10.1136/jmg.28.9.644-b.
- Ramos FJ, McDonald-McGinn DM, Emanuel BS, Zackai EH. Tricho-rhinophalangeal syndrome type II (Langer-Giedion) with persistent cloaca and prune belly sequence in a girl with 8q interstitial deletion. *Am J Med Genet*. 1992; 44: 790–4. DOI: 10.1002/ajmg.1320440614. PMID: 1481848.
- Bernardini L, Gimelli S, Gervasini C, Carella M, Baban A, Frontino G, et al. Recurrent microdeletion at 17q12 as a cause of Mayer-Rokitansky-Kuster-Hauser (MRKH) syndrome: two case reports. *Orphanet J Rare Dis*. 2009; 4: 25. PubMed: 19889212.
- Cheroki C, Krepschi-Santos AC, Szuhai K, Brenner V, Kim CA, Otto PA, Rosenberg C. Genomic imbalances associated with müllerian aplasia. *J Med Genet*. 2008; 45: 228–32. PubMed: 18039948.
- Nik-Zainal S, Strick R, Storer M, et al: High incidence of recurrent copy number variants in patients with isolated and syndromic Müllerian aplasia. *J Med Genet* 2011; 3: 197–204.
- Gericke GS, Fialkov J: The Langer-Giedion phenotype associated with a unique skeletal finding in a mentally retarded adolescent male. *S Afr Med J*. 1980; 57: 548.
- Fryns JP. Trichorhinophalangeal syndrome type 2: another syndromic form of hydrometrocolpos. *Am J Med Genet*. 1997; 73: 233. DOI: 10.1002/(sici)1096--8628(1997)73:2<233::aid-ajmg23>3.0.co;2-u. PMID: 9409879.
- Plaza-Benhumea L, Valdes-Miranda JM, Toral-López J, Pérez-Cabrera A, Cuevas-Covarrubias S. Trichorhinophalangeal syndrome type II due to a novel 8q23.3-q24.12 deletion associated with imperforate hymen and vaginal stenosis. DOI: 10.1111/bjd.13177. PMID: 24909397.
- Plaza-Benhumea L, Valdes-Miranda JM, Toral-López J, et al. Trichorhinophalangeal syndrome type II due to a novel 8q23.3-q24.12 deletion associated with imperforate hymen and vaginal stenosis. *Br J Dermatol*. 2014; 171: 1581–3. DOI: 10.1111/bjd.13177. Epub 2014 Oct 30.
- Boyle MI, Jespersgaard C, Brøndum-Nielsen K, Bisgaard AM, Tümer Z. Cornelia de Lange syndrome. *Clin Genet*. 2015; 88 (1): 1–12. DOI: 10.1111/cge.12499. Epub 2014 Oct 28. PMID: 25209348.

DETECTION OF *SMN1* LOSS WITH PCR-BASED SCREENING TESTNazarov VD¹, Cherebillo CC¹✉, Lapin SV, Sidorenko DV¹, Devyatkina YA¹, Musonova AC¹, Petrova TV², Nikiforova AI², Ivanova AV²¹ Federal State Budgetary Educational Institution of Higher Education Academician I.P. Pavlov First St. Petersburg State Medical University of the Ministry of Healthcare of Russian Federation, St. Petersburg, Russia² DNA-Technology LLC, Moscow, Russia

Spinal muscular atrophy (SMA) is an inherited neuromuscular disease characterized by progressive skeletal muscular weakness and atrophy. The newborn screening for spinal muscular atrophy should define all molecular forms of SMA. The aim of this study is to compare a PCR-based test for detection of homozygous *SMN1* loss with multiple ligation probe amplification (MLPA) in patients with spinal muscular atrophy and other numerical changes of the *SMN1* gene. PCR-based test was used to detect exon 7 of *SMN1* gene homozygous loss. The study included 341 samples of patients with clinical suspicion of SMA from Biobank of Centre of Molecular Medicine of Pavlov State Medical University (Saint-Petersburg, Russia). Group 1 included 206 whole blood samples and Group 2 included 135 dried blood spot (DBS) samples. Copy number of the *SMN1* and *SMN2* genes had been evaluated with MLPA as a reference method. The results showed that kit was able to detect homozygous *SMN1* loss in all samples from group 1 and 2 (Group 1: $n = 67$; 33%; Group 2: $n = 19$; 14%). At the same time in all samples with 1–3 copies of the *SMN1* gene, the results of the kit were negative for homozygous loss of *SMN1* gene (Group 1: $n = 139$; 67%; Group 2: $n = 116$; 86%). Kit showed high effectiveness in the detection of homozygous loss *SMN1* gene. The kit detects all possible molecular forms of homozygous *SMN1* gene loss in both DNA samples extracted from the whole blood and DBS.

Keywords: Spinal muscular atrophy, *SMN1* gene, newborn screening, real-time PCR**Funding:** All tests was provided by DNA-Technology LLC.**Author contribution:** Nazarov VD, Lapin SV — concept; Sidorenko DV, Devyatkina YA, Musonova AC — investigation; Petrova TV, Nikiforova AI, Ivanova AV — methodology; Nazarov VD, Cherebillo CC — wrining, original draft preparation; Cherebillo CC, Lapin SV, Petrova TV, Nikiforova AI, Ivanova AV — writing, review & editing.**Compliance with ethical standards:** this study was approved by the local Ethics Committee of the Pavlov First Saint Petersburg State Medical University (№ 274 from 26.06.2023). Written informed consent was obtained from all participants or their parents. The 1975 Declaration of Helsinki was rigorously adhered to secure the rights of the patients.✉ **Correspondence should be addressed:** Carina C. Cherebillo
6/8, Lva Tolstogo, Saint-Petersburg, 197022, Russia: k.cherebillo@mail.ru**Received:** 30.05.2023 **Accepted:** 22.06.2023 **Published online:** 30.06.2023**DOI:** 10.24075/brsmu.2023.025ДЕТЕКЦИЯ РАЗЛИЧНЫХ ФОРМ ПОТЕРИ ГЕНА *SMN1* С ПОМОЩЬЮ НАБОРА ДЛЯ ПЦР-РВВ. Д. Назаров¹, К. К. Чербило¹✉, С. В. Лапин¹, Д. В. Сидоренко¹, Е. А. Девяткина¹, А. К. Мусонова¹, Т. В. Петрова², А. И. Никифорова², А. В. Иванова²¹ Первый Санкт-Петербургский государственный медицинский университет имени И. П. Павлова Министерства здравоохранения Российской Федерации, Санкт-Петербург, Россия² ООО «ДНК-Технология», Москва, Россия

Проксимальная спинальная мышечная атрофия 5q (5q-CMA) — аутомно-рецессивное нервно-мышечное заболевание, характеризующееся потерей двигательных нейронов в передних рогах спинного мозга. С 2023 г. CMA включена в обязательный неонатальный скрининг на территории Российской Федерации. Неонатальный скрининговый тест на 5q-CMA должен выявлять все типы гомозиготной потери гена *SMN1*. Целью исследования была сравнительная оценка возможности определения гомозиготной потери экзона 7 гена *SMN1* с помощью теста на основе ПЦР-РВ с методом MLPA у пациентов с 5q-CMA, а также с различными изменениями числа копий гена *SMN1*. С помощью набора было проанализировано 206 образцов ДНК (группа 1), выделенных и очищенных из цельной крови, и 135 образцов ДНК (группа 2), выделенных и очищенных из сухих пятен крови, с известным количеством копий генов *SMN1* и *SMN2*. Количество копий генов *SMN1* и *SMN2* определяли методом MLPA, который был выбран в качестве референсного метода. Показано, что набор обнаруживает гомозиготную потерю гена *SMN1* во всех образцах, у которых подтверждена гомозиготная потеря гена *SMN1* с помощью MLPA (группа 1: $n = 67$; 33%; группа 2: $n = 19$; 14%). В то же время во всех образцах с 1–3 копиями гена *SMN1* результаты набора были отрицательными (группа 1: $n = 139$; 67%; группа 2: $n = 116$; 86%). Набор демонстрирует высокую эффективность и позволяет обнаруживать все возможные молекулярные формы гомозиготной потери гена *SMN1* как в образцах ДНК, выделенных из цельной крови, так и из сухих пятен крови.

Ключевые слова: спинальная мышечная атрофия, ген *SMN1*, неонатальный скрининг, ПЦР-РВ**Финансирование:** все наборы ПЦР-детекции в режиме реального времени были предоставлены компанией ООО «ДНК-технология».**Вклад авторов:** В. Д. Назаров, С. В. Лапин — концепция; Д. В. Сидоренко, Е. А. Девяткина, А. К. Мусонова — исследование; Т. В. Петрова, А. И. Никифорова, А. В. Иванова — методология; В. Д. Назаров, К. К. Чербило — написание и подготовка оригинального проекта; К. К. Чербило, С. В. Лапин, Т. В. Петрова, А. И. Никифорова, А. В. Иванова — написание, рецензирование и редактирование.**Соблюдение этических стандартов:** исследование одобрено этическим комитетом Первого Санкт-Петербургского государственного медицинского университета им. И. П. Павлова (протокол № 274 от 26 июня 2023 г.); проведено с соблюдением принципов Хельсинкской декларации 1975 г. Письменное информированное согласие было получено от всех участников или их родителей.✉ **Для корреспонденции:** Карина Константиновна Чербило
ул. Льва Толстого, 6-8, г. Санкт-Петербург, 197022, Россия; k.cherebillo@mail.ru**Статья получена:** 30.05.2023 **Статья принята к печати:** 22.06.2023 **Опубликована онлайн:** 30.06.2023**DOI:** 10.24075/vrgmu.2023.025

Proximal spinal muscular atrophy 5q (5q-SMA) is autosomal recessive neuromuscular disease, characterized by the loss of motor neurons in the anterior horns of the spinal cord, that leads to progressive muscle weakness and skeletal muscle atrophy. 5q-SMA is caused by the mutation in the survival motor neuron 1 gene (*SMN1*), situated on the chromosome 5q13. The incidence of SMA is 1 per 6000–10,000 newborns [1]. Rapid and irreversible loss of the motor neurons in SMA begins during the first 3 months of life, and 95% of motor neurons are affected in the patients under the age of 6 months [2]. Delayed molecular genetic diagnosis of SMA leads to untimely initiation of the treatment, which causes a limited clinical effectiveness of therapeutical intervention.

High incidence of the disease is related to the innate genetic instability of 5q13 region due to the presence of an inverted sequence of functional genes *SMN1*, *SERF1A*, *NAIP*, *GTF2H2A* and their centromeric pseudogenes *SMN2*, *SERF1B*, *NAIPΔ5*, *GTF2H2B* [1]. In 95% of cases, 5q-SMA results from the homozygous loss of the *SMN1* gene. The remaining cases of the disease occur in compound heterozygotes when the loss of the *SMN1* gene on one allele is combined with point mutations in the *SMN1* gene on another allele [3]. Today these forms of SMA are not detected in neonatal testing programs in any country of the world [4]. The prevalence of heterozygous loss of the *SMN1* gene in the Russian population is 1 : 36 [5]. Besides, the duplication of the *SMN1* is a frequent finding in general population, but it is not associated with SMA [1]. The pseudogene of the *SMN1* is the *SMN2* gene, which also consists of 9 exons and encodes the same SMN protein. The genes differ in 5 nucleotide in region from the 6-th intron to the 8-th exon. The key difference is exchange of cytosine to thymine in the 7-th exon of the *SMN2* gene (c. 840 C > T), which leads to the loss of the binding site for the exon splicing enhancer and the formation of the binding site for the exon silencer. As a result of this nucleotide change, the 7-th exon is excluded in 90% of *SMN2* transcripts. The resultant *SMNΔ7* protein becomes functionally defective and unstable, which causes its rapid degradation by the ubiquitin-proteasome system [1]. Nevertheless 10% of SMN protein, produced from *SMN2* gene, retains 7-th exon and can perform its function [6]. Therefore, copy number variation of *SMN2* can modify the severity of the disease in persons with *SMN1* deletion. SMA type 0 is characterized by absence of *SMN1* gene and 1 copy of *SMN2* gene. This SMA form presents antenatally with severely decreased fetal movements. SMA type I (Werdnig–Hoffmann disease) is the most frequent type of SMA, accounting for approximately half of patients (*SMN2* gene — 2–3 copies) [3,7]. Affected infants appear normal at birth, but subsequently develop hypotonia, delayed motor milestones, and feeding difficulties within the first 6 months of life. Infants with SMA type I never sit independently. In the less severe SMA type II (Dubowitz disease), children present between 6 and 18 months of age and are able to sit independently, but never walk. The majority of these patients survive into adulthood (*SMN2* gene — 2-4 copies). SMA type III (Kugelberg–Welander disease) includes patients who walk at some point (and for any period of time) during childhood (*SMN2* gene — 3–5 copies). SMA type IV is the mildest and least common form of SMA with onset in adulthood [3,7].

The loss of functional *SMN1* genes plays the main role in the pathogenesis of this disease. There are several types of the *SMN1* gene loss: complete deletion, conversion of the *SMN1* gene into *SMN2*, the formation of hybrid *SMN1/SMN2* structures, and loss of only a few exons of the *SMN1* gene (partial deletion). The complete deletion of the *SMN1* gene

occurs without an increase in the number of copies of the *SMN2* gene. Partial deletion is characterized by the isolated loss of several exons, including 7 exon, of the *SMN1* gene without changes of the number of copies of these exons in the *SMN2* gene [8]. During the conversion, loss of *SMN1* gene is accompanied by an increase in the number of copies of the *SMN2* gene [9]. The formation of chimeric *SMN1/SMN2* genes, in which there are sites belonging to both the *SMN1* gene and the *SMN2* pseudogene and which are characterized by an homozygous loss *SMN1*'s 7 exons and heterozygous loss *SMN1*'s 8 exon and unequal ratio of 7 and 8 exons in the *SMN2* gene, is another mechanism for the loss of the *SMN1* gene [10]. It should be noted that in patients with SMA, homozygous loss of the *SMN1* gene can be associated with both the individual types of "deletion" described, and with combined cases.

Restitution of SMN protein levels in patients with proximal SMA is valuable treatment option. Experimental models have shown that the time of switching off the SMN protein determined the life expectancy — the earlier the shutdown occurs, the worse observable survival [11]. Moreover, early reconstitution of SMN protein in SMA-models led to almost complete recovery [12]. In accordance with this data, presymptomatic therapy in newborns who have a pathological aberration in the *SMN1* gene has been investigated. The phase 2 NURTURE study demonstrated substantial clinical benefit of presymptomatic nusinersen therapy in infants with two or three copies of the *SMN2* gene [13]. In a multicenter phase III clinical trial for gene replacement therapy (SPR1NT), which was aimed at studying the efficiency and the safety of onasemnogene abeparvovec treatment in children with biallelic deletion of the *SMN1* gene and 3 copies of the *SMN2* gene (SMA type 2, respectively), recently published results also confirmed high clinical efficiency of presymptomatic treatment of children with SMA [14]. The available therapy and the possibility of effective usage of disease-modifying treatment in presymptomatic stage of disorder currently justify the screening of newborns for 5q-SMA. Australia, Belgium, Canada, Germany, Italy, Japan, Norway, the Netherlands, Poland and Taiwan, as well as 46 states in the United States have introduced mandatory screening of newborns for SMA. Mandatory screening for SMA for all newborns was launched in 2023 in the Russian Federation [15].

Multiplex ligation probes amplification (MLPA) is the "gold standard" for the diagnosis of SMA, which is able to detect not only homozygous deletions of the *SMN1* gene, but also other types of numerical changes in the *SMN1* and *SMN2* genes. However, this method is not applicable as a screening method due to the complexity and high cost [16, 17]. The most acceptable screening method for the homozygous loss of the *SMN1* gene is various modifications of the polymerase chain reaction method with real-time signal detection (RT-PCR), detecting the homozygous loss of the 7-th exon of the *SMN1* gene. The benefits of this approach have been confirmed by a number of studies and meta-analyses [18, 19, 20]. Taking into account the high clinical relevance of early diagnosis of SMA, as well as the beginning of mandatory screening for SMA of all newborns in the Russian Federation from 2023, there is a need for diagnostic molecular genetic tests that would allow identifying all possible forms of homozygous loss of the *SMN1* gene with high accuracy. It is also should be noted, that one of the most important requirement for neonatal screening test for SMA is possibility to detect homozygous loss of *SMN1* gene in dried blood spots (DBS) samples.

Russian company «DNA-Technology» recently issued new PCR kit for molecular screening for SMA in newborn, but

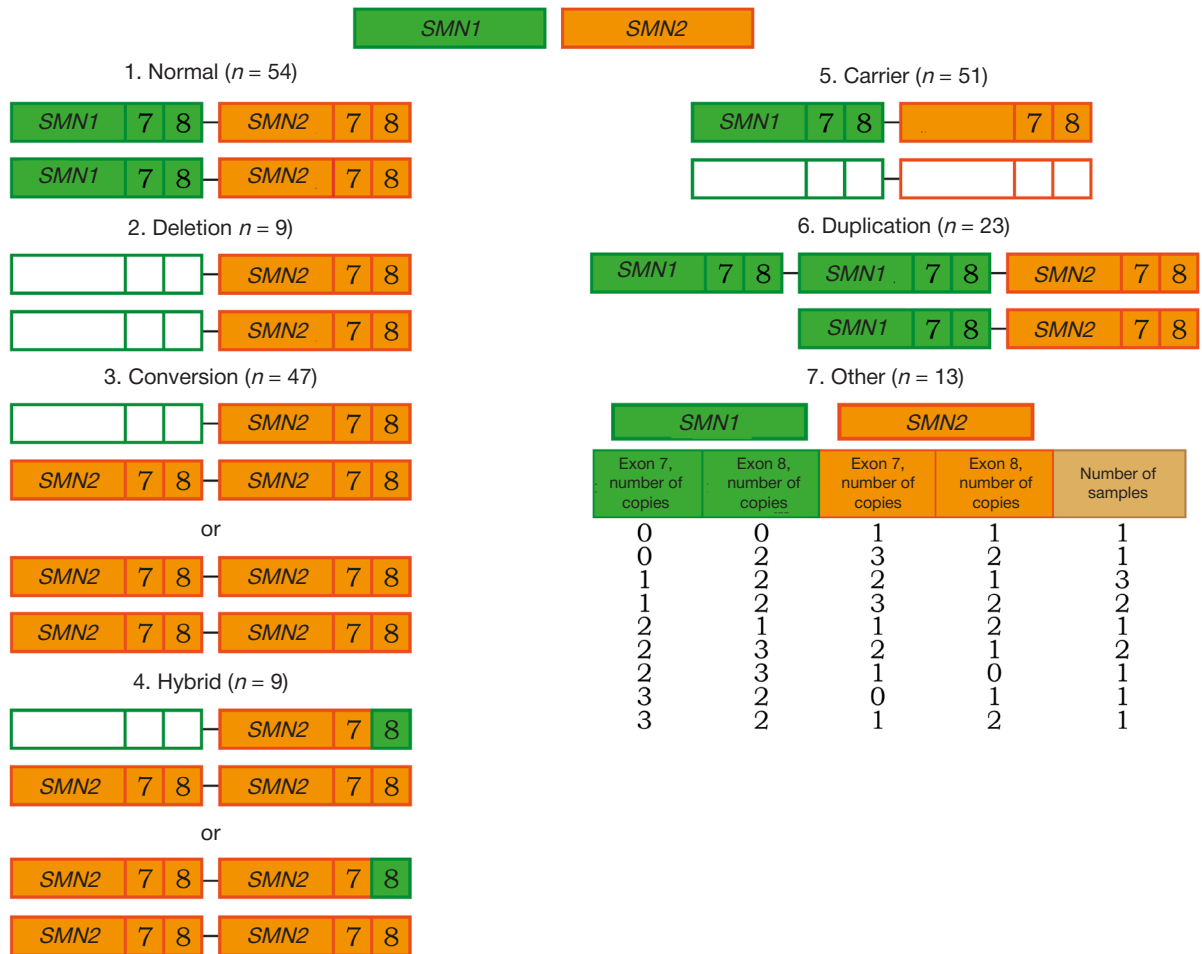


Fig. Schematic representation of SMN1 and SMN2 genotypes in each subgroup

extended approbation of this kit for detection of all form of SMN1 gene loss, detected by MLPA test, is highly needed.

The aim of this study is to compare a PCR-based screening test for detection of homozygous SMN1 loss with multiple ligation pro be amplification in patients with spinal muscular atrophy and other numerical changes of SMN1 gene.

METHODS

Sample collection and DNA extraction and purification

DNA samples extracted and purified from the whole blood (Group 1)

To evaluate possibility of detection of different types of SMN1 copy number variation the cohort consisted of 206 samples from Biobank of Centre of Molecular Medicine of Pavlov State Medical University (Saint-Petersburg, Russia) was collected. Patients with clinical suspicion of SMA were referred to laboratories of Pavlov Medical University from 2019 to 2021. Genomic DNA was extracted from peripheral blood using ExtractDNA Blood & Cells (Evrogen; Russia) according to the manufacturer’s instructions, and adjusted to a final concentration of 50 ng/μl. Copy number of SMN1 and SMN2 genes had been routinely evaluated with multiplex ligation-dependent probe amplification (MLPA) assay using SALSA® MLPA® Probemix P060-B2 SMA Carrier (MRC-Holland®, The Netherlands) in accordance with manufacturer’s instructions.

All the samples were divided into 7 subgroups according to SMN1 and SMN2 genotype status. Subgroup 1 «Normal»

(54 samples): 2 copies of SMN1 and SMN2 genes — so called «Reference genotype». Subgroup 2 «Deletion» (9 samples): absence of SMN1 gene without increase of SMN2 copy number. Subgroup 3 «Conversion» (47 samples): absence of SMN1 gene with increase of SMN2 copy number. Subgroup 4 «Hybrid» (9 samples): homozygous deletion of exon 7 and heterozygous deletion of exon 8 SMN1 gene with increase of exon 7 SMN2 copy number. Subgroup 5 «Carrier» (51 samples): heterozygous deletion of SMN1 gene. Subgroup 6 «Duplication» (23 samples): 3 copies of SMN1 gene. Subgroup 7 «Other» (13 samples): different combinations of SMN1 and SMN2 copy number that did not meet the criteria of other subgroups. Confidence interval for diagnostic sensitivity and specificity was chosen as 95% according to MedCalc® instrument (https://www.medcalc.org/calc/diagnostic_test.php) (Figure).

DNA samples extracted and purified from DBS (Group 2)

To confirm the possibility of detecting a homozygous loss of SMN1 in DNA isolated from DBS samples, a group of 135 patients, whose blood was transported in a dried state on a membrane, was collected from Biobank of Centre of Molecular Medicine of Pavlov State Medical University (Saint-Petersburg, Russia). Patients with clinical suspicion of SMA were referred to laboratories of Pavlov Medical University from 2019 to 2021. Genomic DNA was extracted from DBS using PREP-CITO DBS (DNA-Technology; Russia) according to the manufacturer’s instructions. For all patients copy number of SMN1 and SMN2 genes was evaluated by SALSA® MLPA® Probemix P060-B2

Table 1. The number of copies *SMN1* and *SMN2* genes according to MLPA assay in Group 2

Subgroup	MLPA assay results				Number of samples
	<i>SMN1</i> gene		<i>SMN2</i> gene		
	Exon 7	Exon 8	Exon 7	Exon 8	
Normal	2	2	4	4	10
	2	2	3	3	35
	2	2	2	2	54
Deletion	0	0	2	2	3
Conversion	0	0	4	4	2
	0	0	3	3	11
Hybrid	0	1	3	2	2
Carrier	1	1	2	2	9
Other	0	1	2	1	1
	1	2	1	1	4
	1	2	3	2	4

SMA Carrier (MRC-Holland®, Netherlands) in accordance with protocol for DBS membrane.

All the samples were divided into 6 subgroups: «Normal», «Deletion», «Conversion», «Hybrid», «Carrier», «Other» (Table 1).

Multiplex ligation-dependent probe amplification (MLPA) assay

The MLPA assay was performed using SALSA® MLPA® Probemix P060-B2 SMA Carrier (MRC-Holland®; The Netherlands) following the manufacturer's instructions for DNA extracted and purified from whole blood (Group 1) and from DBS membrane (Group 2). The commercial kit contains 17 reference probes and 4 specific probes detecting sequences presented in exon 7 and 8 of either *SMN1* and *SMN2* genes. MLPA products were analyzed with ABI 3500 genetic analyzer (Thermo Fisher Scientific®, USA). The relative peak height of each sample was calculated and compared with normal controls using MLPA analysis application by GeneMarker® software (SoftGenetics®, USA). The evaluation criteria of deletion/duplication were based on the MLPA kit instructions.

Table 2. Detection channels of PCR-products

Fam	Hex	Rox	Cy5
TREC	<i>SMN1</i> (exon 7 of <i>SMN1</i> gene)	KREC	IC (Internal control)

Table 3. PCR cycling conditions

Step	Temperature, °C	Min	Sec	Number of cycles	Optical measurements	Type of the step
1	80	2	00	1		Cycle
	94	5	00			
2	94	0	30	5	√	Cycle
	64	0	15			
3	94	0	10	45	√	Cycle
	64	0	15			
4	94	0	5	1		Cycle
5	10	Holding		Holding

PCR-based screening test

The NeoScreen SMA/TREC/KREC was performed for all patients from Group 1 and Group 2. NeoScreen SMA/TREC/KREC Real-time PCR Detection Kit (DNA-Technology, Russia) is intended to detect exon 7 of *SMN1* gene homozygous deletion and assess levels of T cell receptor excision circles (TREC) and kappa-deleting recombination excision circle (KREC) in newborns' dried blood spots (DBS) of whole blood for spinal muscular atrophy and primary immunodeficiencies screening by real-time PCR. The method is based on amplification of TREC, KREC, exon 7 of *SMN1* gene, and a fragment of the normalizing gene LTC4S (or endogenous internal control (IC), a single-copy genomic locus of Leukotriene C4 Synthase gene) by multiplex polymerase chain reaction (PCR). The use of several fluorescent dyes allows to simultaneously register the results of different amplification reactions taking place in the same tube. Table 2 shows detection channels of amplification products.

NeoScreen SMA/TREC/KREC assay was carried out using DTprime Real-time Detection Thermal Cycler (DNA-Technology;

Table 4. Comparison of the results obtained by MLPA assay and PCR-based test assay technology in Group 1

Subgroup	Number of samples in each subgroup	MLPA assay results (number of samples depending on exon 7 <i>SMN1</i> copy number)			Test results (number of samples depending on exon 7 <i>SMN1</i> copy number)		TP	FP	TN	FN
		>1	1	0	Normal (≥ 1)	Deletion (0)				
1. Reference	54	54	0	0	54	0	0	54	0	
2. Deletion	9	0	0	9	0	9	0	0	0	
3. Conversion	47	0	0	47	0	47	0	0	0	
4. Hybrid	9	0	0	9	0	9	0	0	0	
5. Carrier	51	0	51	0	51	0	0	51	0	
6. Duplication	23	23	0	0	23	0	0	23	0	
7. Other	13	6	5	2	11	2	0	11	0	
Total	206	83	56	67	139	67	0	139	0	

Note: TP — true positive; FP — false positive; TN — true negative; FN — false negative.

Protvino, Russia) by following the manufacturer's instructions (Table 3.). To assess the performance of the assay a positive control (included in PCR Detection Kit) and a negative control were included in each PCR-run. Positive control C+ № 1, containing DNA plasmids with specified targets — *TREC*, *KREC*, *SMN1*, *IC*, in equal concentration, is intended to evaluate PCR efficiency. Positive control C+ № 2 with plasmid equivalent exon 7 of *SMN2* gene allows to assess blocking of *SMN2* amplification (control of the *SMN1* amplification specificity).

Analysis of *SMN1* exon 7 deletion is based on the estimation of the indicator cycle difference (ΔC_p) between the C_p of *SMN1* (Hex channel) and *IC* (Cy5 channel) ($\Delta C_p = C_p(\text{Hex}) - C_p(\text{Cy5})$).

Evaluation of homozygous deletion of exon 7 of *SMN1* gene was performed according to the PCR Detection Kit instruction for result's analysis algorithm (performed automatically by the thermocycler software).

RESULTS

The PCR-based screening method was used on 341 samples with known *SMN1* and *SMN2* copy numbers (DNA extracted and purified from whole blood — Group 1, 206 samples; DNA extracted and purified from DBS membrane — Group 2, 135 samples). The MLPA assay was used as a reference method (Table 4, Table 5). The PCR-based test results was considered true positive if homozygous deletion of exon 7 *SMN1* gene is detected for samples with 0 copies of exon 7 *SMN1* gene, established by MLPA assay. Presence of at least one exon 7 of

SMN1 gene identified by MLPA assay and detection of exon 7 *SMN1* signal by test was considered true negative.

The results in Group 1 were as follows. In subgroup 1 «Normal» 54 participants (26%) carried 2 copies of exon 7 *SMN1* gene and all samples were true negative by PCR-based screening. In subgroup 2 «Deletion», subgroup 3 «Conversion», subgroup 4 «Hybrid» all samples were true positive ($n = 65$, 32%). In subgroup 5 «Carrier» all 51 participants (25%) had single copy of searched exon and all of the were true negative. In subgroup 6 «Duplication» all 23 samples (11%) carries 3 copies of exon 7 *SMN1* were true negative by PCR protocol. Finally subgroup 7 «Other» consisted of 13 probes with different *SMN1* and *SMN2* exon count. 6 samples (3%) carried more than 1 copy of exon 7 *SMN1* gene and were true negative. 5 samples (2%) in group 8 had single copy of *SMN1* gene and also were true negative. And 2 probes did not contain any of exon 7 *SMN1* and were true positive (1%). See results in Table 4.

The results in Group 2 are presented below. In subgroup «Normal» 99 participants (73%) had 2 copies of exon 7 *SMN1* gene and all samples were true negative by PCR-based screening. In subgroup «Deletion», subgroup «Conversion», subgroup «Hybrid» all samples were true positive by PCR-based screening ($n = 18$, 13,3%). Group 2 did not contain samples with *SMN1* gene duplication according to MLPA assay. In subgroups «Carrier» all 9 samples (7%) were true negative. In subgroup «Other» 1 probe (0,7%) did not contain any of exon 7 *SMN1* and were true positive. And 8 samples (6%) had single copy of *SMN1* gene and were true negative by PCR protocol. See results in Table 5.

Table 5. Comparison of the results obtained by MLPA assay and PCR-based test assay technology in Group 2

Subgroup	Number of samples in each subgroup	MLPA assay results (number of samples depending on exon 7 <i>SMN1</i> copy number)			Test results (number of samples depending on exon 7 <i>SMN1</i> copy number)		TP	FP	TN	FN
		>1	1	0	Normal (≥ 1)	Deletion (0)				
1. Reference	99	99	0	0	99	0	0	99	0	
2. Deletion	3	0	0	3	0	3	0	0	0	
3. Conversion	13	0	0	13	0	13	0	0	0	
4. Hybrid	2	0	0	2	0	2	0	0	0	
5. Carrier	9	0	9	0	9	0	0	9	0	
6. Duplication	0	0	0	0	0	0	0	0	0	
7. Other	9	0	8	1	8	1	0	8	0	
Total	135	99	17	19	116	19	0	116	0	

Note: TP — true positive; FP — false positive; TN — true negative; FN — false negative.

DISCUSSION

Spinal muscular atrophy is an autosomal recessive neurodegenerative disease, characterized by progressive skeletal muscle weakness. A laboratory test for neonatal screening of SMA should detect all types of *SMN1* loss in DNA isolated and purified from whole samples and from DBS samples.

There are several methodological approaches for homozygous *SMN1* loss, however, different modifications of real-time PCR proved to be the most suitable for neonatal SMA screening [16, 21]. Approaches, based on PCR, are highly robust, characterized by a very low number of false negative and false positive results, simple in handling, have a low cost and compatible with DBS samples [2, 22]. Screening for homozygous *SMN1* loss with test is based on the detection of homozygous loss of the 7 exon of *SMN1* gene by real-time PCR [6].

SMN1 gene is located in a highly unstable genome region, which is saturated with repeating inverted genes and Alu-sequences. Due to that fact, there is a wide spectrum of genetic aberrations, characterized by variation in copy number of *SMN1*. In order to assess the specificity of detection of homozygous *SMN1* loss with PCR-based kit in Group 1, which consist of DNA samples extracted and purified from the whole blood, 139 samples with 1–3 copies of *SMN1* gene were selected (subgroups «Normal», «Carrier», «Duplication», 11 samples from subgroup «Other»). In all 139 samples screened for homozygous *SMN1* loss with PCR-based test results were negative. Predictably, this emphasizes that a benign change in the copy number of the *SMN1* genes does not affect the effectiveness of detection of homozygous *SMN1* loss.

Detection of different types of homozygous loss of *SMN1* is the main task of neonatal SMA screening. In Group 1 PCR-based kit was able to detect homozygous *SMN1* loss in all samples ($n = 67$), included in the study. PCR-based test showed high sensitivity and specificity for detection of *SMN1* loss. This is in line with a number of studies, dedicated to the methodological problem of SMA screening [2, 23].

To confirm the effectiveness of the kit to detect a homozygous loss of *SMN1* gene in DNA isolated from DBS samples, patients in Group 2 were selected. For all patients DNA was isolated and purified from DBS samples by PREP-CITO DBS kit for subsequent evaluations by PCR-based test. For all patient MLPA analysis was also performed in parallel. In all samples with 1–3 copies of the *SMN1* gene ($n = 116$), the results of the test were negative for homozygous loss of *SMN1* gene. This highlights that a benign change in the copy number of *SMN1* genes does not affect the specificity of detecting homozygous loss of *SMN1* in DNA isolated from DBS samples with PCR-based test. For samples with 0 copies of exon 7 *SMN1* gene results of screening of homozygous *SMN1* loss by kit were positive for all patients.

A limitation of the PCR-based test is the inability to detect rare forms of 5q-SMA associated with heterozygous loss of one copy of the *SMN1* gene and pathogenic variants on the second copy of the gene (compound heterozygosity). According to research results, the prevalence of this form of 5q-SMA is up to 5% of all cases [3]. However, it should be noted that at the moment this subtype of the disease are not detected in neonatal testing programs in any country of the world [4]. When clinical signs and symptoms of 5q-SMA are identified and screening is negative for homozygous *SMN1* gene loss, an extended study is required to detect *SMN1* gene loss at one allele in combination with *SMN1* gene point mutations on another allele.

CONCLUSIONS

This pilot study showed, that PCR-based screening test is able to detect homozygous *SMN1* gene loss in both DNA samples extracted and purified from the whole blood and samples DNA isolated from DBS. Also, according to the results of this study, the test detects all possible molecular forms of homozygous *SMN1* gene loss.

References

- Butchbach MER. Genomic variability in the survival motor neuron genes (SMN1 and SMN2): Implications for spinal muscular atrophy phenotype and therapeutics development. *Int J Mol Sci.* 2021; 22 (15): 7896. DOI: 10.3390/ijms22157896.
- Chien YH, Chiang SC, Weng WC, Lee NC, Lin CJ, Hsieh WS, et al. Presymptomatic Diagnosis of Spinal Muscular Atrophy Through Newborn Screening. *J Pediatr.* 2017; 190: 124–129. DOI: 10.1016/j.jpeds.2017.06.042.
- Nicolau S, Waldrop MA, Connolly AM, Mendell JR. Spinal Muscular Atrophy. *Semin Pediatr Neurol.* 2021; 37: 100878. DOI: 10.1016/j.spn.2021.100878.
- Clermont O, Buret P, Benit P, Chanterau D, Saugier-Verber P, Munnich A, et al. Molecular analysis of SMA patients without homozygous SMN1 deletions using a new strategy for identification of SMN1 subtle mutations. *Hum Mutat.* 2004; 24 (5): 417–27. DOI: 10.1002/humu.20092.
- Zabnenkova VV, Dadali EL, Spiridonova MG, Zinchenko RA, Polyakov AV. Spinal muscular atrophy carrier frequency in Russian Federation. *ASHG.* 2016. DOI: 10.13140/RG.2.2.16245.60642.
- Arnold ES, Fischbeck KH. Spinal muscular atrophy. *Handb Clin Neurol.* 2018; 148: 591–601. DOI: 10.1016/B978-0-444-64076-5.00038-7.
- Министерство здравоохранения Российской Федерации. Клинические рекомендации «Проксимальная спинальная мышечная атрофия 5q». М., 2023. Russian.
- Gambardella A, Mazzei R, Toscano A, Annesi G, Pasqua A, Annesi F, et al. Spinal muscular atrophy due to an isolated deletion of exon 8 of the telomeric survival motor neuron gene. *Ann Neurol.* 1998; 44 (5): 836–39. DOI: 10.1002/ana.410440522.
- Stabley DL, Holbrook J, Scavina M, Crawford TO, Swoboda KJ, Robbins KM, et al. Detection of SMN1 to SMN2 gene conversion events and partial SMN1 gene deletions using array digital PCR. *Neurogenetics.* 2021; 22 (1): 53–64. DOI: 10.1007/s10048-020-00630-5.
- Niba ETE, Nishio H, Wijaya YOS, Lai PS, Tozawa T, Chiyonobu T, et al. Clinical phenotypes of spinal muscular atrophy patients with hybrid SMN gene. *Brain Dev.* 2021; 43 (2): 294–302. DOI: 10.1016/j.braindev.2020.09.005.
- Lutz CM, Kariy S, Patruni S, Osborne MA, Liu D, Henderson CE, et al. Postsymptomatic restoration of SMN rescues the disease phenotype in a mouse model of severe spinal muscular atrophy. *J Clin Invest.* 2011; 121 (8): 3029–41. DOI: 10.1172/JCI57291.
- Comley LH, Kline RA, Thomson AK, Woschitz V, Landeros EV, Osman EY, et al. Motor unit recovery following Smn restoration in mouse models of spinal muscular atrophy. *Hum Mol Genet.* 2022; 31 (18): 3107–19. DOI: 10.1093/hmg/ddac097.
- De Vivo DC, Bertini E, Swoboda KJ, Hwu WL, Crawford TO, Finkel RS, et al. Nusinersen initiated in infants during the presymptomatic stage of spinal muscular atrophy: Interim efficacy and safety results from the Phase 2 NURTURE study. *Neuromuscul Disord.* 2019; 29 (11): 842–56. DOI: 10.1016/j.nmd.2019.09.007.
- Strauss KA, Farrar MA, Muntoni F, Saito K, Mendell JR, Servais L,

- et al. Onasemnogene abeparvovec for presymptomatic infants with three copies of SMN2 at risk for spinal muscular atrophy: the Phase III SPR1NT trial. *Nat Med.* 2022; 28 (7): 1390–7. DOI: 10.1038/s41591-022-01867-3.
15. Order of the Ministry of Health of the Russian Federation № 274n dated 21.04.2022 "On approval of the Procedure for providing medical care to patients with congenital and (or) hereditary diseases".
 16. Stuppia L, Antonucci I, Palka G, Gatta V. Use of the MLPA Assay in the Molecular Diagnosis of Gene Copy Number Alterations in Human Genetic Diseases. *Int J Mol Sci.* 2012; 13: 3245–76. DOI: 10.3390/ijms13033245.
 17. Arkblad EL, Darin N, Berg K, Kimber E, Brandberg G, Lindberg C, et al. Multiplex ligation-dependent probe amplification improves diagnostics in spinal muscular atrophy. *Neuromuscul Disord.* 2006; 16: 830–38.
 18. Feldkötter M, Schwarzer V, Wirth R, Wienker TF, Wirth B. Quantitative analyses of SMN1 and SMN2 based on real-time lightCycler PCR: fast and highly reliable carrier testing and prediction of severity of spinal muscular atrophy. *Am J Hum Genet.* 2002; 70 (2): 358–68. DOI: 10.1086/338627.
 19. Gómez-Curet I, Robinson KG, Funanage VL, Crawford TO, Scavina M, Wang W. Robust quantification of the SMN gene copy number by real-time TaqMan PCR. *Neurogenetics.* 2007; 8 (4): 271–8. DOI: 10.1007/s10048-007-0093-1.
 20. Gutierrez-Mateo C, Timonen A, Vaahtera K, Jaakkola M, Hougaard DM, Bybjerg-Grauholm J. Development of a Multiplex Real-Time PCR Assay for the Newborn Screening of SCID, SMA, and XLA. *Int J Neonatal Screen.* 2019; 5 (4): 39. DOI: 10.3390/ijns5040039.
 21. Lefebvre S, Bürglen L, Reboullet S, Clermont O, Bulet P, Viollet L, et al. Identification and characterization of a spinal muscular atrophy-determining gene. *Cell.* 1995; 80 (1): 155–65. DOI: 10.1016/0092-8674(95)90460-3.
 22. Kraszewski JN, Kay DM, Stevens CF, Koval C, Haser B, Ortiz V, et al. Pilot study of population-based newborn screening for spinal muscular atrophy in New York state. *Genet Med.* 2018; 20 (6): 608–13. DOI: 10.1038/gim.2017.152.
 23. Kariyawasam DST, Russell JS, Wiley V, Alexander IE, Farrar MA. The implementation of newborn screening for spinal muscular atrophy: the Australian experience. *Genet Med.* 2020; 22 (3): 557–65. DOI: 10.1038/s41436-019-0673-0.

Литература

1. Butchbach MER. Genomic variability in the survival motor neuron genes (SMN1 and SMN2): Implications for spinal muscular atrophy phenotype and therapeutics development. *Int J Mol Sci.* 2021; 22 (15): 7896. DOI: 10.3390/ijms22157896.
2. Chien YH, Chiang SC, Weng WC, Lee NC, Lin CJ, Hsieh WS, et al. Presymptomatic Diagnosis of Spinal Muscular Atrophy Through Newborn Screening. *J Pediatr.* 2017; 190: 124–129. DOI: 10.1016/j.jpeds.2017.06.042.
3. Nicolau S, Waldrop MA, Connolly AM, Mendell JR. Spinal Muscular Atrophy. *Semin Pediatr Neurol.* 2021; 37: 100878. DOI: 10.1016/j.spen.2021.100878.
4. Clermont O, Bulet P, Benit P, Chanterau D, Saugier-Verber P, Munnich A, et al. Molecular analysis of SMA patients without homozygous SMN1 deletions using a new strategy for identification of SMN1 subtle mutations. *Hum Mutat.* 2004; 24 (5): 417–27. DOI: 10.1002/humu.20092.
5. Zabnenkova VV, Dadali EL, Spiridonova MG, Zinchenko RA, Polyakov AV. Spinal muscular atrophy carrier frequency in Russian Federation. *ASHG.* 2016. DOI: 10.13140/RG.2.2.16245.60642.
6. Arnold ES, Fischbeck KH. Spinal muscular atrophy. *Handb Clin Neurol.* 2018; 148: 591–601. DOI: 10.1016/B978-0-444-64076-5.00038-7.
7. Министерство здравоохранения Российской Федерации. Клинические рекомендации «Проксимальная спинальная мышечная атрофия 5q». М., 2023.
8. Gambardella A, Mazzei R, Toscano A, Annesi G, Pasqua A, Annesi F, et al. Spinal muscular atrophy due to an isolated deletion of exon 8 of the telomeric survival motor neuron gene. *Ann Neurol.* 1998; 44 (5): 836–39. DOI: 10.1002/ana.410440522.
9. Stabley DL, Holbrook J, Scavina M, Crawford TO, Swoboda KJ, Robbins KM, et al. Detection of SMN1 to SMN2 gene conversion events and partial SMN1 gene deletions using array digital PCR. *Neurogenetics.* 2021; 22 (1): 53–64. DOI: 10.1007/s10048-020-00630-5.
10. Niba ETE, Nishio H, Wijaya YOS, Lai PS, Tozawa T, Chiyonobu T, et al. Clinical phenotypes of spinal muscular atrophy patients with hybrid SMN gene. *Brain Dev.* 2021; 43 (2): 294–302. DOI: 10.1016/j.braindev.2020.09.005.
11. Lutz CM, Kariy S, Patruni S, Osborne MA, Liu D, Henderson CE, et al. Postsymptomatic restoration of SMN rescues the disease phenotype in a mouse model of severe spinal muscular atrophy. *J Clin Invest.* 2011; 121 (8): 3029–41. DOI: 10.1172/JCI57291.
12. Comley LH, Kline RA, Thomson AK, Woschitz V, Landeros EV, Osman EY, et al. Motor unit recovery following Smn restoration in mouse models of spinal muscular atrophy. *Hum Mol Genet.* 2022; 31 (18): 3107–19. DOI: 10.1093/hmg/ddac097.
13. De Vivo DC, Bertini E, Swoboda KJ, Hwu WL, Crawford TO, Finkel RS, et al. Nusinersen initiated in infants during the presymptomatic stage of spinal muscular atrophy: Interim efficacy and safety results from the Phase 2 NURTURE study. *Neuromuscul Disord.* 2019; 29 (11): 842–56. DOI: 10.1016/j.nmd.2019.09.007.
14. Strauss KA, Farrar MA, Muntoni F, Saito K, Mendell JR, Servais L, et al. Onasemnogene abeparvovec for presymptomatic infants with three copies of SMN2 at risk for spinal muscular atrophy: the Phase III SPR1NT trial. *Nat Med.* 2022; 28 (7): 1390–7. DOI: 10.1038/s41591-022-01867-3.
15. Order of the Ministry of Health of the Russian Federation № 274n dated 21.04.2022 "On approval of the Procedure for providing medical care to patients with congenital and (or) hereditary diseases".
16. Stuppia L, Antonucci I, Palka G, Gatta V. Use of the MLPA Assay in the Molecular Diagnosis of Gene Copy Number Alterations in Human Genetic Diseases. *Int J Mol Sci.* 2012; 13: 3245–76. DOI: 10.3390/ijms13033245.
17. Arkblad EL, Darin N, Berg K, Kimber E, Brandberg G, Lindberg C, et al. Multiplex ligation-dependent probe amplification improves diagnostics in spinal muscular atrophy. *Neuromuscul Disord.* 2006; 16: 830–38.
18. Feldkötter M, Schwarzer V, Wirth R, Wienker TF, Wirth B. Quantitative analyses of SMN1 and SMN2 based on real-time lightCycler PCR: fast and highly reliable carrier testing and prediction of severity of spinal muscular atrophy. *Am J Hum Genet.* 2002; 70 (2): 358–68. DOI: 10.1086/338627.
19. Gómez-Curet I, Robinson KG, Funanage VL, Crawford TO, Scavina M, Wang W. Robust quantification of the SMN gene copy number by real-time TaqMan PCR. *Neurogenetics.* 2007; 8 (4): 271–8. DOI: 10.1007/s10048-007-0093-1.
20. Gutierrez-Mateo C, Timonen A, Vaahtera K, Jaakkola M, Hougaard DM, Bybjerg-Grauholm J. Development of a Multiplex Real-Time PCR Assay for the Newborn Screening of SCID, SMA, and XLA. *Int J Neonatal Screen.* 2019; 5 (4): 39. DOI: 10.3390/ijns5040039.
21. Lefebvre S, Bürglen L, Reboullet S, Clermont O, Bulet P, Viollet L, et al. Identification and characterization of a spinal muscular atrophy-determining gene. *Cell.* 1995; 80 (1): 155–65. DOI: 10.1016/0092-8674(95)90460-3.
22. Kraszewski JN, Kay DM, Stevens CF, Koval C, Haser B, Ortiz V, et al. Pilot study of population-based newborn screening for spinal muscular atrophy in New York state. *Genet Med.* 2018; 20 (6): 608–13. DOI: 10.1038/gim.2017.152.
23. Kariyawasam DST, Russell JS, Wiley V, Alexander IE, Farrar MA. The implementation of newborn screening for spinal muscular atrophy: the Australian experience. *Genet Med.* 2020; 22 (3): 557–65. DOI: 10.1038/s41436-019-0673-0.

TYPE 1 DIABETES MELLITUS: FEATURES OF DIFFERENTIAL DIAGNOSIS

Gantsgorn EV , Denisenko OV, Osipenko YaO, Kalmykova DA, Ivanov AV, Gerasyuta SS, Bulguryan GA, Ivanova MH, Saakyan DA

Rostov State Medical University of the Ministry of Health of the Russian Federation, Rostov-on-Don, Russia

Type 1 diabetes mellitus is a condition caused by autoimmune damage to insulin-producing beta cells of the pancreatic islets, leading to endogenous insulin deficiency. Despite the sufficient knowledge of the disease and the availability of clinical recommendations for substitution therapy, the number of patients with this pathology is growing worldwide. At the same time, their cohort is very heterogeneous, including amid different etiology, concomitant genetic background, variations in the manifestation of the disease and severity. In this regard, traditional ideas about type 1 diabetes mellitus are being questioned, which requires special attention when managing patients with a clinical picture of the disease that differs from the traditional one. The article presents a clinical case of type 1 diabetes mellitus in a young patient, which demonstrates the importance of a personalized approach to the diagnosis and treatment of diabetic patients with a "non-classical" history.

Keywords: type 1 diabetes mellitus, latent autoimmune diabetes in adults, differential diagnosis, diabetic neuropathy

Author contribution: Gantsgorn EV — study concept, interpretation of results, manuscript editing; Denisenko OV, Osipenko YaO — literature analysis, data analysis, interpretation of results, manuscript writing; Kalmykova DA, Ivanov AV, Gerasyuta SS, Bulguryan GA, Ivanova MH, Saakyan DA — literature analysis, data analysis.

Compliance with ethical standards: the patient signed a voluntary informed consent to the publication of personal medical information in an anonymized form.

✉ **Correspondence should be addressed:** Elena V. Gantsgorn
1-ya Mayskaya, 8/10, 16, Rostov-on-Don, 344019, Russia; gantsgorn@inbox.ru

Received: 13.05.2023 **Accepted:** 14.06.2023 **Published online:** 26.06.2023

DOI: 10.24075/brsmu.2023.023

САХАРНЫЙ ДИАБЕТ 1-ГО ТИПА: ОСОБЕННОСТИ ДИФФЕРЕНЦИАЛЬНОЙ ДИАГНОСТИКИ

Е. В. Ганцгорн , О. В. Денисенко, Я. О. Осипенко, Д. А. Калмыкова, А. В. Иванов, С. С. Герасюта, Г. А. Булгурян, М. Х. Иванова, Д. А. Саакян

Ростовский государственный медицинский университет Министерства здравоохранения Российской Федерации, Ростов-на-Дону, Россия

Диабет 1-го типа — это состояние, вызванное аутоиммунным повреждением инсулин-продуцирующих β -клеток островков поджелудочной железы, приводящее к эндогенному дефициту инсулина. Несмотря на достаточную изученность заболевания и наличие клинических рекомендаций по проведению заместительной терапии, количество больных с данной патологией растет по всему миру. При этом их когорта очень неоднородна, в том числе ввиду различной этиологии, сопутствующего генетического фона, вариаций манифестации заболевания и степени тяжести. В связи с этим, традиционные представления о сахарном диабете 1-го типа ставятся под сомнение, что требует особого внимания при ведении пациентов с клинической картиной заболевания, отличающейся от традиционной. В статье представлен клинический случай течения сахарного диабета 1-го типа у молодого пациента, который демонстрирует важность персонализированного подхода к диагностике и лечению больных сахарным диабетом с «неклассическим» анамнезом.

Ключевые слова: сахарный диабет 1-го типа, аутоиммунный диабет взрослых, дифференциальная диагностика, диабетическая нейропатия

Вклад авторов: Е. В. Ганцгорн — концепция, интерпретация результатов, научное редактирование; О. В. Денисенко, Я. О. Осипенко — анализ литературы, анализ данных, интерпретация результатов, написание статьи; Д. А. Калмыкова, А. В. Иванов, С. С. Герасюта, Г. А. Булгурян, М. Х. Иванова, Д. А. Саакян — анализ литературы, анализ данных.

Соблюдение этических стандартов: пациент подписал добровольное информированное согласие на публикацию персональной медицинской информации в обезличенной форме.

✉ **Для корреспонденции:** Елена Владимировна Ганцгорн
ул. 1-я Майская, д. 8/10, кв. 16, г. Ростов-на-Дону, 344019; Россия; gantsgorn@inbox.ru

Статья получена: 13.05.2023 **Статья принята к печати:** 14.06.2023 **Опубликована онлайн:** 26.06.2023

DOI: 10.24075/vrgmu.2023.023

Type 1 diabetes mellitus (DM1) continues to be one of the global medical and social problems due to its widespread prevalence, polymorphism, the development of severe sequelae and the irreversibility of changes. The number of patients in the Russian Federation with DM1 at the beginning of 2023 was 277,092 [1].

Despite the high degree of coverage of DM1 and the existing traditional paradigms of diagnosis and treatment approaches, it is not always possible to correctly diagnose this type of DM, which is associated with a variable onset and course, the presence of "non-classical" manifestations, as well as the existence of intermediate forms of the disease that combine the clinical signs of DM1 and type 2 DM (DM2), for example, such as latent autoimmune diabetes in adults (LADA) [2]. These factors also cause disadvantages in treatment, because the majority of people suffering from DM1 do not have an optimized glycemic profile [3].

In the clinical observation presented by us, the clinical picture of the course of DM1 with a "non-classical" history is shown and attention is focused on the need for diagnostic search and an individual approach to patient management.

Clinical case description*Primary hospitalization*

Patient H. 26 years old, on 12.08.2022 entered the emergency department of the emergency hospital with complaints of general weakness, dry mouth, thirst, fatigue. During the initial examination, the following were revealed: hyperglycemia — 17 mmol/L, glucosuria, ketonuria. The patient was admitted to the therapeutic department of the hospital with a preliminary diagnosis of type 1 diabetes mellitus for the purpose of additional examination and selection of glucose-lowering therapy.

Table 1. Assessment of the level of glycemia (mmol/L) by a glucometer at using of insulin therapy (soluble insulin + insulin-isophane) in the period from 13.08.2022 to 22.08.2022

Date	Before breakfast	2 h after eating	Before lunch	2 h after eating	Before dinner	2 h after eating	At night
13.08.2022	15.7	16.1	12.5	13.6	11.0	13.2	12.1
14.08.2022	12.0	13.2	11.9	14.5	9.8	14.0	11.2
15.08.2022	10.9	11.8	10.5	9.3	10.0	10.9	9.1
16.08.2022	8.9	10.5	9.2	8.9	10.0	11.4	10.2
17.08.2022	11.3	10.5	9.3	9.8	10.1	11.3	9.2
18.08.2022	10.8	11.0	8.7	9.5	9.1	10.0	8.1
19.08.2022	8.8	9.1	7.3	8.8	7.9	9.1	8.5
20.08.2022	7.9	8.0	7.1	8.1	5.8	7.5	5.6
21.08.2022	7.7	8.3	6.0	7.2	5.8	6.3	5.3
22.08.2022	6.3	7.1	5.8	6.8	9.1	6.3	5.5

According to the patient, episodes of hyperglycemia up to 8–9 mmol/L were detected earlier during medical preventive examinations for two years, but he did not attach any importance to this, referring to violations of the rules for testing. In addition, for two months before going to the hospital, the patient had noted increased thirst and weight loss of 5 kg. He did not seek medical help.

It is known from the life history that the patient developed according to gender and age, has no bad habits. There are no chronic diseases and a burdened hereditary history, endocrinopathy included.

Objective findings: height — 190 cm, weight — 84 kg. The body mass index (BMI) is 23.3 kg/m². The skin and visible mucous linings are of the usual color and moisture content, skin tightness is retained. The thyroid gland is not palpable. There is no peripheral swelling. The heart tones are clear, rhythmic. Heart rate (HR) — 65 beats/min, blood pressure (BP) — 120/80 mm Hg. Breathing is auscultatory vesicular on both sides. Percussion — clear pulmonary sound. Respiratory rate (RR) is 16 per minute. The abdomen is of the correct shape, participates in the act of breathing, with palpation — soft, painless. The stool is formed, without any pathological admixtures. The urination is unimpeded, painless. The kidneys are not palpable. Pounding symptom (Pasternatsky's symptom) is negative on both sides.

1. Full blood count (FBC) from 12.08.2022: without pathological findings.

2. Urine analysis (UA) from 12.08.2022: glucosuria (+++), ketonuria (+), hypersthenuria (1,028 g/L).

3. Biochemical blood test: hyperglycemia: 12.08.2022 — 17.5 mmol/L, 19.08.2022 — 18.3 mmol/L, 20.08.2022 — 7.7 mmol/L, 23.08.2022 — 6.8 mmol/L. Glycated hemoglobin (HbA1c) — 10.5%. Indicators of protein metabolism, bilirubin fractions, iron, alanine aminotransferase (AlAT), aspartate aminotransferase (AsAT), gamma-glutamyl transferase (GGT), alkaline phosphatase, creatinine, urea, uric acid, C-reactive protein, Na⁺, K⁺, Ca²⁺, Mg²⁺ ions are within normal limits.

4. Lipid profile: total cholesterol — 4.9 mmol/L, triglycerides (TG) — 1.8 mmol/L, high density lipoproteins (HDL) — 1.40 mmol/L, low density lipoproteins (LDL) — 3.1 mmol/L, very low-density lipoproteins (VLDL) — 0.8 mmol/L, atherogenicity index — 2.5.

5. Coagulation profile indicators are within the normal range.

6. The analysis of acid-alkali balance showed no abnormal changes.

7. The glomerular filtration rate (GFR) was calculated: 123.81 ml/min/1.73 m².

The patient was treated in the medical ward from 12.08.2022 to 24.08.2022.

The patient was treated in the form of basal bolus insulin therapy: soluble insulin and insulin-isophane.

During the entire treatment period, blood glucose was monitored (Table 1). The patient was discharged with a diagnosis of type 1 diabetes mellitus, first identified, the goal of HbA1c < 6.5%. It was recommended to continue treatment with insulin aspart subcutaneously (s/c) for 10–12 units before meals and insulin glargine s/c for 30 units in the evening once under the control of glycemia levels with possible dose adjustment, as well as to keep a diary of self-monitoring of blood glucose levels and adhere to a diet with a restriction of easily digestible carbohydrates. Preventive counseling on treatment issues was carried out, but group counseling at the Diabetes School was not practiced.

A few days after discharge, the patient began to present with thirst, dry mouth, frequent urination, and a feeling of crawling goosebumps in the area of the feet. Within a week, the glucose level began to rise again and was in the range of 10–13 mmol/L.

Repeated hospitalization

The patient was admitted on 30.08.2022 to the medical ward in a day hospital, taking into account clinical and laboratory decompensation of DM.

Upon admission: height — 190 cm, weight — 82 kg, BMI — 22.7 kg/m². Blood pressure — 115/68 mm Hg, heart rate — 71 beats/min, RR — 17 in min. There were no other changes in the objective status of the patient compared to the examination on 12.08.22. FBC, UA, lipid profile, coagulogram — within the normal range. The biochemical analysis revealed glucosuria — 13.9 mmol/L, the remaining parameters are without pathological findings. The HbA1c level from 30.08.2022 is 10.5%. Glycemic profile from 30.08.2022 (venous blood): 13.49 mmol/L (on an empty stomach); 17.4 mmol/L — 2 hours after meals, 4 hours — 16.6 mmol/L.

Ultrasonography of the abdominal organs from 31.08.2022 revealed no pathology.

Due to the presence of complaints about the feeling of "crawling goosebumps" in the area of the feet, a neurologist was consulted with. A symmetrical decrease in biceps reflexes, carporadial, hock reflex, a significant decrease in the Achilles reflex, impaired surface sensitivity of the polyneuritic type (according to the type of "stockings" from the lower tertile level of the shin) was revealed. When evaluated on the Neuropathy Symptom Scale (NSS), the total score was 4, which corresponds to moderate neuropathy [4]. Conclusion:

Table 2. Assessment of the level of glycemia (mmol/L) by a glucometer at using of insulin therapy (glulisin + degludec) in the period from 31.08.2022 to 09.09.2022

Date	Before breakfast	2 h after eating	Before lunch	2 h after eating	Before dinner	2 h after eating	At night
31.08.2022	10.1	12.5	8.3	13.0	10.0	10.8	7.9
01.09.2022	8.8	15.6	12.0	13.2	9.8	10.2	9.3
02.09.2022	7.9	10.2	9.8	9.5	7.6	8.1	7.8
03.09.2022	7.1	9.2	7.9	8.1	6.9	7.1	6.1
04.09.2022	6.3	7.5	5.9	7.1	5.6	7.8	5.6
05.09.2022	5.3	6.8	5.5	7.5	6.3	7.0	5.5
06.09.2022	5.6	7.0	6.0	6.9	5.8	7.1	5.8
07.09.2022	5.3	5.9	6.3	6.9	5.3	6.2	4.9
08.09.2022	5.6	6.9	5.0	5.2	5.3	6.2	5.4
09.09.2022	5.4	6.5	4.8	–	–	–	–

diabetic distal polyneuropathy, sensory form, moderate manifestations.

During the entire time of the patient's stay in the hospital, carbohydrate metabolism was monitored (Table 2).

The patient was treated with insulin degludec 25 units at 22.00, insulin glulisin at the rate of 1 bread unit (BU): 2 units before meals to eliminate persistent postprandial hyperglycemia.

Starting from 05.09.2022, the glucose level began to gradually approach the goal, on 09.09.2022, reaching 5.4 mmol/L on an empty stomach and 6.5 mmol/L 2 hours after eating.

In order to verify the diagnosis, the patient was recommended to perform a study for the presence of autoantibodies to glutamic acid decarboxylase (GAD) and islet cells (ICA). The result from 09.09.2022: GADA — more than 1000 ME/ml; ICA — 256 U/ml.

Final diagnosis: type 1 diabetes mellitus, goal of HbA1c < 6.5%. Complications of the main diagnosis: diabetic distal polyneuropathy, sensory form, mild malfunctions.

The patient was discharged on 10.09.2022. To continue treatment, he was prescribed 25 units insulin degludec in the evening at 22.00, insulin glulisin at the rate of 1 BU: 2 units before meals.

Clinical case discussion

In this clinical case, the diagnosis of DM1 was more probable, since the patient's common complaints (weakness, dry mouth, thirst, fatigue), hyperglycemia, glucosuria, ketonuria, weight loss over the last 2 months, age < 30 years and BMI < 25 kg/m², absence of signs of metabolic syndrome indicate this pathological condition. However, the slow progression of DM, the absence of an acute onset, autoimmune diseases and predisposing factors are not quite definitive of the "classic" insulin-dependent diabetes. These characteristics are observed both with DM2, and, together with the onset at a young age and normal weight, with LADA [2, 5]. Due to the discrepancy of these signs, there is a need for an extended differential diagnosis.

For this purpose, an enzyme immunoassay was performed for the presence of antibodies to GAD and ICA. The positive result obtained disproves the presence of DM2, but does not exclude LADA. However, DM1 in young patients has a greater immunogenic load with faster damage to β -cells and a high need for insulin [2, 6–8], which was observed in the described clinical case. This fact can be confirmed by the determination of sharply decreased levels of C-peptide in DM1 than in LADA, in which this indicator decreases gradually [9, 10].

Anamnestic data indicate a similarity with LADA diabetes, however, a high concentration of autoantibodies, indicating a rapidly progressive decrease in the function of β -cells with the development of an acute hyperglycemic condition, comes more under the phenotype of DM1. There is also a classification that distinguishes stages in the development of DM1, including those with an asymptomatic onset [2, 11]. HLA genotyping can help in clarifying the diagnosis, since studies describe differences in the genetic profile of patients with LADA and DM1 in terms of the frequency of predisposing, protective genotypes and haplotypes [12, 13]. However, this method is not routine and it is not used for diagnosis in normal clinical practice, and therefore, the main role in such a diagnostic search will be played by the clinical picture.

One of the peculiarities of this case is the rapid development of complications of DM: diabetic distal neuropathy was diagnosed almost immediately after the diagnosis. Such rapid progression of complications is rare. Several cases of early onset of polyneuropathy have been described [14, 15]. It is possible that the symptoms of polyneuropathy occurred earlier, as well as episodes of hyperglycemia, but the patient did not complain before the induction of more serious malfunctions.

Defining the type of diabetes and taking into account the "non-classical" symptoms are necessary for the correct selection of insulin therapy, especially due to the fact that the patient had decompensation of diabetes mellitus, it was not immediately possible to achieve a stable tendency to decrease glycemia and there are complications already. Since the insufficiency of β -cell function is significant, insulin therapy is the right treatment tactic. However, repeated hospitalization with deterioration of health and persistent hyperglycemia may indicate both low patient adherence to treatment between admissions and inappropriate insulin dosages, in connection with which the drugs and therapy regimen were changed. The importance of differential diagnosis is confirmed in respect of the aspect of the fact that if this case is attributed to LADA diabetes, combination therapy with sugar-lowering oral drugs would be possible with a residual β -cell function, for the evaluation of which the laboratory workup of C-peptide is recommended.

CONCLUSION

Summarizing all available data, it can be claimed that in the described clinical case, the diagnosis of DM 1 is most likely. However, in our opinion, in such "non-classical" clinical setting, it is advisable to conduct the widest workup of DM: identification of the level of C-peptide for accurate diagnosis

verification, assessment of diabetes progression; performing electromyography to exclude other causes of neuropathic symptoms; consultation with an ophthalmologist to search for other possible microvascular complications. It is also important to monitor and maintain a sufficient level of patient

compliance. The clinical observation presented by us indicates the importance of an individual approach to the management of patients with DM1, especially in the presence of similar signs with other types of DM, for timely therapy correction and prevention of progression, development of complications.

References

1. Federal'nyj Registr saxarnogo diabeta RF; 2023 [Elektronnyj resurs] [data obrashheniya: 11.06.2023]. Dostupno po ssylke: <https://sd.diaregistry.ru/content/o-proekte.html#content>. Russian.
2. Buzzetti R, Tuomi T, Mauricio D, Pietropaolo M, Zhou Z, Pozzilli P, et al. Management of latent autoimmune diabetes in adults: a consensus statement from an international expert panel. *Diabetes*. 2020; 69 (10): 2037–47. PMID: 32847960; PMCID: PMC7809717.7.
3. DiMeglio LA, Evans-Molina C, Oram RA. Type 1 diabetes. *Lancet*. 2018; 391 (10138): 2449–62. PMID: 29916386; PMCID: PMC6661119.
4. Meijer JW, Smit AJ, Sonderen EV, Groothoff JW, Eisma WH, Links TP. Symptom scoring systems to diagnose distal polyneuropathy in diabetes: the diabetic neuropathy symptom score. *Diabet Med*. 2002; 19 (11): 962–5. PMID: 12421436.
5. Furlanos S, Perry C, Stein MS, Stankovich J, Harrison LC, Colman PG. A clinical screening tool identifies autoimmune diabetes in adults. *Diabetes Care*. 2006; 29 (5): 970–5. PMID: 16644622.
6. Pieralice S, Pozzilli P. Latent autoimmune diabetes in adults: a review on clinical implications and management. *Diabetes Metab J*. 2018; 42 (6): 451–64. PMID: 30565440; PMCID: PMC6300440.
7. Zampetti S, Capizzi M, Spoletini M, Campagna G, Leto G, Cipolloni L, et al. GADA titer-related risk for organ-specific autoimmunity in LADA subjects subdivided according to gender (NIRAD study 6). *J Clin Endocrinol Metab*. 2012; 97 (10): 3759–65. PMID: 22865904.
8. Leslie RD, Williams R, Pozzilli P. Clinical review: Type 1 diabetes and latent autoimmune diabetes in adults: one end of the rainbow. *J Clin Endocrinol Metab*. 2006; 91 (5): 1654–9. PMID: 16478821.
9. Hernandez M, Mollo A, Marsal JR, Esquerda A, Capel I, Puig-Domingo M, et al. Insulin secretion in patients with latent autoimmune diabetes (LADA): half way between type 1 and type 2 diabetes: action LADA 9. *BMC Endocr Disord*. 2015; 15: 1. PMID: 25572256; PMCID: PMC4297398.
10. American Diabetes Association Professional Practice Committee; 2. Classification and Diagnosis of Diabetes: Standards of Medical Care in Diabetes — 2022. *Diabetes Care*. 2022; 45 (Supplement 1): S17–S38.
11. Akil AA, Yassin E, Al-Maraghi A, Aliyev E, Al-Malki K, Fakhro KA. Diagnosis and treatment of type 1 diabetes at the dawn of the personalized medicine era. *J Transl Med*. 2021; 19 (1): 137. PMID: 33794915; PMCID: PMC8017850.
12. Timakova AA, Saltykov BB. Osobennosti razvitiya latentnogo diabeta vzroslykh (LADA). *Arxiv patologii*. 2019; 81 (4): 78–82. Russian.
13. Hernández M, Nóvoa-Medina Y, Faner R, Palou E, Esquerda A, Castelblanco E, et al. Genetics: Is LADA just late onset type 1 diabetes? *Front Endocrinol (Lausanne)*. 2022; 13: 916698. PMID: 36034444; PMCID: PMC9404871.
14. Said G, Goulon-Goeau C, Slama G, Tchobroutsky G. Severe early-onset polyneuropathy in insulin-dependent diabetes mellitus. A clinical and pathological study. *N Engl J Med*. 1992; 326 (19): 1257–63. PMID: 1560802.
15. Shafi OM, Latief M. Early onset symptomatic neuropathy in a child with Type 1 Diabetes mellitus. *Diabetes & Metabolic Syndrome: Clinical Research & Reviews*. 2017; 11 (Suppl 1): S477–S479.

Литература

1. Федеральный Регистр сахарного диабета РФ; 2023 [Электронный ресурс] [дата обращения: 11.06.2023]. Доступно по ссылке: <https://sd.diaregistry.ru/content/o-proekte.html#content>.
2. Buzzetti R, Tuomi T, Mauricio D, Pietropaolo M, Zhou Z, Pozzilli P, et al. Management of latent autoimmune diabetes in adults: a consensus statement from an international expert panel. *Diabetes*. 2020; 69 (10): 2037–47. PMID: 32847960; PMCID: PMC7809717.7.
3. DiMeglio LA, Evans-Molina C, Oram RA. Type 1 diabetes. *Lancet*. 2018; 391 (10138): 2449–62. PMID: 29916386; PMCID: PMC6661119.
4. Meijer JW, Smit AJ, Sonderen EV, Groothoff JW, Eisma WH, Links TP. Symptom scoring systems to diagnose distal polyneuropathy in diabetes: the diabetic neuropathy symptom score. *Diabet Med*. 2002; 19 (11): 962–5. PMID: 12421436.
5. Furlanos S, Perry C, Stein MS, Stankovich J, Harrison LC, Colman PG. A clinical screening tool identifies autoimmune diabetes in adults. *Diabetes Care*. 2006; 29 (5): 970–5. PMID: 16644622.
6. Pieralice S, Pozzilli P. Latent autoimmune diabetes in adults: a review on clinical implications and management. *Diabetes Metab J*. 2018; 42 (6): 451–64. PMID: 30565440; PMCID: PMC6300440.
7. Zampetti S, Capizzi M, Spoletini M, Campagna G, Leto G, Cipolloni L, et al. GADA titer-related risk for organ-specific autoimmunity in LADA subjects subdivided according to gender (NIRAD study 6). *J Clin Endocrinol Metab*. 2012; 97 (10): 3759–65. PMID: 22865904.
8. Leslie RD, Williams R, Pozzilli P. Clinical review: Type 1 diabetes and latent autoimmune diabetes in adults: one end of the rainbow. *J Clin Endocrinol Metab*. 2006; 91 (5): 1654–9. PMID: 16478821.
9. Hernandez M, Mollo A, Marsal JR, Esquerda A, Capel I, Puig-Domingo M, et al. Insulin secretion in patients with latent autoimmune diabetes (LADA): half way between type 1 and type 2 diabetes: action LADA 9. *BMC Endocr Disord*. 2015; 15: 1. PMID: 25572256; PMCID: PMC4297398.
10. American Diabetes Association Professional Practice Committee; 2. Classification and Diagnosis of Diabetes: Standards of Medical Care in Diabetes — 2022. *Diabetes Care*. 2022; 45 (Supplement 1): S17–S38.
11. Akil AA, Yassin E, Al-Maraghi A, Aliyev E, Al-Malki K, Fakhro KA. Diagnosis and treatment of type 1 diabetes at the dawn of the personalized medicine era. *J Transl Med*. 2021; 19 (1): 137. PMID: 33794915; PMCID: PMC8017850.
12. Тимакова А. А., Салтыков Б. Б. Особенности развития латентного диабета взрослых (LADA). *Архив патологии*. 2019; 81 (4): 78–82.
13. Hernández M, Nóvoa-Medina Y, Faner R, Palou E, Esquerda A, Castelblanco E, et al. Genetics: Is LADA just late onset type 1 diabetes? *Front Endocrinol (Lausanne)*. 2022; 13: 916698. PMID: 36034444; PMCID: PMC9404871.
14. Said G, Goulon-Goeau C, Slama G, Tchobroutsky G. Severe early-onset polyneuropathy in insulin-dependent diabetes mellitus. A clinical and pathological study. *N Engl J Med*. 1992; 326 (19): 1257–63. PMID: 1560802.
15. Shafi OM, Latief M. Early onset symptomatic neuropathy in a child with Type 1 Diabetes mellitus. *Diabetes & Metabolic Syndrome: Clinical Research & Reviews*. 2017; 11 (Suppl 1): S477–S479.

THE ROLE OF CAUCASIAN, IRANIAN AND STEPPE POPULATIONS IN SHAPING THE DIVERSITY OF AUTOSOMAL GENE POOL OF THE EASTERN CAUCASUS

Balanovska EV^{1,2}, Gorin IO¹, Petrushenko VS¹, Ponomarev GYu¹, Belov RO¹, Pocheshkhova EA^{1,3}, Salaev VA¹, Iskandarov NA¹, Pylev VYu^{1,2} ✉

¹ Bochkov Research Centre of Medical Genetics, Moscow, Russia

² Biobank of North Eurasia, Moscow, Russia

³ Kuban State Medical University, Krasnodar, Russia

Eastern Caucasus is home to more than 30 peoples speaking Caucasian, Iranian and Turkic languages. Fusion of multiple migration flows together with the complex population structure of the Eastern Caucasus make it more difficult to analyze its gene pool: this is the most poorly studied one among all regions of the Caucasus. The study is aimed to identify the main patterns of the autosomal gene pool variation in this region. A total of 356 genomes of 29 ethnic groups were studied using the large panels of SNP markers: 243 genomes of 22 peoples of the Eastern Caucasus and 113 genomes of 7 peoples living in adjacent regions. The bioinformatics analysis involved the use of the ADMIXTURE ancestral component method and the gene pool variability principal component analysis (PCA). The hypothesis of three genetic strata, the interaction of which forms the structure of gene pool of the Eastern Caucasus, was put forward. The "Dagestan" stratum carries information about the gene pool of the ancient autochthonous population of the Eastern Caucasus. The "Iranian" stratum represents the legacy of ancient and middle-aged migrations surges of the Iranian-speaking population: it constitutes three quarters of the gene pool of modern Azerbaijan and about one third of the Dagestan peoples' gene pool. The "Steppe" stratum represents a negligible influence of the Eurasian steppe. Interaction of three genetic strata is only indirectly related to the peoples' linguistic affiliation, however, the association with linguistics is more obvious in the Caucasian-speaking peoples. Four genetically distinct groups of indigenous population of the Eastern Caucasus have been identified, the combination of which should be included in the characteristics of its autosomal gene pool: 1) Dargins, Laks; 2) Avars, Lezghins, Tabasarans, Aghuls, Rutul people, Tsakhur people; 3) Kumyks, Tat people and Azerbaijanis living in Dagestan; 4) Azerbaijanis and Talysh living in Azerbaijan. The directions of further research have been defined.

Keywords: gene geography, gene pool, population genetics, autosomal SNP markers, Eastern Caucasus, population

Funding: the study was supported by the RSF grant № 21-74-00156 (bioinformatics analysis of gene pools of the Eastern Caucasus and Transcaucasia), State Assignment of the Ministry of Science and Higher Education of the Russian Federation for the Research Centre of Medical Genetics (cartographic analysis, data interpretation), Biobank of North Eurasia (expedition survey).

Acknowledgements: the authors would like to thank all members of the expedition survey (sample donors) and the autonomous non-profit organization "Biobank of North Eurasia" for access to DNA collections and the genotyping results.

Author contribution: Balanovska EV — management, design, manuscript writing and expedition survey of the Dagestani peoples; Gorin IO, Petrushenko VS — bioinformatics analysis; Ponomarev GYu — work with DNA collections, cartographic analysis; Belov RO — work with DNA collections, manuscript formatting; Pocheshkhova EA — expedition survey of the Dagestani peoples; Salaev VA — organization and conducting the expedition survey of the Talysh living in Azerbaijan; Iskandarov NA — organization and conducting the expedition survey of the Azerbaijanis living in Azerbaijan; Pylev VYu — organization of genotyping, statistical analysis.

Compliance with ethical standards: the study was approved by the Ethics Committee of the Bochkov Research Centre of Medical Genetics (protocol № 1 of 29 June 2020).

✉ **Correspondence should be addressed:** Vladimir Yu. Pylev
Moskvorechye, 1, 115522, Moscow, Russia; freetrust@yandex.ru

Received: 26.04.2023 **Accepted:** 13.05.2023 **Published online:** 29.05.2023

DOI: 10.24075/brsmu.2023.017

РОЛЬ КАВКАЗСКОГО, ИРАНСКОГО И СТЕПНОГО НАСЕЛЕНИЯ В ФОРМИРОВАНИИ МНОГООБРАЗИЯ АУТОСОМНОГО ГЕНОФОНДА ВОСТОЧНОГО КАВКАЗА

Е. В. Балановская^{1,2}, И. О. Горин¹, В. С. Петрушенко¹, Г. Ю. Пономарёв¹, Р. О. Белов¹, Э. А. Почешхова^{1,3}, В. А. Салаев¹, Н. А. Искандаров¹, В. Ю. Пылёв^{1,2} ✉

¹ Медико-генетический научный центр, Москва, Россия

² Биобанк Северной Евразии, Москва, Россия

³ Кубанский государственный медицинский университет, Краснодар, Россия

На Восточном Кавказе проживают более 30 народов, говорящих на кавказских, иранских и тюркских языках. Слияние многих миграционных потоков и сложная популяционная структура Восточного Кавказа затрудняют анализ его генофонда: из всех регионов Кавказа он наименее изучен. Цель работы — выявить основные закономерности в изменчивости аутосомных генофондов этого региона. По обширным панелям SNP-маркеров изучено 356 геномов 29 этносов: 243 генома 22 народов Восточного Кавказа и 113 геномов 7 народов окружающих регионов. Биоинформатический анализ проведен методами предковых компонент ADMIXTURE и главных компонент изменчивости генофонда (PCA). Выдвинута гипотеза трех основных пластов генофонда Восточного Кавказа, взаимодействие которых формирует его структуру. «Дагестанский» пласт несет информацию о генофонде древнего автохтонного населения Северного Кавказа. «Иранский» пласт отражает наследие древних и средневековых волн миграций ираноязычного населения: он составляет три четверти генофонда современного Азербайджана и около трети генофонда народов Дагестана. «Степной» пласт фиксирует слабое влияние евразийской степи. Взаимодействие трех генетических пластов лишь косвенно связано с языковой принадлежностью народов, но у кавказоязычных народов связь с лингвистикой проявляется ярче. Выявлены четыре генетически своеобразные группы коренного населения Восточного Кавказа, комплекс которых должен включаться в характеристику его аутосомного генофонда: 1) даргинцы, лакцы; 2) аварцы, лезгины, табасараны, агулы, рутульцы, цахуры; 3) кумыки, таты и азербайджанцы Дагестана; 4) азербайджанцы и талыши Азербайджана. Определены направления дальнейших исследований.

Ключевые слова: геногеография, генофонд, популяционная генетика, аутосомные SNP-маркеры, Восточный Кавказ, народонаселение

Финансирование: исследование выполнено при поддержке гранта РНФ №21-74-00156 (биоинформационный анализ генофондов Восточного Кавказа и Закавказья), Государственного задания Министерства науки и высшего образования РФ для Медико-генетического научного центра им. академика Н. П. Бочкова (картографический анализ, интерпретация результатов), Биобанка Северной Евразии (экспедиционное исследование).

Благодарности: авторы благодарят всех участников экспедиционного обследования (доноров образцов), АНО «Биобанк Северной Евразии» — за предоставление коллекций ДНК и результатов генотипирования.

Вклад авторов: Е. В. Балановская — руководство, дизайн и написание статьи, организация и проведение экспедиционного обследования народов Дагестана; И. О. Горин, В. С. Петрушенко — биоинформатический анализ; Г. Ю. Пономарев — работа с ДНК-коллекциями, картографический анализ; Р. О. Белов — работа с ДНК-коллекциями, оформление статьи; Э. А. Почешхова — проведение экспедиционного обследования народов Дагестана; В. А. Салаев — организация и проведение обследования талышей Азербайджана; Н. А. Искандаров — организация и проведение обследования азербайджанцев Азербайджана; В. Ю. Пылёв — организация генотипирования, статистический анализ.

Соблюдение этических стандартов: исследование одобрено этическим комитетом Медико-генетического научного центра имени Н. П. Бочкова (протокол № 1 от 29 июня 2020 г.).

✉ **Для корреспонденции:** Владимир Юрьевич Пылёв
ул. Москворечье, д. 1, 115522, г. Москва, Россия; freetrust@yandex.ru

Статья получена: 26.04.2023 **Статья принята к печати:** 13.05.2023 **Опубликована онлайн:** 29.05.2023

DOI: 10.24075/vrgmu.2023.017

The gene pool of the Caucasian peoples has long attracted the attention of population genetic scientists. This region, small in area, that is located between Europe and Asia, is home to more than 60 peoples speaking languages of three linguistic families: Caucasian, Indo-European, and Altaic. Among all regions of the Caucasus, the Eastern Caucasus, where the largest number of peoples (more than 30) representing three language families is concentrated, is the most poorly studied region in terms of genetics. Since the Western Caspian Sea region served as a bridge between Europe and Asia over millennia, it is necessary to involve data on both steppes in the north of the region and populations of the Iranian plateau to understand the gene pool of the Eastern Caucasus. Bizarre structure of peoples of the Eastern Caucasus together with fusion of multiple migration flows make it extremely difficult to analyze its gene pool. While there are some papers on genetics of the populations of Dagestan, the population of Azerbaijan represents one of the largest blank spots in the genetic map. And it's the key to understanding the centuries-old influence of Persia on the gene pools of the Eastern Caucasus: did this influence extend throughout the Caspian Sea region or was it concentrated only on the southern border gene pools? The genetic history of a number of small peoples living in the North Caucasus can also be reconstructed only by the systematic genetic study of the Eastern Caucasus in the context of knowledge about the peoples of Iran.

The complex structure of the multi-ethnic region, the Eastern Caucasus, requires thorough analysis. That is why our study is focused on its autosomal gene pool only. In parallel, we will publish a paper on the Y-chromosome variation in the same populations of the Eastern Caucasus. Such "binocular vision" will make it possible to get the most impartial and fair picture of the gene pool variation in the Eastern Caucasus.

There are very little published data on the populations of Dagestan and Azerbaijan obtained using the genome-wide panels that are among the most popular and effective systems of DNA markers over the last 10 years. In almost all of these papers, the data on the Eastern Caucasus were not analyzed separately, these were just an integral part of research focused on much larger region, the entire Caucasus or Eurasia.

The populations of Dagestan were assessed using the Illumina panel (~600,000 SNPs) in the study [1] of gene pool of the Caucasus as a whole, and using the Human Origin panel (~600,000 SNPs) [2].

The gene pool of Azerbaijanis living in the Northwestern Iran is discussed in the paper on the traces of Turkic expansion [3], in which they showed a 5% contribution of the East Eurasian ancestral component that could be explained by the spread of Turkic languages westwards in accordance with the "elite dominance" model (language change without significant gene pool changes). Assessment of Azerbaijanis living in Azerbaijan in comparison with other gene pools using the Human Origin genome-wide panel is provided only in paper [2].

The majority of papers discuss a broad spectrum of issues: formation of the Caucasian gene pool based on the contribution of migration in the Middle East [1], legacy of the Turkic-speaking groups' migration [3] or the eco-geographical zoning of North Eurasia [2]. However, none of the papers is focused on assessing the features of gene pool of the Eastern Caucasus. Certain small samples of peoples of the Eastern Caucasus are represented in other two large studies focused on the completely different issues [4, 5]. Unfortunately, some of the above samples were assessed using only the HumanOrigin panel (Affimetrix) that was hardly comparable with the Illumina panels.

Among studies conducted in recent years, the whole genome and whole exome studies of the gene pools of Iran and Turkey should be noted. The authors of one of the papers [6] study genomic variation in peoples of Iran. Since the study is focused on compiling the database on genomic variation in Iran, there is much emphasis on the genetic structure of Iran itself, while adjacent regions (specifically Azerbaijan) are not addressed in depth. A similar situation in the paper [7], where the genetic structure of the populations of Turkey is assessed, however, the impact of the Eastern Caucasus is described only in a short comment about its admixture with certain populations of Turkey.

In general, the published data contain genotypes of only 43 samples obtained from peoples of the Eastern Caucasus. These samples were assessed using mainly small Illumina panels, while in our study we assessed 243 samples using a large Illumina panel.

Thus, the world literature on genome-wide panels provides no conclusions about the gene pool of the Eastern Caucasus and reports just a few data that are restricted to specific groups. In contrast, our paper discusses populations of 22 peoples living in the Eastern Caucasus.

In the paper of our team focused on the search for traces of Alans in the autosomal gene pools of the North Caucasus [8] the main attention is paid to the ethnic groups of the Central and Western Caucasus. The gene pool of peoples living in the Eastern Caucasus is represented by four Dagestani peoples. The results obtained highlight the need for the detailed review of this data on the gene pool of the Eastern Caucasus, as well as for the targeted analysis of autosomal gene pools of all peoples living in this region and identification of the main patterns underlying variation, which is the aim of our study.

METHODS

In this paper the whole population of Dagestan (17 ethnic groups), Azerbaijan (Azerbaijanis, Azerbaijanis-Karapapakhs, Talysh) together with the other Iranian-speaking Kurds and Yazidis studied in the Caucasus (including migrants from various populations of the Caucasus and Iran; in our study they are considered as representatives of the Iranian-speaking population of the Eastern Caucasus, which is part of their ethnic range) are referred to as "peoples of the Eastern Caucasus". These 22 ethnic groups of the Eastern Caucasus are represented (Table 1) by original data on 243 genomes obtained by our team. These are assessed in the context of original data on the neighbouring peoples living in the Central Caucasus (Chechens), Transcaucasia (Georgians), Caspian Sea region (Astrakhan Nogais), Transcaspiya (Karakalpaks, Turkmens), as well as the literature data on the peoples of Iran, using the same panel of SNP markers [3, 9].

The overall sample size was 356 genomes of 29 ethnic groups: original data (318 genomes of 27 ethnic groups) were assessed using the Illumina4M and Illumina750K panels; the literature data (38 genomes of 2 ethnic groups) were assessed using the Illumina750K and HumanOrigin panels. PLINK 1.9 [10] was used for filtering by quality of the genome reads; kinship of individuals (below the 3rd degree according to KING 2.3.0 [11]); DNA markers' linkage and monomorphism.

The principal component analysis (PCA) of genomic variation was performed using the smartpca utility of the EIGENSTRAT software package [12]. Conversion from the plink format (bed-bim-fam) to the eigensoft format (eigenstratgeno-

Table 1. Linguistic affiliation and number of the studied genomes

LINGUISTIC CLASSIFICATION				Peoples	N of genomes	
Family	Branch	Sub-branch	Group			
Caucasian	Nakho-Dagestanian	Lezgin-Dargin-Lak	Dargin	Kubachins	6	
				Dargins	8	
				Kaitags	8	
			Lak	Laks	11	
			Lezgin	Tabasarans	11	
				Aghuls	1	
				Rutul people	9	
				Tsakhur people	8	
			Avar-Ando-Cesian	Lezgins	Lezgins	43
					Avar	Avars
		Andian			Tindi people	6
		Nakh	Cesian (Didoi)	Didoi people	5	
				Hinukh people	5	
		Kartvelian	South-Kartvelian	Chechens	15	
Altai	Turkic	Polovtsian-Kipchak	Caucasian	Georgians	19	
		Oguz	Essentially Oguz	Kumyks	27	
				Azerbaijanis: Dagestan,	9	
				Azerbaijan,	13	
				Iran*	18	
				Karapapakhs	6	
		Kipchak	Kipchak-Nogai	Turkmens	19	
				Karanogai people	11	
				Astrakhan Nogais	5	
		Indo-European	Aryan	New Iranian	South-Western	Karakalpaks
Tat people living in Dagestan	13					
North-Western	Iranian-speaking peoples of Iran**			Iranian-speaking peoples of Iran**	20	
				Talysh	10	
				Yazidis	10	
				Kurds	16	

Note: literature data on peoples of Iran [3, 9].

snp-ind) was carried out with the convertf tool of the same software package (using the default settings). Calculation was performed for five principal components with five iterations of outlier removal, the results were visualized in Python 3 using the pandas [13], matplotlib [14], and seaborn [15] libraries. The centroid for each population was defined (and designated by a larger dot) for each population on the principal component plot. It was determined as an average of all calculated components for all samples included in the population.

Analysis of the ancestral components by the ADMIXTURE method was performed using ADMIXTURE v1.3.0 [16], the number of the modelled ancestral components (K) varied between 2 and 20. Cross-validation is performed for each K-value in order to estimate error. The ADMIXTURE results were visualized in Python 3 using the *pandas*, *matplotlib*, and *seaborn* libraries.

RESULTS

Preliminary assessment of contributions of the ADMIXTURE ancestral components to the gene pools of four Dagestan peoples

In the earlier published report [8] the autosomal gene pool of the Eastern Caucasus was represented by genomes of the Dagestan peoples: Caucasian-speaking (Dargins, Laks, Tabasarans) and Iranian-speaking (Tat people). In the ADMIXTURE model of ancestral components (ACs) with $K = 11$ the contribution of the Dagestanian AC to these genomes was 77%. But the question remains, how valid is such pooling? Genomes of which large peoples of the Eastern Caucasus can represent it correctly in the study of the large regions of Eurasia?

Changes in the contribution of the "Dagestanian" component with increasing number of ACs (Fig. 1) reveals the differences

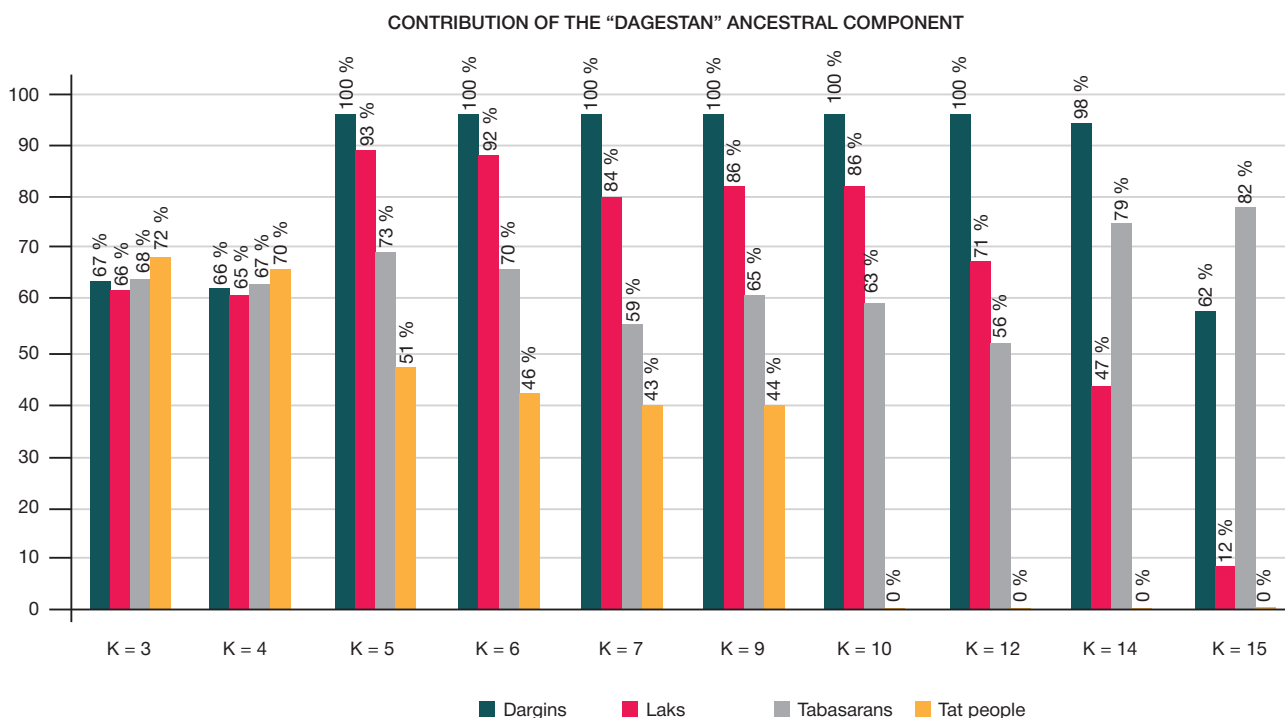


Fig. 1. Dynamic changes in the contribution of the "Dagestan" ADMIXTURE ancestral component to the genomes of Dargins, Laks, Tabasarans, and Tat people in the models with K-values between 3 and 15

between ethnic groups even with a small number of ACs ($K = 5$). When $K = 10$, the Tat people of Dagestan form their own AC, separating from the Caucasian-speaking peoples. Furthermore (Fig. 1), Dargins are the major contributors to the gene pool of Dagestan: the contribution of the "Dagestani" AC to their genomes within the interval of $4 < K < 15$ is 98–100%, it drops to 62% only when $K = 15$. Laks demonstrate different dynamics: when the K-value increases from 5 to 15, the contribution of the "Dagestani" AC to their genomes drops from 93 to 29%, as the Laks' AC shows itself. Tabasarans demonstrate a specific pattern: when the K-value increases from 5 to 12, the contribution of the "Dagestani" AC to their genomes drops from 73 to 56% and then increases to 82% when $K = 15$.

The comparison has revealed an unexpected phenomenon: the Dagestani AC represents the gene pools of different ethnic groups of Dagestan with different number of ACs ($3 < K < 15$). Their contributions are equal only when the number of ACs is low ($K = 3$ and $K = 4$), however, when $K > 4$ the contributions of the Tat people and Laks gradually diminish, and the contributions of Dargins and Tabasarans change. Such results show that it is necessary to generate the genetic portraits of autosomal gene pools for each people of the Eastern Caucasus and then form clusters of ethnic groups to be used as the basis for analysis of autosomal gene pools of the Caucasus and other large regions of Eurasia.

Position of 22 peoples of the Eastern Caucasus in the principal component space

To answer the above questions correctly, it is important to extend the study to the broadest possible spectrum of peoples living in the Eastern Caucasus and to use basic independent methods for population genetics analysis.

Fig. 2 shows positions of 22 peoples of the Eastern Caucasus and six reference groups within the space of the gene pool variation principal components (PC) 1 and 2. Six clusters of genomes are clearly distinguished showing that similarity

of peoples living in the Eastern Caucasus loosely matches classification of their languages. Almost all clusters include peoples speaking not only different branches of languages, but the languages of different linguistic families (Table 2). The first PC clearly divides all peoples into steppe peoples and all other peoples. In contrast, the second PC demonstrates a long chain containing all other genomes, from Kubachins to Kurds (Fig. 2).

The **Dargin-Lak-Ando-Cesian cluster** includes representatives of five ethnic groups of four groups speaking different sub-branches of the Nakho-Dagestani languages (Table 2): Dargins, Kaitags, Kubachins, Laks, Tindi people, Didoi people, Hinukh people. It should be noted that the genomes of isolated populations differ sharply from the whole set by other PCs: the Didoi people and Hinukh people differ by PC 3, the ethnic group of Kubachins living in one mountain village differs by PC 4, and the Tindi people differ by PC 5.

The **Lezgin-Avar cluster** includes representatives of six ethnic groups speaking both sub-branches of the Nakho-Dagestani languages (Table 2). In the Avar group only Avars have been included in the cluster. Despite the fact that their centroid is located among the genomes of Lezgin peoples, individual genomes of Avars are extremely diverse (Fig. 2; red dots): these stretch along the entire Lezgin-Avar cluster and extend to the Ando-Cesian one beyond its boundaries. As for Lezgin peoples, no differences between genomes of the East-Lezghin (Lezghins, Tabasarans, Aghuls) and the Rutul-Tsakhur (Rutul people, Tsakhur people) subgroups are observed. Furthermore, the genomes of Lezghins (purple dots in Fig. 2) extend to the other cluster that includes the Tat people and Azerbaijanis living in Dagestan.

The **Turkic-Iranian cluster of Dagestan** brings together the genomes of the Iranian-speaking Tat people and the Turkic-speaking Kumyks and Azerbaijanis living in Dagestan (Table 2). Similarity of genomes of the Tat people and Azerbaijanis of Dagestan is no surprise, since there was a tradition in Dagestan to register the Tat people as Azerbaijanis, and the boundary was drawn based on their compact settlement in Dagestan. The genomes of all three ethnic groups are extremely diverse and

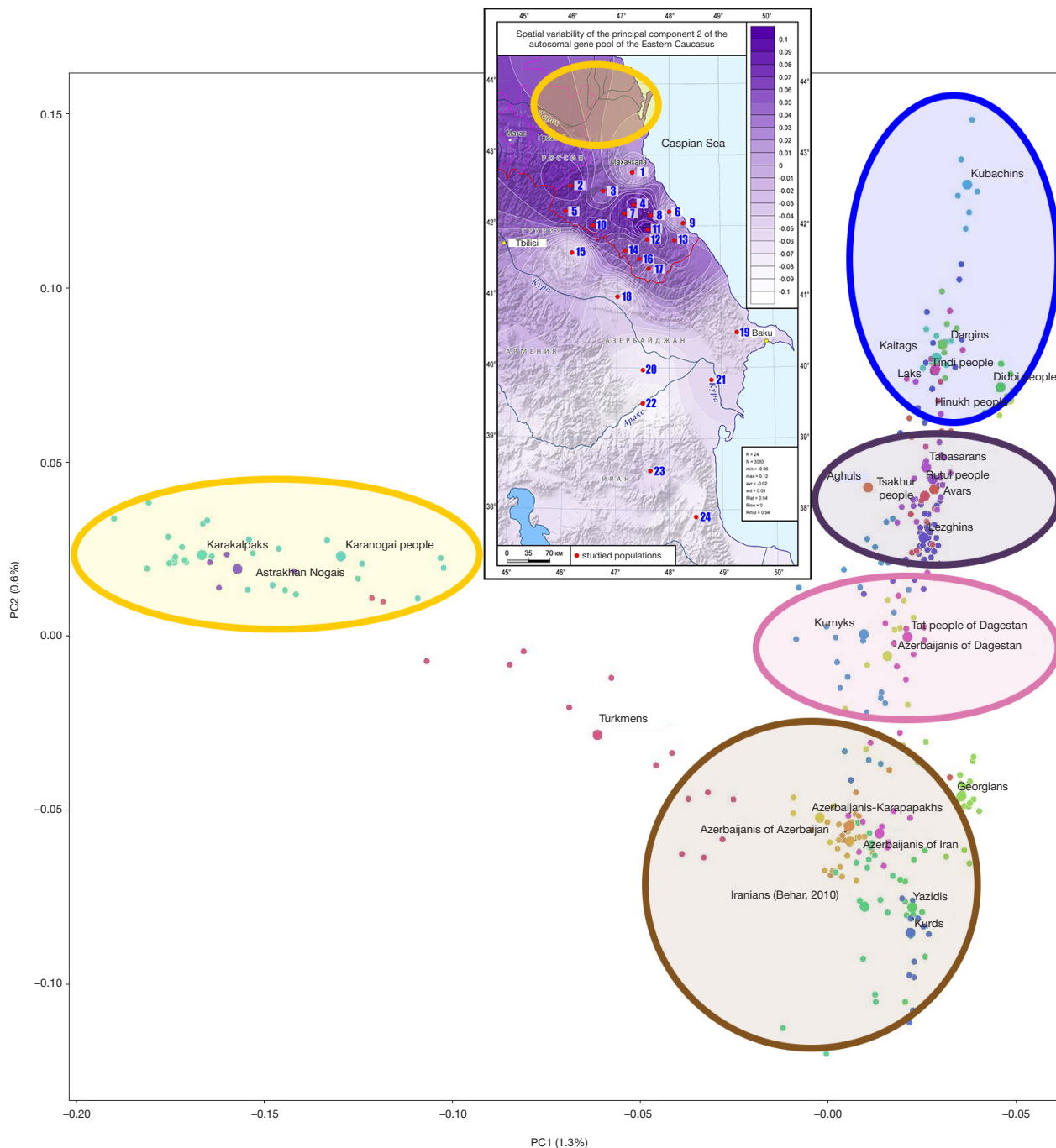


Fig. 2. Plot of principal components 1–2 (PCA) of the genome variability in peoples of the Eastern Caucasus in the context of neighboring populations. The map of the principal component 2 is provided in the inset. 1 — Kumyks; 2 — Tindi people; 3 — Avars; 4 — Dargins; 5 — Hinukh people; 6 — Azerbaijanis living in Dagestan; 7 — Laks; 8 — Kaitags; 9 — Tat people living in Dagestan; 10 — Didoi people; 11 — Kubachins; 12 — Aghuls; 13 — Tabasarans; 14 — Tsakhur people; 15 — Georgians; 16 — Rutul people; 17 — Lezghins; 18 — Azerbaijanis-Karapapakhs; 19 — Azerbaijanis living in Azerbaijan; 20 — Yazidis; 21 — Talysh; 22 — Kurds; 23 — Azerbaijanis living in Iran [3]; 24 — Iranian-speaking Iranians [9]

gravitate towards the Azerbaijan-Iranian cluster. However, Kumyks, that are also included in the Lezgin-Avar cluster, demonstrate the excess diversity of genomes (Fig 2; blue dots).

The **Azerbaijan-Iranian cluster of Dagestan** brings together the genomes of the Turkic-speaking (Azerbaijanis living in Azerbaijan and Iran) and Iranian-speaking (Talysh, Kurds, Yazidis and the aggregate group of Iran) peoples too. Based on PC 1, only one group of Azerbaijanis (Karapapakhs) shows a slight shift towards peoples of the Eurasian steppe. However, the genomes of Turkmen (Fig 2; pink dots) have become a bridge between the Azerbaijan-Iranian and steppe clusters. The other pole of the Azerbaijan-Iranian cluster is fixed by the Georgian

genomes that move closer to peoples of the North Caucasus in other PC variants.

The **steppe cluster** brings together the Karanogai people living in Dagestan and other steppe peoples of the Caspian steppe (Astrakhan Nogais) and Transcaspians (Karakalpaks). The sharp difference shown by the steppe cluster genomes generates the differences by PC 1 reflecting the greatest variability of the assessed genomes.

Spatial variability of principal components

On the map of PC 2 (Fig. 2; inset) we have placed a yellow oval within the range of the Karanogai people in the northern

Table 2. Clusters in the genetic space of principal components 1–2 (PCA) and ethno-linguistic affiliation of genomes in each cluster

Cluster	LINGUISTIC CLASSIFICATION				Peoples				
	Family	Branch	Sub-branch	Group					
Dargin-Lak-Ando-Cesian	Caucasian	Nakho-Dagestanian	Lezgin-Dargin-Lak	Dargin	Kubachins, Dargins, Kaitags				
				Lak	Laks				
				Andian	Tindi people				
			Avar-Ando-Cesian	Cesian (Didoi)	Didoi people Hinukh people				
				Lezgin-Avar	Caucasian	Nakho-Dagestanian	Lezgin-Dargin-Lak	Lezgin	Tabasarans
									Aghuls
Rutul people									
Tsakhur people									
Lezgins									
Avars									
Turkic-Iranian of Dagestan	Altai	Turkic	Polovtsian-Kipchak	Caucasian	Kumyks				
			Oguz	Essentially Oguz	Azerbaijanis living in Dagestan				
	Indo-European	Aryan	New Persian	South-Western	Tat people living in Dagestan				
Azerbaijan-Iranian	Altai	Turkic	Oguz	Essentially Oguz	Azerbaijanis living in Azerbaijan, Iran Karapapakhs				
					Indo-European	Aryan	New Iranian	North-Western	Talysh Yazidis
									South-Western
	Steppe Turkic	Altai	Turkic	Kipchak				Kipchak-Nogai	
					Separate	Altai	Turkic		Oguz
	Separate	Caucasian	Kartvelian	South-Kartvelian					

Dagestan suggesting the influence of the Eurasian steppe based on PC 1. The map makes it possible to see interaction of three genetic strata within the range of the Eastern Caucasus. The influence of Iran covering the entire Azerbaijan and wading into Dagestan along the edge of the Caspian Sea extends from the south. Dagestan retains genetic specificity of the autochthonous population of the Eastern Caucasus eastern outskirts. The most recent influence of the Eurasian steppe extends from the north. And these three genetic strata are loosely related to three linguistic divisions: Iranian-speaking, Caucasian-speaking, and Turkic-speaking peoples. An independent bioinformatics method was further applied to test the “three strata” hypothesis.

Contribution of the ADMIXTURE ancestral components to the gene pools of peoples living in the Eastern Caucasus

After considering positions of the Eastern Caucasus genomes in the variation principal component space, let's move to analysis by more informative method, i.e. to the ADMIXTURE ancestral component modeling. Recall that each model was calculated based on the same set of genomes as was used in the previous analysis (only Chechens were added, who became outliers in the PC analysis). The models differed only in the number of ancestral components (K) set for each model.

Among all models with K-values between 2–20 three models (K = 3, K = 10, K = 20) allowing one to trace the changes with increasing number of hypothetical ancestral populations were selected for thorough investigation (Fig. 3).

Model of three ancestral components

The contribution of each of three ancestral components (AC) to each genome is highlighted in specific color. The resulting ADMIXTURE image can serve as confirmation of the hypothesis of three genetic strata in the gene pool of the Eastern Caucasus: the orange color that is typical for the Karanogai people represents the hypothetical steppe genetic stratum; the green color that is pronounced in Kurds and Iranian-speaking Iranians represents the Iranian stratum; the yellow color that predominates in genomes of the peoples of Dagestan represents the contribution of the Caucasian-speaking population of the region. If we accept this interpretation of the color scheme, we will be able to estimate the contribution of each of three genetic strata to the genomes of peoples of the Eastern Caucasus and test the hypothesis of three strata in its gene pool. For that let's merge the genomes in accordance with the clusters (Table 2) and represent the AC contributions as a bar graph (Fig. 4; for quantitative data see fig. A in Appendix).

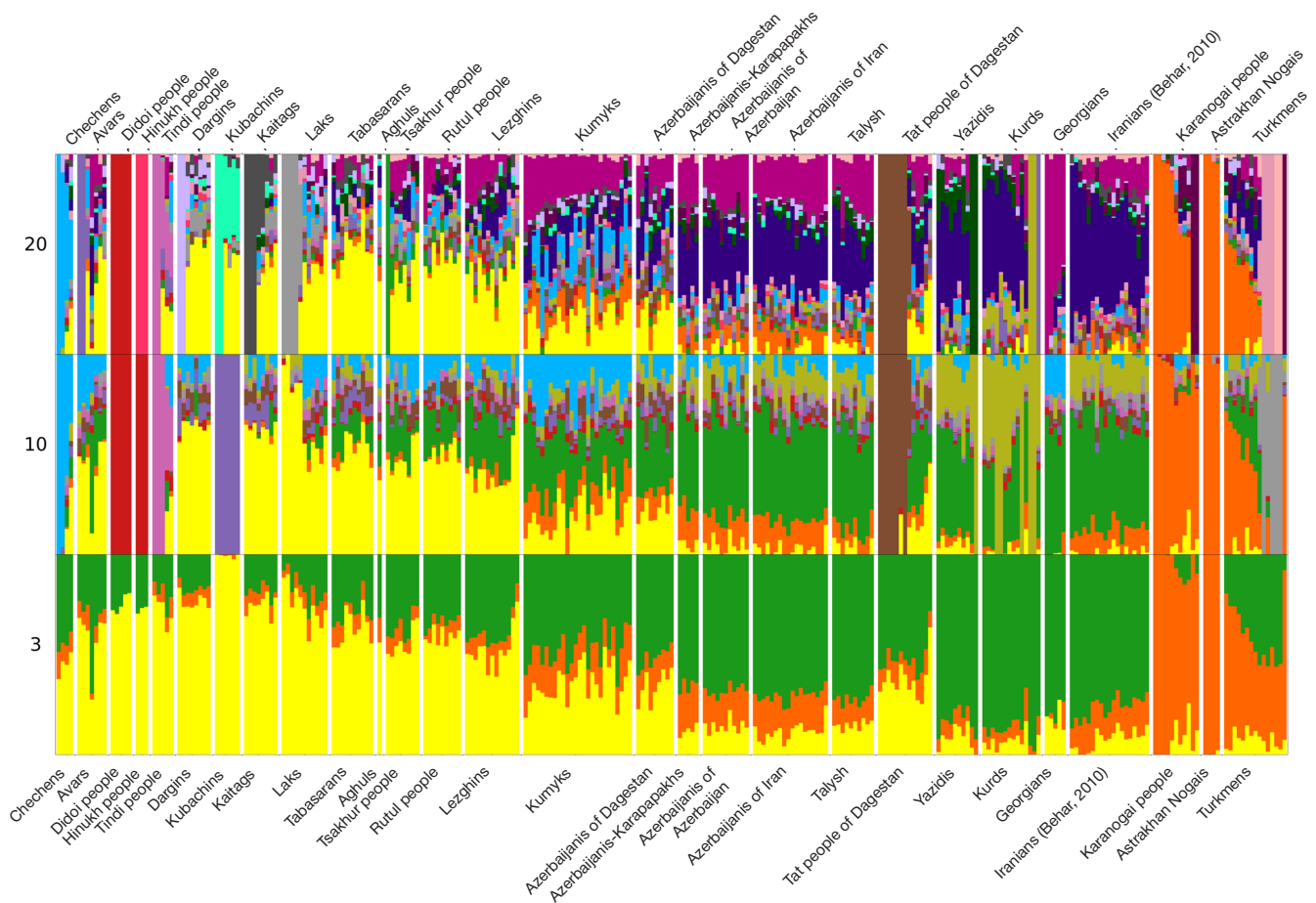


Fig. 3. Contributions of the ADMIXTURE ancestral components (%) to the genomes of peoples of the Eastern Caucasus, $K = 3$, $K = 10$, $K = 20$

The AC genomic profiles show very close agreement with the PC clusters based on the correlation of “three strata”. The “Caucasian” contribution to the genomes of the Dargin-Lak cluster is 75%; the contribution to the Lezgin-Avar cluster is slightly more than a half of the gene pool; the contribution to the Turkic-Iranian cluster is about one third, and the contribution to the Azerbaijan-Iranian cluster is about 10%. As the “Caucasian” stratum descends, the Iranian stratum dramatically increases: 17%, 35%, 50%, 75%. The “Steppe” stratum turns out to be potent in the steppe cluster only (91%): it constitutes only 7–8% in the Caucasian-speaking peoples and 14–19% in the Turkic-speaking ones.

Model of 10 ancestral components

When modeling 10 ancestral components for the same set of genomes, preservation of three original ACs (“Steppe”, “Iran”, “Caucasian”) is observed. However the correlation of strata changes due to the emergence of new ACs. Specific new components that make little contribution to the genomes of other peoples (Fig. 3) are merged into one AC, referred to as “Other” (Fig. 4). These include ACs of small ethnic groups (Kubachins, Didoi people, Hinukh people, Tindi people) that usually reflect the closely related genomes within ethnic groups, and specific AC variants found in some Tat people and Turkmens.

Such merging into models with $K = 10$ (Fig. 4; also see fig. B in Appendix) results in the emergence of only two new components reflecting the impact of peoples living in other regions of the Caucasus: the first one predominates among Georgians, and the second one prevails among Chechens. The “Caucasian” stratum is the major contributor to the “Nakhi” AC, while the “Iranian”

stratum is the main contributor to the “Transcaucasia” AC. Since the contribution of the “Transcaucasia” AC to the genomes of the Iranian-speaking population of Iran (54%) is almost equal to its contribution to the genomes of Georgians (58%), it can be assumed that the “Transcaucasia” AC represents an ancient Southwest Asian stratum in the gene pools of the Caucasus and Transcaucasia.

Model of 20 ancestral components

When modeling 20 ancestral components for the same set of genomes, we see four new ACs that have diverged from the “Caucasian” AC in addition to two original ACs found when $K = 3$ (“Steppe”, “Iran”). These new ACs reflect the genetic diversity of peoples of the Dargin and Lezgin groups, as well as of Avars and Laks (Fig. 4; also see fig. C in Appendix). Among them the “Lezgin” AC is the major contributor to the genomes of other peoples: it defines one third of gene pools of the Dargin-Lak and Avar cluster, a half of the Lezgin gene pool, and one fifth of the Kumyk gene pool.

It is extremely important that a common genetic stratum that is highlighted in yellow in Fig. 3 and 4 is preserved in the genomes of all peoples of Dagestan, along with the diverged inherent ACs. Previously we called this stratum “Caucasian”. However, other ACs predominate in the genomes of other Caucasian peoples, that is why we have every right to propose a more accurate name for this genetic stratum: “Dagestan” AC.

DISCUSSION

Two independent methods for bioinformatics analysis of genomic variation in peoples of the Eastern Caucasus make it possible to reveal similar patterns and complement each other.

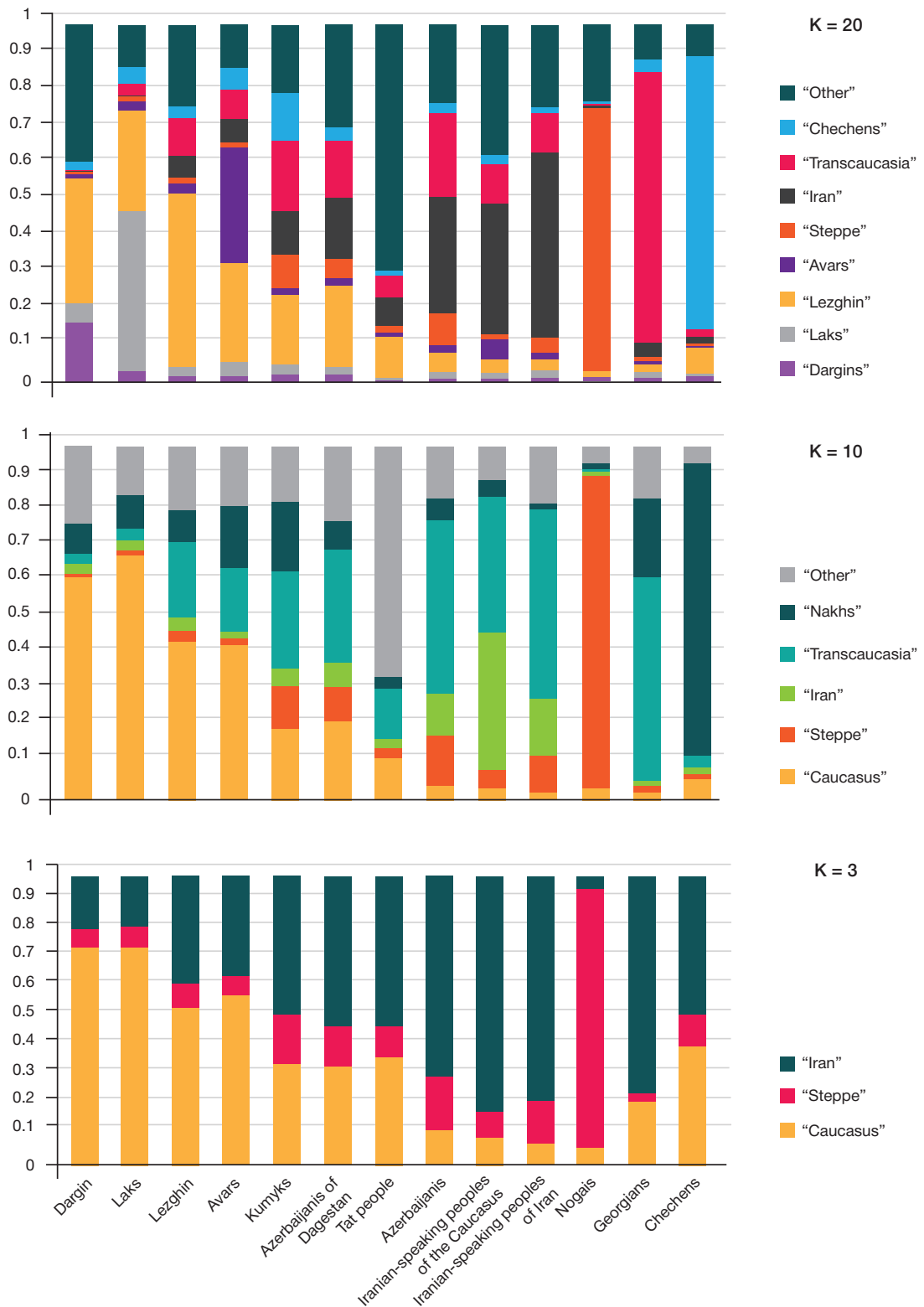


Fig. 4. Relative contributions of the ADMIXTURE ancestral components (%) to the genomes of peoples of the Eastern Caucasus, K = 3, K = 10, K = 20

Three genetic strata

Both methods identify three genetic strata: the first one is associated with multiple surges in the Iranian population, the second one with the recent influence of the Eurasian steppe, and the third one with the ancient population formed within the range of modern Dagestan. The strength of these genetic strata among different groups of population of the Eastern Caucasus varies.

In the Eastern Caucasus, the "Steppe" genetic stratum constitutes almost the entire gene pool only in the Karanogai people, and in the other genomes of the region the share varies between 7% in peoples of Dagestan and 19% in Azerbaijan. However, the findings show that this "Steppe" stratum forms the basis of the gene pools of many peoples living in the Caspian Sea region (Astrakhan Nogais, Karakalpak, Turkmens), representing a strong genetic component in the vast area.

The “Iranian” genetic stratum of the Eastern Caucasus plays an important role, since it permeates all gene pools of Azerbaijan and “fades” as it travels through Dagestan from its south border (Lezgin peoples) and the Caspian Sea region (Kumyks, Tat people) to the center and north.

The “Dagestan” genetic stratum forms the basis of all Dagestan peoples. Despite the fact that original ancestral component is found in almost all the assessed Dagestan peoples when the K-values are high, all ethnic groups of Dagestan are united by the common ancient genetic stratum. This is an important conclusion of the study.

All three genetic strata are well placed within the Eastern Caucasus geographical space. The “Steppe” stratum is only limited by the small area of the Eurasian steppe in the north of the region. In contrast, the south “Iranian” stratum that flows from the Iranian plateau as a powerful stream constitutes three quarters of the gene pool of modern Azerbaijan and one third of the gene pools of peoples of Dagestan on average. The “Dagestan” genetic stratum is geographically located between other strata, it constitutes more than a half of the gene pool of Caucasian-speaking peoples (52–100%). The Caspian Sea region is a crossroads and a meeting place of all three strata: the “Iranian” stratum constitutes a half of the gene pool of Kumyks, Azerbaijanis living in Azerbaijan, and the Tat people, the “Dagestan” stratum makes up one third, and the “Steppe” stratum make up about 15%.

Genetics and linguistics

In contrast to geography, the correlation between genetics and linguistics is very weak. This is mainly due to the fact that peoples of the Eastern Caucasus (Kumyks and Azerbaijanis) started speaking Turkic languages, but their gene pool still remained mostly “pre-Turkic”. However, we clearly see that the neighboring peoples also have an impact on the genomes of peoples that have retained their languages. Thus, the share of the “Dagestan” genetic stratum in the Tat people of Dagestan reaches 38%, while in other Iranian-speaking peoples of the Eastern Caucasus (Kurds, Yazidis, and Talysh) it reaches only 9%. The “Dagestan” stratum strength in the Caucasian-speaking peoples of Dagestan is two-thirds of the gene pool (66%) on average, it varies depending on the contacts with other peoples. And these are not the only ones showing a broken relationship between genetics and linguistics. For example, original “Georgian” ancestral component is found in Georgians only when $K = 19$, and all models with $K < 19$ show that three quarters of their gene pool come from the “Iranian” stratum.

References

1. Yunusbayev B, Metspalu M, Järve M, Kutuev I, Rootsi S, Metspalu E, et al. The Caucasus as an asymmetric semipermeable barrier to ancient human migrations. *Molecular biology and evolution*. 2012; 29 (1): 359–65.
2. Jeong C, Balanovsky O, Lukianova E, Kahbatkyzy N, Flegontov P, Zaporozhchenko V, et al. The genetic history of admixture across inner Eurasia. *Nature ecology & evolution*. 2019; 3(6): 966–76.
3. Yunusbayev B, Metspalu M, Metspalu E, Valeev A, Litvinov S, Valiev R, et al. The genetic legacy of the expansion of Turkic-speaking nomads across Eurasia. *PLoS Genetics*. 2015; 11 (4): e1005068.
4. Behar DM, Metspalu M, Baran Y, Kopelman NM, Yunusbayev B, Gladstein A, et al. No evidence from genome-wide data of a Khazar origin for the Ashkenazi Jews. *Human biology*. 2013; 85 (6): 859–900.
5. Lazaridis I, Patterson N, Mittnik A, Renaud G, Mallick S, Kirsanov K, et al. Ancient human genomes suggest three ancestral populations for present-day Europeans. *Nature*. 2014; 513 (7518): 409–13.
6. Fattahi Z, Beheshtian M, Mohseni M, Poustchi H, Sellars E, Nezhadi SH, et al. Iranome: A catalog of genomic variations in the Iranian population. *Human mutation*. 2019; 40 (11): 1968–84.
7. Kars ME, Başak AN, Onat OE, Bilguvar K, Choi J, Itan Y, et al. The genetic structure of the Turkish population reveals high levels of variation and admixture. *Proceedings of the National Academy of Sciences*. 2021; 118 (36): e2026076118.
8. Balanovska EV, Agdzhoyan AT, Gorin IO, Petrushenko VS, Pylev VY, Kulemin NA, i dr. V poiskax alanskogo sleda: geneticheskaya istoriya Severnogo Kavkaza po polnogenomnym dannym ob

Selection of “model” gene pools

One of the objectives of the study was to search for such groups of ethnicities that could credibly represent the Eastern Caucasus in the Eurasian space. Two independent methods suggest the need to include four such groups: 1) Dargins, Laks; 2) Avars, Lezghins, Tabasarans, Aghuls, Rutul people, Tsakhur people; 3) Kumyks, Tat people and Azerbaijanis living in Dagestan; 4) Azerbaijanis and Talysh living in Azerbaijan. The combination of those provides a correct representation of the Eastern Caucasus diversity. Since in this case the “steppe” contribution of the Karanogai genomes is small, it is more appropriate to consider genomes of the Karanogai people in the context of gene pool of the Eurasian steppe or its Caspian part.

Planning further research

The study covers the main range of genomes of the Eastern Caucasus and generally reflects the polyphony of its genomes, however, it should be considered only as a general contour of its diversity architectonics. The findings suggest that there is a need to perform a specific thorough assessment of autosomal gene pools of each of four groups of the indigenous population: Dagestan, Azerbaijan, Iranian-speaking population, steppe populations of six countries of the Caspian Sea region and the Ciscaucasia.

CONCLUSIONS

The hypothesis of three genetic strata, the interaction of which forms “unity in diversity” of gene pool of the Eastern Caucasus, is put forward. The “Iranian” stratum is formed by multiple surges of Iranian population within the range of the Eastern Caucasus; the “Steppe” stratum is related to the recent negligible influence of the Eurasian steppe; the “Dagestan” stratum represents the gene pool of ancient population of the Eastern Caucasus. Modeling of a large number of ancestral components reveals the original ancestral component in the majority of Dagestan peoples, however, all ethnic groups of Dagestan are united by a strong common ancient genetic stratum. The interaction of these three genetic strata results from geographic features of the region and is only indirectly related to linguistics. Four groups of indigenous population of the Eastern Caucasus have been identified, the combination of which should be included in the characteristics of its autosomal gene pool.

- autosomnom genofonde. Vestnik Moskovskogo universiteta. Seriya 23. Antropologiya. 2022 (3): 4–62. Russian.
9. Behar DM, Yunusbayev B, Metspalu M, Metspalu E, Rosset S, Parik J, et al. The genome-wide structure of the Jewish people. *Nature*. 2010; 466 (7303): 238–42.
 10. Chang CC, Chow CC, Tellier LC, Vattikuti S, Purcell SM, Lee JJ. Second-generation PLINK: rising to the challenge of larger and richer datasets. *Gigascience*. 2015; 4: 1–16.
 11. Manichaikul A, Mychaleckyj JC, Rich SS, Daly K, Sale M, Chen WM. Robust relationship inference in genome-wide association studies. *Bioinformatics*. 2010; 26 (22): 2867–73.
 12. Price AL, Patterson NJ, Plenge RM, Weinblatt ME, Shadick NA, Reich D. Principal components analysis corrects for stratification in genome-wide association studies. *Nature genetics*. 2006; 38 (8): 904–9.
 13. McKinney W. Data structures for statistical computing in python. In: *Proceedings of the 9th Python in Science Conference*. 2010; 28–445 (1): 51–56.
 14. Hunter JD. Matplotlib: A 2D graphics environment. *Computing in science & engineering*. 2007; 9 (03): 90–5.
 15. Waskom M, Botvinnik O, O'Kane D, Hobson P, Lukauskas S, Gemperline DC, et al. *Mwaskom/Seaborn: V0. 8.1*. Zenodo. 2017.
 16. Alexander DH, Novembre J, Lange K. Fast model-based estimation of ancestry in unrelated individuals. *Genome research*. 2009; 19 (9): 1655–64.

Литература

1. Yunusbayev B, Metspalu M, Järve M, Kutuev I, Rootsi S, Metspalu E, et al. The Caucasus as an asymmetric semipermeable barrier to ancient human migrations. *Molecular biology and evolution*. 2012; 29 (1): 359–65.
2. Jeong C, Balanovsky O, Lukianova E, Kahbatkyzy N, Flegontov P, Zaporozhchenko V, et al. The genetic history of admixture across inner Eurasia. *Nature ecology & evolution*. 2019; 3(6): 966–76.
3. Yunusbayev B, Metspalu M, Metspalu E, Valeev A, Litvinov S, Valiev R, et al. The genetic legacy of the expansion of Turkic-speaking nomads across Eurasia. *PLoS Genetics*. 2015; 11 (4): e1005068.
4. Behar DM, Metspalu M, Baran Y, Kopelman NM, Yunusbayev B, Gladstein A, et al. No evidence from genome-wide data of a Khazar origin for the Ashkenazi Jews. *Human biology*. 2013; 85 (6): 859–900.
5. Lazaridis I, Patterson N, Mittnik A, Renaud G, Mallick S, Kirsanow K, et al. Ancient human genomes suggest three ancestral populations for present-day Europeans. *Nature*. 2014; 513 (7518): 409–13.
6. Fattahi Z, Beheshtian M, Mohseni M, Poustchi H, Sellars E, Nezhadi SH, et al. Iranome: A catalog of genomic variations in the Iranian population. *Human mutation*. 2019; 40 (11): 1968–84.
7. Kars ME, Başak AN, Onat OE, Bilguvar K, Choi J, Itan Y, et al. The genetic structure of the Turkish population reveals high levels of variation and admixture. *Proceedings of the National Academy of Sciences*. 2021; 118 (36): e2026076118.
8. Балановская Е. В., Агджоян А. Т., Горин И. О., Петрушенко В. С., Пылёв В. Ю., Кулемин Н. А., и др. В поисках аланского следа: генетическая история Северного Кавказа по полногеномным данным об аутосомном генофонде. *Вестник Московского университета. Серия 23. Антропология*. 2022 (3): 48–62.
9. Behar DM, Yunusbayev B, Metspalu M, Metspalu E, Rosset S, Parik J, et al. The genome-wide structure of the Jewish people. *Nature*. 2010; 466 (7303): 238–42.
10. Chang CC, Chow CC, Tellier LC, Vattikuti S, Purcell SM, Lee JJ. Second-generation PLINK: rising to the challenge of larger and richer datasets. *Gigascience*. 2015; 4: 1–16.
11. Manichaikul A, Mychaleckyj JC, Rich SS, Daly K, Sale M, Chen WM. Robust relationship inference in genome-wide association studies. *Bioinformatics*. 2010; 26 (22): 2867–73.
12. Price AL, Patterson NJ, Plenge RM, Weinblatt ME, Shadick NA, Reich D. Principal components analysis corrects for stratification in genome-wide association studies. *Nature genetics*. 2006; 38 (8): 904–9.
13. McKinney W. Data structures for statistical computing in python. In: *Proceedings of the 9th Python in Science Conference*. 2010; 28–445 (1): 51–56.
14. Hunter JD. Matplotlib: A 2D graphics environment. *Computing in science & engineering*. 2007; 9 (03): 90–5.
15. Waskom M, Botvinnik O, O'Kane D, Hobson P, Lukauskas S, Gemperline DC, et al. *Mwaskom/Seaborn: V0. 8.1*. Zenodo. 2017.
16. Alexander DH, Novembre J, Lange K. Fast model-based estimation of ancestry in unrelated individuals. *Genome research*. 2009; 19 (9): 1655–64.

IMMUNOGENICITY OF FULL-LENGTH AND MULTI-EPIOTOPE MRNA VACCINES FOR *M. TUBERCULOSIS* AS DEMONSTRATED BY THE INTENSITY OF T-CELL RESPONSE: A COMPARATIVE STUDY IN MICE

Vasileva OO¹, Tereschenko VP¹, Krapivin BN¹, Muslimov AR^{1,2}, Kukushkin IS¹, Pateev II¹, Rybtsov SA¹, Ivanov RA¹, Reshetnikov VV^{1,3}✉

¹ Translational Medicine Research Center, Sirius University of Science and Technology (Autonomous Non-Commercial Higher Education Organization), Sirius, Russia

² Pavlov First Saint Petersburg State Medical University, St. Petersburg, Russia

³ Institute of Cytology and Genetics, Siberian Branch of the Russian Academy of Sciences, Novosibirsk, Russia

Development of the new tuberculosis vaccines that would be effective in adults is an urgent task: worldwide, the annual death toll of this disease exceeds 1.5 million. In the recent decades, the matter has been addressed in numerous studies, but none has yielded an effective vaccine so far. There are many factors to resistance against tuberculosis; this study focuses on the T-cell response, a mechanism that enables elimination of intracellular pathogens, such as *M. tuberculosis*. We aimed to develop an mRNA vaccine capable of triggering a pronounced T-cell response to the *M. tuberculosis* antigens. The *in silico* analysis allowed us to select epitopes of the *M. tuberculosis* secreted protein ESAT6 (Rv3875) and design a multi-epitope mRNA vaccine thereon. We assessed the intensity of T-cell response in mice immunized with mRNA vaccines that encode a full-length or multi-epitope antigen. The results of this study in mice show that immunization with a multi-epitope mRNA vaccine produces twice as many IFN γ -secreting splenocytes in response to specific stimulation than immunization with an mRNA vaccine encoding the full-length protein. Thus, the developed multi-epitope mRNA vaccine can be an effective *M. tuberculosis* prevention agent the mode of action of which involves formation of a pronounced T-cell response.

Keywords: mRNA vaccine, multi-epitope vaccine, T-cell response, ELISpot

Funding: the study was supported by the Ministry of Science and Higher Education of the Russian Federation (agreement № 075-10-2021-113, unique project identifier RF----193021X0001).

Acknowledgements: the authors express their gratitude to the staff of the Sirius University: Terenin IM for *in vitro* transcription, Zaborova OV for the formulation of mRNA into lipid nanoparticles, Gavriyak MA and Golovin EV for purification and characterization of the Rv3875 protein; Shevrev DV for setting up the intracellular staining experiment and Sitikova VA for assistance in the context of the animal experiment.

Author contribution: Vasileva OO, Tereschenko VP — work with the cells, data analysis, article authoring, figures authoring; Krapivin BN, Pateev II, Rybtsov SA — work with the cells, animal experiment, data analysis; Muslimov AR, Kukushkin IS — design of structures, cloning; Ivanov RA, Reshetnikov VV — text editing, data analysis, project coordination.

Compliance with the ethical standards: animal study was approved by the Ethics Committee of the Institute of Cytology and Genetics (2022); carried out in accordance with the laboratory animals care guidelines (2010), Directive 2010/63/EU of the European parliament and of the Council on the protection of animals used for scientific purposes (2010), Good Laboratory Practice guidelines (2016).

✉ **Correspondence should be addressed:** Vasily V. Reshetnikov
Olympiyskiy prospekt, 1, Sochi, 354340, Russia; reshetnikov.vv@talantiuspeh.ru

Received: 24.04.2023 **Accepted:** 15.06.2023 **Published online:** 29.06.2023

DOI: 10.24075/brsmu.2023.021

СРАВНИТЕЛЬНОЕ ИССЛЕДОВАНИЕ ИММУНОГЕННОСТИ ПОЛНОРАЗМЕРНОЙ И МУЛЬТИЭПИТОПНОЙ МРНК-ВАКЦИН ПРОТИВ *M. TUBERCULOSIS* ПО ВЫРАЖЕННОСТИ Т-КЛЕТОЧНОГО ОТВЕТА У МЫШЕЙ

О. О. Васильева¹, В. П. Терещенко¹, Б. Н. Крапивин¹, А. Р. Муслимов^{1,2}, И. С. Кукушкин¹, И. И. Патеев¹, С. А. Рыбцов¹, Р. А. Иванов¹, В. В. Решетников^{1,3}✉

¹ Научный центр трансляционной медицины, Автономная некоммерческая образовательная организация высшего образования «Научно-технологический университет «Сириус», Сириус, Россия

² Первый Санкт-Петербургский государственный медицинский университет имени И. П. Павлова, Санкт-Петербург, Россия

³ Институт цитологии и генетики СО РАН, Новосибирск, Россия

Разработка новых вакцин против туберкулеза, эффективных в том числе и у взрослых, является актуальной задачей, поскольку ежегодная смертность от этого заболевания во всем мире превышает 1,5 млн случаев. Несмотря на множество исследований в последние десятилетия, эффективной вакцины все еще не получено. Сопrotивляемость туберкулезу состоит из многих факторов, в этом исследовании сделан акцент на Т-клеточном ответе — механизме, позволяющем элиминировать внутриклеточные патогены, такие как *M. tuberculosis*. Целью исследования было разработать мРНК-вакцину, способную формировать выраженный Т-клеточный ответ на антигены *M. tuberculosis*. С помощью анализа *in silico* были выбраны эпitопы секреторного белка ESAT6 (Rv3875) *M. tuberculosis* для дизайна мультиэпитопной мРНК-вакцины. Проведена оценка эффективности Т-клеточного ответа у мышей, иммунизированных мРНК-вакцинами, которые кодируют полноразмерный или мультиэпитопный антиген. Результаты показали, что при иммунизации мультиэпитопной мРНК-вакциной количество IFN γ -секретирующих спленцитов в ответ на специфичную стимуляцию в два раза выше, в сравнении с количеством IFN γ -секретирующих клеток у мышей, иммунизированных мРНК-вакциной, кодирующей полноразмерный белок. Таким образом, разработанная мультиэпитопная мРНК-вакцина может стать эффективным препаратом для профилактики *M. tuberculosis* посредством формирования выраженного Т-клеточного ответа.

Ключевые слова: мРНК-вакцина, мультиэпитопная вакцина, Т-клеточный ответ, ELISpot

Финансирование: исследование выполнено при поддержке Министерства науки и высшего образования Российской Федерации (соглашение № 075-10-2021-113, уникальный идентификатор проекта РФ----193021X0001).

Благодарности: авторы выражают благодарность сотрудникам АНО ВО «Университет «Сириус»: И. М. Теренину за постановку транскрипции *in vitro*, О. В. Заборовой за формулировку мРНК в липидные наночастицы, М. А. Гавриляк и Е. В. Головину за очистку и характеристику белка Rv3875; Д. В. Шевыреву за постановку эксперимента по внутриклеточному окрашиванию и В. А. Ситиковой за помощь в проведении эксперимента с животными.

Вклад авторов: О. О. Васильева, В. П. Терещенко — клеточные работы, анализ данных, написание статьи, подготовка рисунков; Б. Н. Крапивин, И. И. Патеев, С. А. Рыбцов — клеточные работы, проведение эксперимента с животными, анализ данных; А. Р. Муслимов, И. С. Кукушкин — дизайн конструкций, клонирование; Р. А. Иванов, В. В. Решетников — редактирование текста, анализ данных, координация проекта.

Соблюдение этических стандартов: исследование на животных одобрено этическим комитетом ИЦиГ СО РАН (2022 г.); проведено в соответствии с руководством по уходу и использованию лабораторных животных (2010 г.), Directive 2010/63/EU of the European parliament and of the council on the protection of animals used for scientific purposes (2010 г.), «Правилами надлежащей лабораторной практики» (2016 г.).

✉ **Для корреспонденции:** Василий Владимирович Решетников
Олимпийский пр-кт, д. 1, г. Сочи, 354340, Россия; reshetnikov.vv@talantiuspeh.ru

Статья получена: 24.04.2023 **Статья принята к печати:** 15.06.2023 **Опубликована онлайн:** 29.06.2023

DOI: 10.24075/vrgmu.2023.021

Every year, more than 10 million new cases of tuberculosis and about 1.5 million deaths from the disease are registered worldwide. The COVID-19 pandemic has boosted the spread of tuberculosis: it develops against the backdrop of the viral infection, and the global incidence of tuberculosis in 2020 and 2021 has grown by 3–6% compared to previous years [1]. Despite this, in the pandemic years of 2020 and 2021, the incidence of tuberculosis in the Russian Federation decreased, but at the same time, its course became more complicated, with more first-time patients suffering from lung tissue destruction, massive bacterial excretion, and fibrous-cavernous variety of tuberculosis [2].

Currently, the only approved tuberculosis prevention vaccine is BCG. It has been used for more than 100 years; in addition to tuberculosis, BCG can help develop non-specific protection against other respiratory and viral diseases, training the immunity [3]. In the Russian Federation, children (provided there are no contraindications) receive 3 injections of BCG after birth. In addition to its protective effect, the vaccine can cause a number of post-vaccination complications, inflammatory reactions manifesting as infiltrates, abscesses, fistulas, and ulcers [4]. Another disadvantage of BCG is that it does not shield adults from pulmonary tuberculosis [5]: if the bacteria is multidrug-resistant or extensively drug-resistant, it is necessary to use expensive and toxic chemotherapy drugs [6]. The foregoing adds urgency to the task of finding new effective vaccines against tuberculosis for adolescents and adults, including for the purposes of prevention and to enable the immunity to combat multidrug-resistant tuberculosis.

The main purpose of vaccination is to prevent development of the disease. In the case of tuberculosis, T-cell response drives elimination of the pathogen, and the vaccine protects by triggering production of CD4⁺ memory cells. In turn, CD8⁺ cells control the spread of mycobacteria in chronic tuberculosis cases. Secretion of the pro-inflammatory IFN γ cytokine by T-cells is associated with the vaccine's protective effect [7].

Searching for the new drugs to fight and prevent tuberculosis, researchers most often consider subunit protein vaccines or viral vectors [8], but the new trend in the scientific community is to suggest mRNA-based vaccine designs. One of the studies has demonstrated the ability of a self-replicating mRNA vaccine to induce a specific response of CD4⁺ and CD8⁺ cells [9]. mRNA vaccines have a number of advantages over vaccines of other types. Compared to the vaccines based on protein antigens, they guarantee an order of magnitude higher antibody titer, and the cost of production and scaling mRNA vaccines is lower, since the process is cell-free. Compared to DNA vaccines, mRNA vaccines are less genotoxic, since they cannot merge with the genome [10], and more effective, since, unlike DNA vaccines, they act in the cell's cytosol and not in the nucleus, which means their performance is independent from the cell cycle stage during transfection [11].

A transition from attenuated vaccines to protein or nucleic acid vaccines raises the problem of selecting the epitope for immunization. The most common choice are subunit vaccines that contain a single protein sequence [12], but there are also vaccine variants with epitopes from one or more pathogen antigens that may induce a synergistic immune response [13]. Such vaccines are called multi-epitope. Humoral and T-cell responses are triggered by different epitopes. B-cell epitopes can be non-linear (repeating the native protein conformation) and linear, and T-cell epitopes are short peptides. Multi-epitope vaccines can induce both types of immune responses simultaneously. Bioinformatic tools are actively used to predict the epitopes for mRNA tuberculosis vaccines [14, 15]. Short peptides in the composition of a multi-epitope vaccine mitigates

the risk of allergic reactions peculiar to attenuated vaccines [16]. In addition, a multi-epitope vaccine can contain epitopes of antigens of various microorganisms, which translates into effective simultaneous immunization against several pathogens [13].

However, there are few experimental studies that compare the effectiveness of mRNA vaccines encoding full-length and multi-epitope variants of antigens. Therefore, this study in mice sought to assess the intensity of T-cell response following immunization with mRNA vaccines that encode the full-length or multi-epitope *M. tuberculosis* antigen.

METHODS

Experiment design

The experiment involved 15 male C57BL6/J mice, age 8–9 weeks, SPF status, weight 19–21 g. The animals were provided by the Center for Genetic Resources of Laboratory Animals of the Institute of Cytology and Genetics of the Siberian Branch of the Russian Academy of Sciences. They were kept in a conventional vivarium with a fixed 12 light/12 dark cycle; there were no restrictions imposed on the standard feed (granules) and water the mice received. The two different variants of mRNA vaccines — mRNA Rv3875 (582 nucleotides) or mRNA mEpitope (699 nucleotides), 50 μ g of RNA each, — were administered intramuscularly. In addition, mice were immunized with full-length Rv3875 protein (25 mg) adjuvanted with mRNA-free lipid nanoparticles in an amount equivalent to (\pm 10%) the number of particles in the RNA vaccine groups. Besides the test groups, there were two control groups in the experiment, first of which received lipid nanoparticles without mRNA, second — a phosphate buffer. Each group included three animals. Second immunization (same doses) took place 4 weeks after the first one. The mice were killed 4 weeks after second immunization and their spleen isolated (Fig. 1).

Selection of epitopes for the Rv3875 multi-epitope construct

The software that enabled prediction of the MHC I epitopes was the MHC Lurry 2.0 version 2.0.4 package [17], and for MHC II epitopes we used the NetMHCIIpan 4.1 package [18]. The "-length" values selected for the epitope calculations were 13, 14, 15, 16, 17, plus the -BA modifier to enable the epitope-allele affinity prediction mode. Quantitative characteristics of the allele frequencies were taken from the published data [19, 20]. Python 3.9 was used to filter the predictions output by MHCFlurry 2.0 and NetMHCIIpan 4.1. The criteria were that each epitope-allele pair should interact with an affinity of no more than 500 nM, and each epitope should bind to at least 5 different alleles. The algorithm allowed selecting two epitopes for MHC I (LLDEGKQSL and AAWGGSGSEAY) and three epitopes for MHC II (WNFAGIEAAASAIQG, KQSLTKLAAAWGGSG and LNNALQNLARTISEA). The final construct contained five epitopes (1 copy of each epitope) connected by linkers (KK for MHCII and AAY for MHC I). In addition, we added to the construct a sequence of the cytoplasmic and transmembrane domain of MHC class I (IVGIVAGLAVLAWVIGAWATVMCRRKSSGGKGGGYSQAASSDSAQGSVDVSLTA), which enables colocalization of the target protein with histocompatibility complexes in various endocytic compartments [21].

Cloning

Seeking to produce the constructs for subsequent *in vitro* transcription of RNA, we extended the pSmart vector (Lucigen;

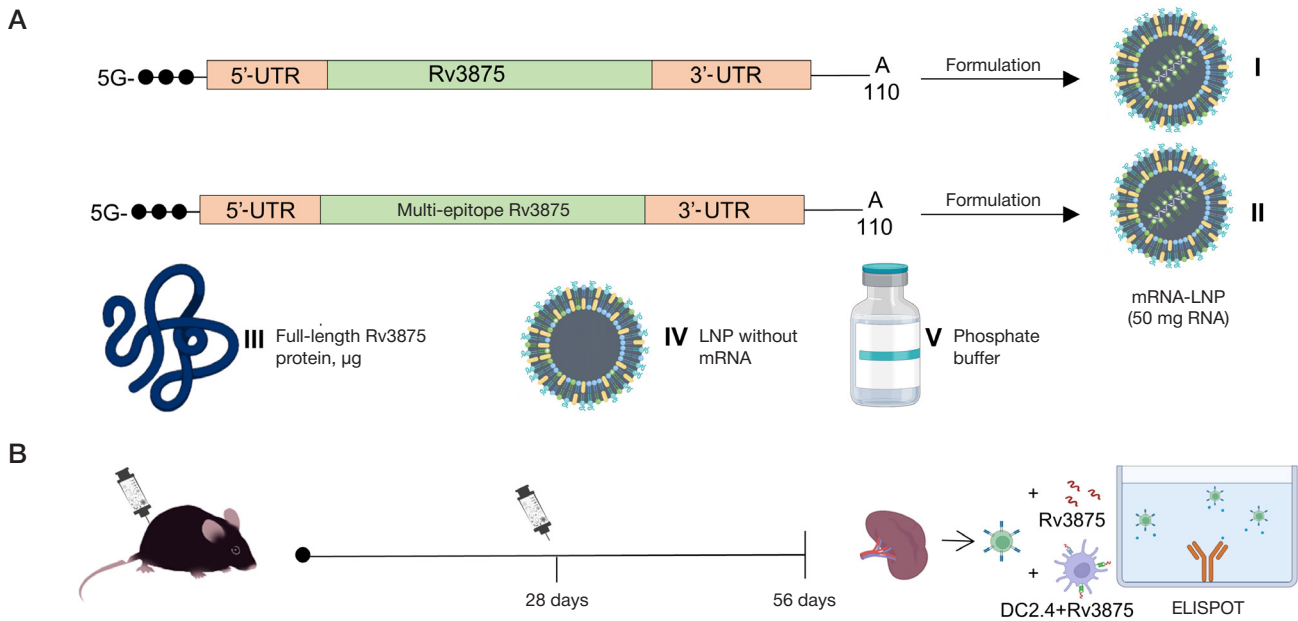


Fig. 1. Experiment design. **A.** Schematic representation of composition of the mRNA-LNP vaccine and other drugs. **B.** Design of the experiment in C57BL6/J mice. The two different variants of mRNA vaccines — mRNA Rv3875 (582 nucleotides) or mRNA mEpitope (699 nucleotides), 50 µg of RNA each, — were administered intramuscularly. In addition, mice were immunized with full-length Rv3875 protein (25 mg) adjuvanted with mRNA-free lipid nanoparticles in an amount equivalent to ($\pm 10\%$) the number of particles in the RNA vaccine groups. Besides the test groups, there were two control groups in the experiment, first of which received lipid nanoparticles without mRNA, second — a phosphate buffer. Each group included three animals. Second immunization (same doses) took place 4 weeks after the first one. The mice were killed 4 weeks after second immunization and their spleen isolated. We used the ELISpot assay to count splenocytes secreting IFN γ in response to the Rv3875 tuberculosis protein post vaccination, and thus measured the level of the resulting T-cell response

USA) with a cassette with 5'UTR (gggaataagagagaaaagaag agtaagaagaaatataagaccccgcgccgccacc) sequence, Rv3875 protein sequence (full-length or multi-epitope), and 3'UTR sequence (gctggagcctcggtggcctagcttcttccccttgggctcccc ccagcccctcctcccctcctgcaccgcgtaccccggtcttgaataaagtctga gtggcgcca). Next, we applied the EcoRI and BglII restriction enzymes to the resulting cassette, purified it on the agarose gel and ligated with a similarly prepared pSmart commercial vector (Lucigen; USA). Chemically competent NEB-stable cells (New England Biolabs; UK) were transformed with a ligation mixture and plated on LB agar with 100 µg/mL of ampicillin. To check the colonies for the insert, we used PCR. The plasmids were verified by Sanger sequencing, and to analyze the sequencing chromatograms, we used the Ugene v38.1 software. *E. coli* NEB-stable with the vector were cultivated at 30°C and 180 rpm. QIAGEN Plasmid Maxi Kit (Qiagen; USA) was used to isolate and purify the plasmid DNA. To obtain a linearized plasmid, we applied SpeI to the preparation at the unique restriction site located after the poly(A) tail.

A pET30 vector (Agilent; United States) was used to build the construct and produce the full length Rv3875 protein. The Rv3875 sequence with an additional sequence for six histidines at the N-terminus was assembled from the oligonucleotides with the help of PCR. We applied the EcoRI and NdeI restriction enzymes to the resulting cassette, purified it on the agarose gel and ligated with a similarly prepared pET30 vector (Lucigen; USA). For transformation, we used the BL21DE3 cells (Agilent; USA). The plasmids were verified by Sanger sequencing.

In vitro mRNA transcription

The *in vitro* transcription was done as described previously [22]. We used 5 µg of linearized plasmid, buffer (20 mM DTT, 2 mM spermidine, 80 mM HEPES-KOH pH 7.4, 24 mM MgCl₂), 500 units of T7 RNA polymerase (Biolabmix; Russia), 200 units of ribonuclease inhibitor RiboCare (Evrogen; Russia) and 1 µl of a mixture of enzymes from the RiboMAX Large Scale RNA

Production System (Promega; USA) as a source of inorganic pyrophosphatase. The reaction mixture also contained 12 mM of the ARCA cap analogue (Biolabmix; Russia) and 3 mM of each of the ribonucleoside triphosphates (Biosan, Russia). The reaction was supported for 2 hours at 37 °C; after that, we added another 3 mM of each of the ribonucleoside triphosphates and incubated for another 2 hours. For DNA hydrolysis, we used the RQ1 nuclease (Promega; USA); the RNA was precipitated by adding LiCl to the concentration of 0.32 M and EDTA pH 8.0 to the concentration of 20 mM, after which the solution was put on ice for 1 hour of incubation. Next, the solution was centrifuged for 15 min (25,000 g at 4 °C). The RNA precipitate was washed with 70% ethanol, dissolved in ultrapure water and then precipitated again with alcohol as per the standard procedure. Spectrophotometry enabled identification of the RNA concentration; we measured absorption at 260 nm. The target length and homogeneity of the synthesized RNA molecules were assessed with the help of capillary electrophoresis done in a TapeStation (Agilent; USA).

Formulation of mRNA into LNP

To formulate mRNA into lipid nanoparticles (LNP), we mixed an aqueous solution (10 mM citrate buffer, pH 3.0) of 0.2 mg/mL mRNA with alcoholic solution of a lipid mixture in a microfluidic cartridge using The NanoAssemblr™ Benchtop (Precision Nanosystems; USA). The components of the lipid mixture were ionizable lipidoid ALC-0315 (BroadPharm; USA), distearoylphosphatidylcholine (DSPC) (Avanti Polar Lipids; USA), cholesterol (Sigma-Aldrich; USA), DMG-PEG-2000 (BroadPharm; USA); the molar ratio (%) was 46.3 : 9.4 : 42.7 : 1.6. The mass fraction of mRNA in LNP was 0.04% wt. To form particles, we mixed aqueous and alcoholic phases 3 : 1 by volume, the overall mixing rate was 10 mL/min.

Next, the particles were filtered (in sterile conditions) through a 0.22 µm PES membrane filter (Merck; USA) and

stored at 4 °C. After filtration, we analyzed the quality of the resulting particles by two parameters, particle size (measured with Zetasizer Nano ZSP, Malvern Panalytical; USA) and mRNA loading. Concentration of the mRNA loaded onto lipid nanoparticles was established by the difference in fluorescent signal levels upon staining with the RiboGreen reagent (Thermo Fischer Scientific; USA) before and after their destruction. To destroy the particles, we used the Triton X-100 detergent (Sigma-Aldrich; USA).

Rv3875 protein production and purification

To produce protein, we incubated *E. coli* BL21DE3 with the vector at 37 °C and 180 rpm until OD(600) equaled 0.65, then added IPTG to the final concentration of 1 mM, and cultured for 6 h at 30 °C. The cells were resuspended in buffer containing 50 mM Tris-HCl pH 8.0 and 300 mM of sodium chloride. Next, we induced lysis of the cells with ultrasound, 15-second pulses every 15 seconds. The amplitude of ultrasonic vibrations was 50% of the maximum. After lysis, the samples were centrifuged for 15 minutes (20,000 g at 4 °C). The pH of the resulting supernatant was adjusted to equal 7.5 by addition of a 1 M Tris-OH solution. Then, we filtered the sample through a polyethersulfone membrane with 0.22 µm pores.

For the first stage of purification of the Rv3875 protein we used a metal chelate affinity sorbent with an average particle size of 30 µm: cell lysate was applied to the sorbent with immobilized chelating ligand (nitrilotriacetic acid) and eluted in an imidazole gradient. Next, the purified protein fractions were dialyzed against a buffer containing 25 mM Tris-HCl. The dialyzed sample was applied onto a potent cation-exchange sorbent (average particle size 45 µm) with immobilized functional sulfo groups (-SO₃⁻). To verify the mass of the Rv3875, we used both the classical polyacrylamide gel electrophoresis method and a maxis 4G ETD mass spectrometer (Bruker; USA).

Assessment of the post vaccination T-cell response level

We used the ELISpot assay to count splenocytes secreting IFN γ in response to the Rv3875 tuberculosis protein post vaccination, and thus measured the level of the resulting T-cell response.

Splenocytes were obtained by rubbing spleens of the experimental and control group animals through a 70 µm filter. Once available, 300,000 splenocytes were seeded onto the ELISpot PVDF membrane plates and simultaneously stimulated with Rv3875 protein (50 µg/mL) and DC2.4 dendritic cells, 30000 cells per well. We did two technical repetitions for each experimental well. With the seeded splenocytes and added stimulants, the total volume of each well was 200 µl of RPMI-1640 nutrient medium (PanEco; Russia) with 10% FCS. Next, we left the splenocytes to culture for 18 hours in a CO₂ incubator (5% CO₂, 37 °C).

After culturing, we identified the IFN γ -secreting splenocytes with the help of a Mouse IFN γ ELISpot Set (BD; USA) and an AEC Substrate Set (BD; USA) as per the manufacturer's instructions. To count the dots of splenocytes secreting IFN γ , we used S6 Ultra (CTL; USA).

Cytometry of the IFN γ -producing cells

Cytometry of the IFN γ -producing cells started with seeding splenocytes of the vaccinated mice onto 200 µl of RPMI-1640 medium in a 96-well culture plate, 300,000 splenocytes per well; there, they were stimulated with the Rv3875 protein (50 µg/mL)

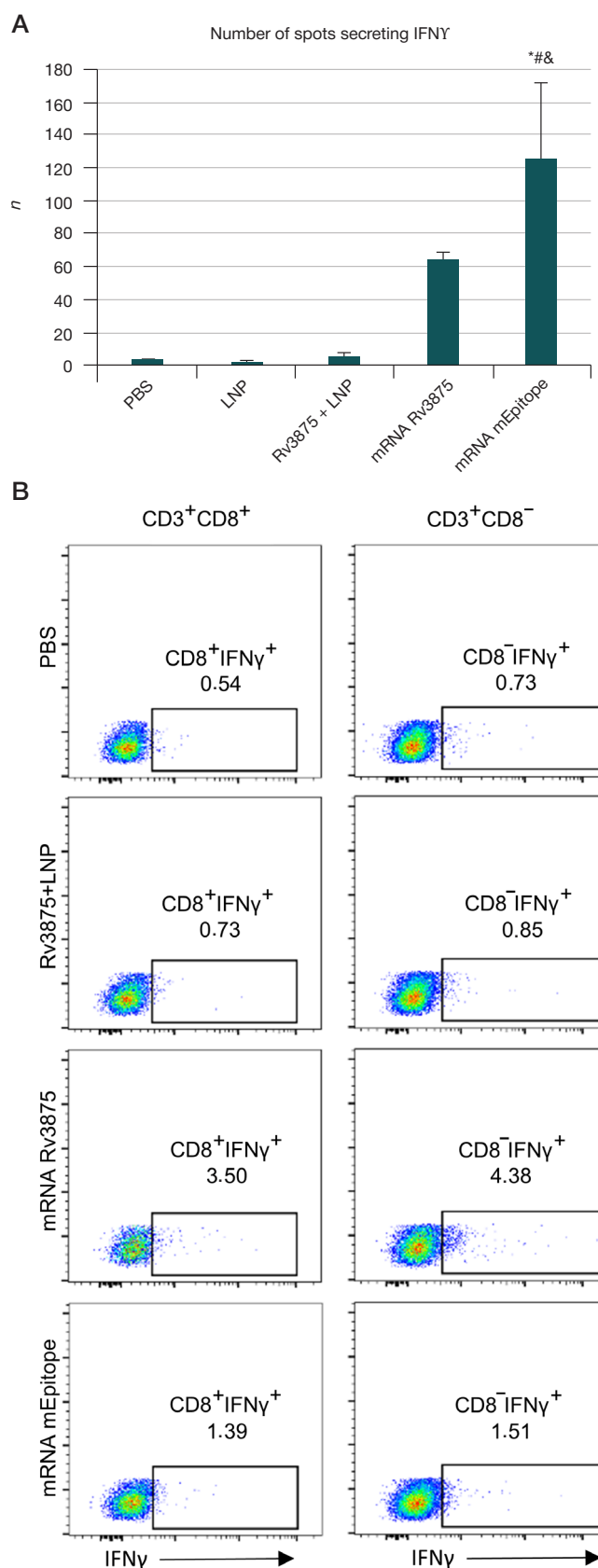


Fig. 2. Evaluation of the T-cell response of splenocytes of the immunized mice. **A.** ELISpot results. Number of cells secreting IFN γ in response to DC2.4 stimulation, activated by the Rv3875 protein. The data are presented as mean \pm error of mean. Three animals per group. * — $p < 0.05$ compared with the PBS group; # — $p < 0.05$ compared with the LNP group; & — $p < 0.05$ compared with the Rv3875 + LNP group. **B.** Representative data on CD3⁺ T lymphocytes (CD8⁺ and CD8⁻) producing IFN γ (intracellular staining). The figures show the percentage of cells from the total pool of CD3⁺ CD8⁺ and CD3⁺ CD8⁻ T-lymphocytes that produce IFN γ

or left unstimulated. Two hours after beginning of the stimulation we added 10 µg/mL of Brefeldin A (Abcam; USA) to the wells. Next, the cells were cultured overnight in a CO₂ incubator. At the end of the incubation, they were stained with anti-CD3 (PE Anti-Mouse CD3, Elabscience) and anti-CD8 antibodies (FITC Anti-Mouse CD8a, Elabscience), the concentration thereof as per the manufacturer's instructions, then immobilized and permeabilized with a commercially available kit (BD; USA) as prescribed by its maker. To analyze the resulting samples, we used the LSRFortessa Cell Analyzer, a flow cytometer (BD; USA). Supplement 1 contains the example of gating. The obtained data were processed with the help of the FlowJo software (Treestar Inc.; USA).

Statistical analysis

We applied the one-way ANOVA and Turkey's test as a post-hoc analysis in the context of statistical processing of the data. Differences between the experimental groups were considered statistically significant at $p < 0.05$. Statistica 6.0 software package (StatSoft; USA) enabled statistical analysis of the data.

RESULTS

ELISpot assay used to analyze the T-cell response through identification of the IFN γ -secreting cells has proven the vaccination to be effective [$F(10.4) = 6.02$; $p = 0.012$]. The number of IFN γ -secreting cells after stimulation with DC2.4+RV3875 was higher in the splenocytes of mice vaccinated with the multi-epitope variant of the mRNA vaccine (mRNA mEpitope) than in the control groups (PBS, LNP) and splenocytes of mice immunized with Rv3875 protein with nanoparticles but without RNA (Rv3875+LNP) (Fig. 2A). As for the mRNA vaccine encoding the full-length Rv3875 protein, the respective experimental group had the number of IFN γ -secreting cells higher than the control group (64 ± 2.7 vs 2.5 ± 1.0), but these changes were not significant. A fact of note is the insignificant growth of the IFN γ -secreting cells count in mice immunized with Rv3875 with LNPs not loaded with mRNA compared to the animals that received mRNA vaccines (Rv3875: 5.7 ± 1.8 ; mRNA Rv3875: 64 ± 2.7 ; mRNA mEpitope: 126.0 ± 46.2). Supplement 2 presents the data on splenocytes from individual animals.

For cytometry, we used splenocytes from one animal of each group. This approach rendered statistical data processing impossible; the respective results are given for the purpose of clarity only. According to our data, the share of CD3⁺CD8⁺ and CD3⁺CD8⁻ T-lymphocytes producing IFN γ is higher in splenocytes of mice immunized with mRNA vaccines (Fig. 2B). Thus, cytometry confirms that the secretion of IFN γ in splenocytes of mice vaccinated with mRNA Rv3875 and mRNA mEpitope grows, inter alia, because of the T-lymphocytes, which is a clear sign of development of the T-cell response to Mycobacterium tuberculosis antigens in the vaccinated mice.

DISCUSSION

Our study has shown that immunization with an mRNA vaccine encoding the *M. tuberculosis* Rv3875 (ESAT6) multi-epitope protein yields a more pronounced T-cell response than both immunization with an mRNA vaccine encoding the full-length variant of the protein and immunization with a recombinant protein vaccine. The possible reasons behind these results are both a more efficient presentation of epitopes by type I and II histocompatibility

complexes and the choice of the most immunogenic epitopes [11]. The enhanced presentation may be caused by the proteasome and lysosomal pathways of breaking of the protein molecule enabled by adding of the sequences of breaking linkers [23]. Another factor affecting immunogenicity is the leader sequence. In our case, we used the sequence of the cytoplasmic and transmembrane domain of MHC class I at the carboxyl end of the protein molecule. It has previously been shown that the leader sequence with the MHC class I transport signal ensures co-localization of the target protein and histocompatibility complexes in various endocytic compartments, which leads to efficient activation and expansion of antigen-specific CD8⁺ and CD4⁺ T-cells [21].

Another clear advantage of multi-epitope vaccines is the possibility to tune the T-cell response by selecting specific epitopes. In our study, we used the vaccine that encodes five Rv3875 epitopes, three presented by MHC class II and two by MHC class I, which guarantees specific activation of CD8⁺ and CD4⁺ T-cells. The epitopes were selected based on their affinity to human alleles rather than mouse alleles, and yet the multi-epitope mRNA vaccine showed high efficiency, probably due to high interspecies cross-reactivity. The T-cell response is one of the key components of the body's fight against *M. tuberculosis*. CD8⁺-T-lymphocytes can destroy infected phagocytic cells with the help of perforin, granzyme and granulysin proteins; they are also capable of inducing apoptosis through the FasL receptor, while the secreted granulysin can kill *M. tuberculosis* directly. The most important function of CD4⁺ cells in the fight against *M. tuberculosis* is the production of IFN γ , which activates macrophages and cytotoxic T-lymphocytes. In some people, insufficient induction of the CD8⁺ T-cells may render BCG not as effective as expected [24].

There are two experimental studies that demonstrated efficacy of the mRNA vaccines against tuberculosis, but their results are inconsistent [9, 25]. One of these studies has shown immunogenic properties of the developed anti-tuberculosis mRNA vaccine based on the full-length MPT83 antigen [25]. Immunization with that vaccine triggered production of specific antibodies. T-cells isolated from the spleens of mice secreted IFN γ in response to the antigen challenge, and CTLs were able to lyse antigen-transfected cells; this is consistent with our results. In a similar 2022 study, the researchers used the ID91 mRNA containing four full-length tuberculosis antigens fused with a synthetic TLR4 agonist; the mRNA in this study was self-replicating [9]. Compared to a protein vaccine, such mRNA vaccine showed the capacity to raise the antibody titer to the same level, but the associated T-cell response was less pronounced. Our study is the first one to use a multi-epitope mRNA vaccine against tuberculosis; we have shown that, compared to the full length mRNA vaccine, the effects of multi-epitope mRNA vaccine are more intense. Use of multi-epitope vaccines for prevention of tuberculosis may be more promising than using protein and full-length mRNA vaccines for the purpose.

CONCLUSIONS

Administered intramuscularly, multi-epitope mRNA vaccine induces a pronounced T-cell response in mice. Enhancement of the T-cell response may be key to the development of an effective *M. tuberculosis* prevention vaccine. Vaccines against new epitopes of tuberculosis could enhance the T-cell response and accelerate the involvement of adaptive immune cells in the immune response within the first two weeks of infection, ensuring a more effective elimination of the pathogen. Thus, mRNA-based multi-epitope vaccines may be a promising direction of development of an effective vaccine against *M. tuberculosis*.

References

- Dartois VA, Rubin EJ. Anti-tuberculosis treatment strategies and drug development: challenges and priorities. *Nat Rev Microbiol*. 2022; 20 (11): p. 685–701.
- Vasileva IA, Testov VV, Sterlikov SA. Ehpidemicheskaya situaciya po tuberkulezu v gody pandemii COVID-19–2020–2021 gg. Tuberkulez i bolezni legkix. 2022. 100 3: 6–12. Russian.
- Ahmed A, et al. A century of BCG: Impact on tuberculosis control and beyond. *Immunological reviews*. 2021; 301 (1): 98–121.
- Shalofast EI, Ershova Yul. Postvaccinal'nye oslozhneniya pri «BCZh» immunizacii. *Vestnik nauki*. 2022; 4, 11 (56): 341–55. Russian.
- Covian C., et al., BCG-Induced Cross-Protection and Development of Trained Immunity: Implication for Vaccine Design. *Front Immunol*. 2019; 10: 2806.
- Nikolenko NYu, Kudlaj DA, Doktorova NP. Farmakoehpideologiya i farmakoehpikomika tuberkuleza s mnozhestvennoj i shirokoj lekarstvennoj ustojchivost'yu vzbudatelya. *Farmakoehpikomika. Sovremennaya farmakoehpikomika i farmakoehpideologiya*. 2021; 14 (2): 235–48. Russian.
- Counoupas C, Triccas JA. The generation of T-cell memory to protect against tuberculosis. *Immunol Cell Biol*. 2019; 97 (7): 656–63.
- Bouzeyen R, Javid B, Therapeutic Vaccines for Tuberculosis: An Overview. *Front Immunol*. 2022; 13: 878471.
- Larsen SE, et al. An RNA-based vaccine platform for use against Mycobacterium tuberculosis. *Vaccines*. 2023; 11 (1): 130.
- Tian Y, Deng Z, Yang P. mRNA vaccines: A novel weapon to control infectious diseases. *Front Microbiol*. 2022; 13: 1008684.
- Melo A, et al. Third-generation vaccines: features of nucleic acid vaccines and strategies to improve their efficiency. *Genes (Basel)*. 2022; 13 (12).
- Heidary M, et al. A comprehensive review of the protein subunit vaccines against COVID-19. *Front Microbiol*. 2022; 13: 927306.
- Teran-Navarro H, et al. A comparison between recombinant listeria GAPDH proteins and GAPDH encoding mRNA conjugated to lipids as cross-reactive vaccines for Listeria, Mycobacterium, and Streptococcus. *Front Immunol*. 2021; 12: 632304.
- Al Tbeishat H. Novel in silico mRNA vaccine design exploiting proteins of M. tuberculosis that modulates host immune responses by inducing epigenetic modifications. *Scientific Reports*. 2022. 12 (1): 1–19.
- Shahrear S, Islam ABMMK. Modeling of MT. P495, an mRNA-based vaccine against the phosphate-binding protein PstS1 of Mycobacterium tuberculosis. *Molecular Diversity*. 2022; 1–20.
- Kar T, et al. A candidate multi-epitope vaccine against SARS-CoV-2. *Sci Rep*. 2020; 10 (1): 10895.
- O'Donnell TJ, Rubinsteyn A, Laserson U. MHCflurry 2.0: improved pan-allele prediction of MHC class I-presented peptides by incorporating antigen processing. *Cell Syst*. 2020; 11 (1): 42–48.
- Reynisson B, et al. Improved prediction of MHC II antigen presentation through integration and motif deconvolution of mass spectrometry MHC eluted ligand data. *J Proteome Res*. 2020; 19 (6): 2304–15.
- Greenbaum J, et al. Functional classification of class II human leukocyte antigen (HLA) molecules reveals seven different supertypes and a surprising degree of repertoire sharing across supertypes. *Immunogenetics*. 2011; 63 (6): 325–35.
- Weiskopf D, et al. Comprehensive analysis of dengue virus-specific responses supports an HLA-linked protective role for CD8⁺ T cells. *Proc Natl Acad Sci U S A*. 2013; 110 (22): E2046–53.
- Kreiter S, et al. Increased antigen presentation efficiency by coupling antigens to MHC class I trafficking signals. *J Immunol*. 2008; 180 (1): 309–18.
- Kirshina A, Kolosova E, Imasheva E, Vasileva O, Zaborova O, Terenin I, et al. Effects of various mRNA-LNP vaccine doses on neuroinflammation in BALB/c mice. *RSMU*. 2022; 6.
- Yano A, et al. An ingenious design for peptide vaccines. *Vaccine*. 2005; 23 (17–18): 2322–6.
- Hess J, Kaufmann SH. Live antigen carriers as tools for improved anti-tuberculosis vaccines. *FEMS Immunol Med Microbiol*. 1999; 23 (2): 165–73.

Литература

- Dartois, V.A. and E.J. Rubin, Anti-tuberculosis treatment strategies and drug development: challenges and priorities. *Nat Rev Microbiol*, 2022. 20 (11): p. 685–701.
- Васильева И. А., Тестов В. В., Стерликов С. А. Эпидемическая ситуация по туберкулезу в годы пандемии COVID-19–2020–2021 гг. *Туберкулез и болезни легких*. 2022. 100 3: 6–12.
- Ahmed A, et al. A century of BCG: Impact on tuberculosis control and beyond. *Immunological reviews*. 2021; 301 (1): 98–121.
- Шалюфаст Е. И., Ершова Ю. И. Поствакцинальные осложнения при «БЦЖ» иммунизации. *Вестник науки*. 2022; 4, 11 (56): 341–55.
- Covian C., et al., BCG-Induced Cross-Protection and Development of Trained Immunity: Implication for Vaccine Design. *Front Immunol*. 2019; 10: 2806.
- Николенко Н. Ю., Кудлай Д. А., Докторова Н. П. Фармакоэпидемиология и фармакоэкономика туберкулеза с множественной и широкой лекарственной устойчивостью возбудителя. *Фармакоэкономика. Современная фармакоэкономика и фармакоэпидемиология*. 2021; 14 (2): 235–48.
- Counoupas C, Triccas JA. The generation of T-cell memory to protect against tuberculosis. *Immunol Cell Biol*. 2019; 97 (7): 656–63.
- Bouzeyen R, Javid B, Therapeutic Vaccines for Tuberculosis: An Overview. *Front Immunol*. 2022; 13: 878471.
- Larsen SE, et al. An RNA-based vaccine platform for use against Mycobacterium tuberculosis. *Vaccines*. 2023; 11 (1): 130.
- Tian Y, Deng Z, Yang P. mRNA vaccines: A novel weapon to control infectious diseases. *Front Microbiol*. 2022; 13: 1008684.
- Melo A, et al. Third-generation vaccines: features of nucleic acid vaccines and strategies to improve their efficiency. *Genes (Basel)*. 2022; 13 (12).
- Heidary M, et al. A comprehensive review of the protein subunit vaccines against COVID-19. *Front Microbiol*. 2022; 13: 927306.
- Teran-Navarro H, et al. A comparison between recombinant listeria GAPDH proteins and GAPDH encoding mRNA conjugated to lipids as cross-reactive vaccines for Listeria, Mycobacterium, and Streptococcus. *Front Immunol*. 2021; 12: 632304.
- Al Tbeishat H. Novel in silico mRNA vaccine design exploiting proteins of M. tuberculosis that modulates host immune responses by inducing epigenetic modifications. *Scientific Reports*. 2022. 12 (1): 1–19.
- Shahrear S, Islam ABMMK. Modeling of MT. P495, an mRNA-based vaccine against the phosphate-binding protein PstS1 of Mycobacterium tuberculosis. *Molecular Diversity*. 2022; 1–20.
- Kar T, et al. A candidate multi-epitope vaccine against SARS-CoV-2. *Sci Rep*. 2020; 10 (1): 10895.
- O'Donnell TJ, Rubinsteyn A, Laserson U. MHCflurry 2.0: improved pan-allele prediction of MHC class I-presented peptides by incorporating antigen processing. *Cell Syst*. 2020; 11 (1): 42–48.
- Reynisson B, et al. Improved prediction of MHC II antigen presentation through integration and motif deconvolution of mass spectrometry MHC eluted ligand data. *J Proteome Res*. 2020; 19 (6): 2304–15.
- Greenbaum J, et al. Functional classification of class II human leukocyte antigen (HLA) molecules reveals seven different supertypes and a surprising degree of repertoire sharing across supertypes. *Immunogenetics*. 2011; 63 (6): 325–35.
- Weiskopf D, et al. Comprehensive analysis of dengue virus-

- specific responses supports an HLA-linked protective role for CD8⁺ T cells. *Proc Natl Acad Sci U S A*. 2013; 110 (22): E2046–53.
21. Kreiter S, et al. Increased antigen presentation efficiency by coupling antigens to MHC class I trafficking signals. *J Immunol*. 2008; 180 (1): 309–18.
 22. Kirshina A, Kolosova E, Imasheva E, Vasileva O, Zaborova O, Terenin I, et al. Effects of various mRNA-LNP vaccine doses on neuroinflammation in BALB/c mice. *RSMU*. 2022; 6.
 23. Yano A, et al. An ingenious design for peptide vaccines. *Vaccine*. 2005; 23 (17–18): 2322–6.
 24. Hess J, Kaufmann SH. Live antigen carriers as tools for improved anti-tuberculosis vaccines. *FEMS Immunol Med Microbiol*. 1999; 23 (2): 165–73.

ACTIVATION OF MICROGLIA IN THE BRAIN OF SPONTANEOUSLY HYPERTENSIVE RATS

Guselnikova VV^{1,2}✉, Razenkova VA¹, Sufieva DA¹, Korzhevskii DE¹¹ Institute of Experimental Medicine, St. Petersburg, Russia² St Petersburg University, St. Petersburg, Russia

Arterial hypertension is one of the most significant medical and social problems, being widespread and associated with the risk of renal failure, cardiovascular and cerebrovascular complications. The aim was to investigate the morphofunctional state of microglia in different regions of the rat brain in the setting of arterial hypertension. Brain samples from spontaneously hypertensive SHR rats aged 3–8 months ($n = 4$) were used as study material. Normotensive WKY rats of the same age ($n = 3$) were used as the control group. The work was performed using immunohistochemical analysis and confocal laser microscopy. During the quantitative analysis, we were seeking to determine the number of microglia cell bodies and the area occupied by the bodies and processes of these cells per 1 mm² of the nervous tissue. An immunohistochemical reaction for calcium-binding protein Iba1 revealed that in rats with arterial hypertension, microglia in the cerebral cortex, striatum, subcortical white matter and subfornical organ showed morphological signs of activation: increased body size and thickening of the processes of these cells. The strongest activation is demonstrated by microglia of the subfornical organ, which is in a preactivated state in normotensive rats. The performed statistical analysis revealed a trend towards an increase in the amount of microglia in the brain in SHR rats compared to animals in the control group. The Iba1/CD68 double immunofluorescence reaction showed no changes in the amount and/or distribution of lysosomal CD68 protein in spontaneously hypertensive rats compared to control group. The results obtained indicate chronic activation of microglia in the brain of spontaneously hypertensive rats. Activation of microglia in this case is not accompanied by an increase in the phagocytic activity of these cells.

Keywords: arterial hypertension, microglia, SHR, Iba1, CD68, subfornical organ

Funding: the study was funded by the Russian Science Foundation, project № 22-25-00105, <https://rscf.ru/project/22-25-00105/>.

Author contribution: Guselnikova VV — literature analysis, analysis and interpretation of the results, preparation of the manuscript; Razenkova VA — development of protocols for immunofluorescent reactions, confocal laser microscopy; Sufieva DA — histological examination of biological material, performing immunohistochemical reactions for light microscopy; Korzhevskii DE — concept development, research planning, manuscript editing.

Compliance with ethical standards: the study was approved by the Ethics Committee of the Federal State Budgetary Scientific Institution "IEM" (protocol № 1/22 dated February 18, 2022, protocol № 3/19 dated April 25, 2019), and was conducted in accordance with the provisions of the Declaration of Helsinki (2013)

✉ **Correspondence should be addressed:** Valeria V. Guselnikova
Acad. Pavlov, 12, Saint-Petersburg, 197376, Russia; guselnicova.valeria@yandex.ru

Received: 05.06.2023 **Accepted:** 20.06.2023 **Published online:** 27.06.2023

DOI: 10.24075/brsmu.2023.024

АКТИВАЦИЯ МИКРОГЛИИ В ГОЛОВНОМ МОЗГЕ СПОНТАННО ГИПЕРТЕНЗИВНЫХ КРЫС

В. В. Гусельникова^{1,2}✉, В. А. Разенкова¹, Д. А. Суфиева¹, Д. Э. Коржевский¹¹ Институт экспериментальной медицины, Санкт-Петербург, Россия² Санкт-Петербургский государственный университет, Санкт-Петербург, Россия

Артериальная гипертензия является одной из наиболее значимых медико-социальных проблем, что обусловлено широкой распространенностью этого заболевания и сопутствующим риском развития почечной недостаточности, сердечно-сосудистых и сосудисто-мозговых осложнений. Целью работы было изучение морфофункционального состояния микроглии разных отделов головного мозга крысы в условиях развития артериальной гипертензии. Материалом для исследования служили образцы головного мозга спонтанно гипертензивных крыс линии SHR в возрасте 3–8 месяцев ($n = 4$). В качестве контроля использовали нормотензивных крыс линии WKY той же возрастной группы ($n = 3$). Работа выполнена с применением методов иммуногистохимического анализа и конфокальной лазерной микроскопии. При проведении количественного анализа определяли количество тел микроглияцитов и площадь, занимаемую телами и отростками этих клеток, на 1 мм² нервной ткани. В результате постановки иммуногистохимической реакции на кальций-связывающий белок Iba1 обнаружено, что у крыс с артериальной гипертензией микроглия в коре головного мозга, стриатуме, субкортикальном белом веществе и субфорникальном органе имеет морфологические признаки активации (увеличение размера тела и утолщение отростков). Наиболее сильную активацию демонстрирует микроглия субфорникального органа, которая у нормотензивных крыс находится в преактивированном состоянии. Проведенный статистический анализ позволил выявить тенденцию увеличения количества микроглии в головном мозге у крыс линии SHR по сравнению с животными контрольной группы. При двойной иммунофлуоресцентной реакции Iba1/CD68 не выявлено изменений в количестве и/или распределении лизосомного белка CD68 у спонтанно гипертензивных крыс по сравнению с контролем. Полученные результаты свидетельствуют о хронической активации микроглии в головном мозге у крыс на фоне развития артериальной гипертензии. Активация микроглии в данном случае не сопровождается усилением фагоцитарной активности этих клеток.

Ключевые слова: артериальная гипертензия, микроглия, SHR, Iba1, CD68, субфорникальный орган

Финансирование: исследование выполнено при финансовой поддержке Российского Научного Фонда, проект № 22-25-00105, <https://rscf.ru/project/22-25-00105/>.

Вклад авторов: Гусельникова В. В. — анализ литературы, анализ и интерпретация результатов, подготовка рукописи; Разенкова В. А. — отработка протоколов иммунофлуоресцентных реакций, проведение конфокальной лазерной микроскопии; Суфиева Д. А. — гистологическая проводка биологического материала, постановка иммуногистохимических реакций для световой микроскопии; Коржевский Д. Э. — разработка концепции, планирование исследования, редактирование рукописи.

Соблюдение этических стандартов: исследование одобрено этическим комитетом ФГБНУ «ИЭМ» (протокол №1/22 от 18 февраля 2022 г., протокол № 3/19 от 25 апреля 2019 г.), проведено в соответствии с положениями Хельсинкской декларации (2013 г.).

✉ **Для корреспонденции:** Валерия Владимировна Гусельникова
ул. Акад. Павлова, д. 12, г. Санкт-Петербург, 197376, Россия; guselnicova.valeria@yandex.ru

Статья получена: 05.06.2023 **Статья принята к печати:** 20.06.2023 **Опубликована онлайн:** 27.06.2023

DOI: 10.24075/vrgmu.2023.024

Today, arterial hypertension (AH) remains one of the most significant health and social problems worldwide. According to a joint study by WHO and Imperial College London, the number of people with AH has almost doubled in 30 years (from 1990 to 2019), from 650 million to 1.28 billion [1]. The prevalence of AH in Russia, according to the ESSE-RF study (Epidemiology of cardiovascular diseases and their risk factors in the regions of the Russian Federation), was 44% in 2014 in a representative sample of patients aged 25–65 years. An epidemiological survey conducted in 2019 involving 20,607 residents of the Russian Federation, reported AH in 14,853 (72.1%) of those surveyed [2]. It is clear that AH is a widespread disease in our country, posing a serious problem for domestic health care. Despite more than a century of research, AH remains poorly treated, probably due to the complexity of the mechanisms of pathogenesis, involving many interacting factors, and our limited understanding of these mechanisms at the cellular and molecular levels [3]. Further research in this area thus looks relevant.

Being widespread in the Russian Federation, featuring inadequate treatment and control, AH remains a poorly managed risk factor for myocardial infarction, chronic heart failure, sudden death, renal failure, and ischaemic and hemorrhagic stroke. The brain is one of the target organs most early affected by AH: small-diameter vessels are the first to be affected, resulting in microbleeds, subcortical lacunar infarcts and diffuse white matter lesions, accompanied by cognitive decline [4]. It has been noted that AH is accompanied by the development of chronic neuroinflammation in the brain [5]. However, the cellular mechanisms of neuroinflammation associated with AH are unknown, and it is unclear whether neuroinflammation contributes to the progression of AH. Since inflammation in the brain is mainly caused and maintained by microglia, a detailed analysis of this cell population in the setting of AH seems relevant. New data on the functional status of brain microglia in the setting of AH may contribute to a better understanding of the molecular and cellular mechanisms underlying the development of the disease. The aim was to investigate the morphofunctional state of microglia in different brain regions of the rat in the setting of AH development.

METHODS

The SHR (Spontaneously Hypertensive Rats) strain was used as an AH experimental model. Animals of this strain, bred by K. Okamoto and K. Aoki (1963) from normotensive Wistar-Kyoto (WKY) rats, develop chronic hypertension spontaneously (without any preceding primary disease), which is a consequence of dysfunction of 1–6 genes involved in blood pressure regulation. Persistent increase in blood pressure to 190–200 mmHg in SHR rats starts from week 12 onwards [6]. The SHR line is considered the most adequate model of human essential hypertension and is widely used to study the pathogenesis of the disease and to develop new approaches to its therapy [7, 8].

Brain samples from spontaneously hypertensive male SHR rats aged 3–8 months ($n = 4$) were used as study material. The brain of male WKY rats of the same age was used as a control group ($n = 3$). Systolic blood pressure in animals was determined in the caudal artery using Sistol, a system for non-invasive blood pressure measurement in rodents (Neurobotics; Russia). Blood pressure readings were 220 mmHg in SHR rats and 85–100 mmHg in WKY rats. Brain samples were fixed in zinc-ethanol-formaldehyde using the previously described method [9], then dehydrated and embedded in Type 6 paraffin (ThermoScientific; USA). Then, 5 μ m thick sections were made from paraffin blocks using a Microm HM 325 rotary microtome

(ThermoScientific; USA). The obtained preparations after deparaffinization and rehydration were subjected to a heat demasking procedure by soaking in 10% aqueous sodium thiosulphate solution for 23 min.

Rabbit polyclonal antibodies to Iba1 (Biocare Medical; USA) at a dilution of 1 : 500 were used for immunohistochemical detection of Iba1. HRP Conjugate reagent from the Reveal Polyvalent HRP DAB Detection System kit (Spring Bioscience; USA) was used as a secondary reagent for the detection of primary antibodies. Peroxidase label was detected using diaminobenzidine chromogen from the DAB+ kit (Agilent; USA). After the immunohistochemical reaction, some of the slices were counterstained with alum hematoxylin.

For simultaneous detection of Iba1 and CD68, a mixture of rabbit polyclonal antibodies to Iba1 (Biocare medical; USA) at a dilution of 1 : 500 and mouse monoclonal antibodies to CD68 (Agilent; USA) at a dilution of 1 : 1000 were applied to slices. The primary antibody mixture was prepared in a 1 : 1 ratio. The secondary reagents were the mixture (1 : 1) of antibodies against biotin-labelled rabbit immunoglobulins (from R&D Systems kit; USA) and EnVision+/HRP-AntiMouse reagent (Agilent; USA) with normal rat serum added to prevent non-specific antibody binding. After incubation in the secondary antibody mixture, the slices were treated with streptavidin conjugate solution with fluorochrome Cy2 (Jackson ImmunoResearch; USA) and then with antibody solution against HRP conjugated with fluorochrome Cy3 (Jackson Immuno Research; USA).

For the negative antibody control, immunohistochemical processing of the preparations was performed without using primary antibodies, instead of which PBS was applied to the slices. There was no positive reaction in this case.

The preparations were examined using a Leica DM750 light microscope (Leica; Germany) and a LSM800 confocal laser microscope (Zeiss; Germany). A laser with a wavelength of 488 nm was used to excite Cy2 fluorescence, and a laser with a wavelength of 561 nm was used for Cy3 excitation. The images were studied using LSM Image Browser and ZEN2012 software (Zeiss, Germany).

In the quantitative testing, we evaluated the number of Iba1⁺ microglial cell bodies and the area occupied by Iba1-immunopositive microglial cell bodies and processes per 1 mm² of nerve tissue. Measurements were made in three 270 × 203 μ m fields of view for each case in each study area (cortex, striatum, white matter, subfornical organ) using Fiji morphometric analysis software (ImageJ). The number of cell bodies was counted using the Cell Counter plug-in. The area occupied by microglial cells was estimated after channel separation (DAB/hematoxylin) using the "Color Deconvolution" option followed by application of the "Threshold" and "Measure Particles" options [10]. Statistical analysis was performed with GraphPad Prism 8 software (GraphPad Software; USA). Data were presented as mean \pm SEM. The data were compared using the Mann-Whitney test. The criterion to deem the differences significant was $p < 0.05$.

RESULTS

After performing an immunohistochemical reaction for the calcium-binding protein Iba1, immunopositive cells were detected in all brain regions studied. The reaction product was concentrated in branching cells, which have a typical microglia structure. A morphological diversity of Iba1⁺ cells was observed depending on their localization within the brain. In the cortex of the control group animals (WKY), typical ramified microglia without signs of activation were present

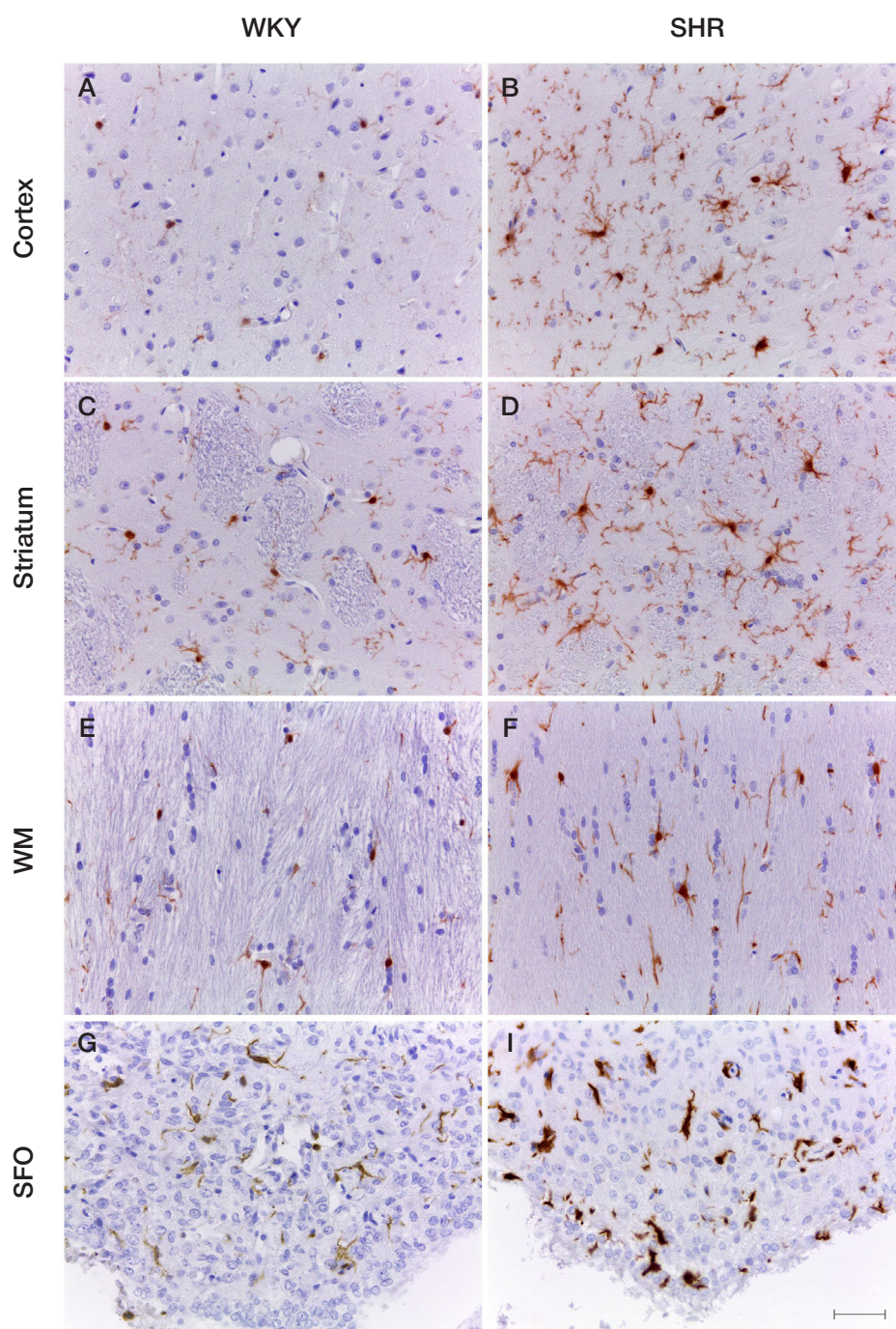


Fig. 1. Microglia in the rat brain. WKY — Wistar-Kyoto normotensive rat line; SHR — spontaneously hypertensive rat line; Cortex — area of the large cerebral cortex; Striatum — striatum (corpus striatum); WM — subcortical white matter; SFO — subformal organ. Immunohistochemical reaction for Iba1, counterstained with alum hematoxylin. Scale bar is 50 μm

(Fig. 1A). Iba⁺ cells in this case were characterized by a small soma and the presence of long thin processes branching in different directions. The cell body was often not in the slice plane, resulting in the visualization of only parts of microglial cell processes in the form of immunopositive strands and/or dots in some cortical areas. The immunopositive elements detected were evenly distributed within the cortex (Fig. 1A). In similar cortical areas of spontaneously hypertensive rats (SHR), microglia had a number of differences (Fig. 1B). As in the control group, the immunopositive cells in this case were evenly distributed without forming clusters, but the density of Iba⁺ cells was visually significantly higher. We observed an increase in the size of the microglial cell body and thickening of their processes, which demonstrated a high branching rate

(Fig. 1B). Such morphological features were characteristic of microglia in all layers of the cerebral cortex of spontaneously hypertensive rats.

The average area occupied by Iba⁺ microglia in the cerebral cortex of the control group animals was $27,547 \pm 3,100 \mu\text{m}^2/\text{mm}^2$, and that with spontaneously hypertensive rats — $18,790 \pm 2,717 \mu\text{m}^2/\text{mm}^2$ ($p = 0.2$). The number of Iba⁺-microglial cell bodies in WKY rats was 89.56 ± 10.86 cell bodies/ mm^2 , and in SHR rats — 130.1 ± 19.9 cell bodies/ mm^2 ($p = 0.2$).

In the striatum of control animals, as in the cortex, a typical ramified microglia were found (Fig. 1B). At the same time, the thickness of microglial processes was greater compared to the cortex of control animals, making the complex branching of microglial outgrowths in this localization more visible. As in

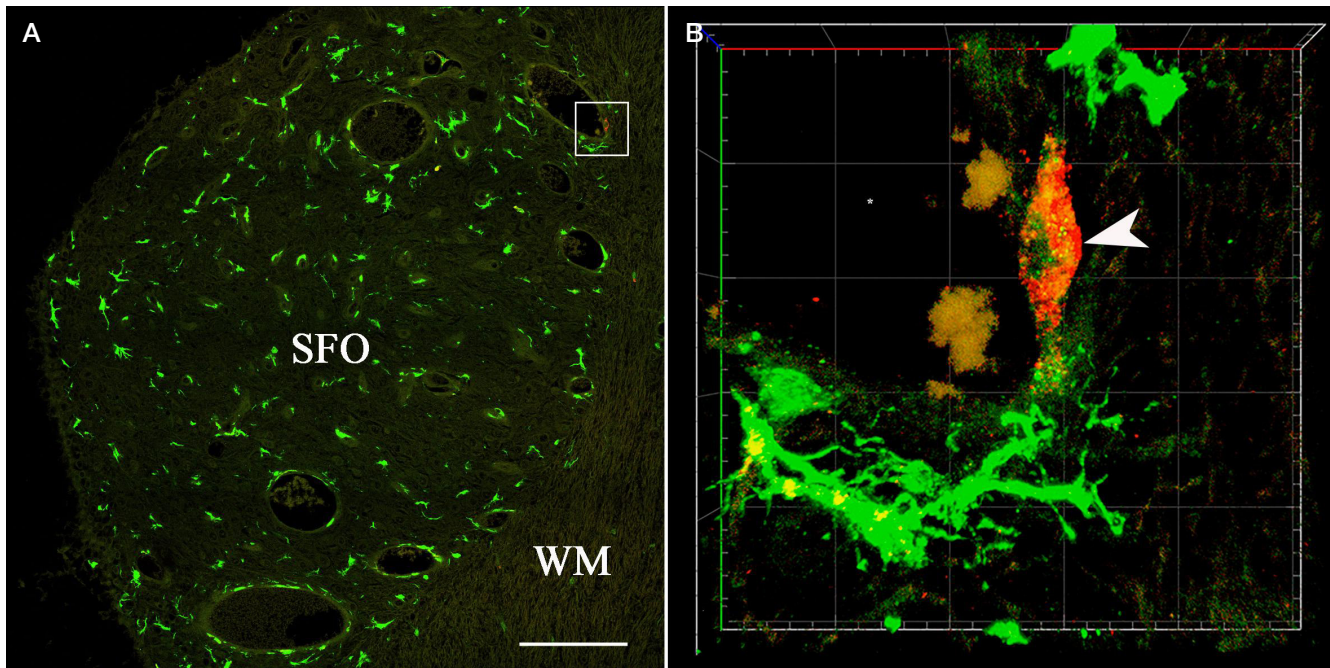


Fig. 2. Subfornical organ of a spontaneously hypertensive rat. Double immunofluorescence reaction for Iba1 (green fluorescence) and CD68 (red fluorescence). The yellow color marks the colocalization areas of the green and red channels. Figure B is an enlarged fragment of Figure A (white box). SFO, subfornical organ; WM, white matter; *asterisk*, blood vessel; *arrowhead* indicates CD68-rich cell. Confocal microscopy. **A.** Panoramic image; the scale bar is 100 μm . **B.** Three-dimensional reconstruction of a series of optical slices, grid cell size 10 \times 10 μm

the large hemisphere cortex, microglia were evenly distributed in the striatum, without forming clusters. Cell bodies were small, rounded or oval in shape and not always in the slice plane. Microglia were localized predominantly in the grey matter of the striatum, and only short sections of these cell processes were visible in the white matter (Fig. 1C). The average area of Iba1⁺ microglia was $33,887 \pm 3,944 \mu\text{m}^2/\text{mm}^2$, the number of Iba1⁺ cell bodies was 111.7 ± 14.31 cell bodies/ mm^2 . In the striatum of spontaneously hypertensive rats, the shape and distribution of microglia did not differ from that of control animals, but there was an increase in the size of these cell bodies and a thickening of their processes, which demonstrated a high branching rate (Fig. 1D). The average area of Iba1⁺ microglia in this case was $21,516 \pm 2,589 \mu\text{m}^2/\text{mm}^2$, and the number of cell bodies was 146.3 ± 12.68 cell bodies/ mm^2 , which had no statistically significant difference to the control group ($p = 0.2$).

In the subcortical white matter of control animals, spindle-shaped Iba1⁺ cells were present, with their bodies and processes oriented along the nerve fibers (Fig. 1D). The microglia detected were characterized by the presence of one or two long unbranched or weakly branched offshoots arising from different poles of the cell body in opposite directions (Fig. 1D). In spontaneously hypertensive rats, an increase in body size and thickness of Iba1⁺ cell processes was observed in the subcortical white matter region. We found not only spindle-shaped microglia but also cells with three processes extending from the body and penetrating white matter fibers in different directions. No increase in the intensity of branching was observed (Fig. 1E). The mean area of Iba1⁺ microglia in the white matter in control animals was $11,791 \pm 4,540 \mu\text{m}^2/\text{mm}^2$; in spontaneously hypertensive rats it was $9,208 \pm 1,368 \mu\text{m}^2/\text{mm}^2$ ($p > 0.9999$). The number of Iba1⁺ microglial cell bodies was 8107.7 ± 26.97 cells/ mm^2 in WKY rats and 111.7 ± 2 cells/ mm^2 in SHR rats ($p = 0.6$).

A large number of Iba1-immunopositive cells, distributed relatively evenly throughout the organ, were present in the subfornical organ of the control group (Fig. 1G). The morphology of microglia in this region of the brain differed significantly

from the typical ramified morphology characteristic of normal microglia. Most of the Iba1⁺ cells present in this locus were uni- or bipolar spindle-shaped. Their processes demonstrated very little branching (often no branching) and lacked a unified direction. Within the subfornical organ, there were also single unprotected microglia characterized by hypertrophy of the bodies and the absence of distinct processes (Fig. 1G). In the subfornical organ of spontaneously hypertensive rats, all detected Iba1⁺ cells had not many processes. They were characterized by marked hypertrophy of the bodies and the presence of few short, thick, unbranched ramifications (Fig. 1H). The mean area of Iba1⁺ microglia in the subfornical organ in control animals was $37,831 \pm 8283 \mu\text{m}^2/\text{mm}^2$, and in spontaneously hypertensive rats it was $45,783 \pm 4,318 \mu\text{m}^2/\text{mm}^2$ ($p = 0.4$). The number of Iba1⁺ microglial cell bodies in WKY rats was 337.4 ± 8.84 cells/ mm^2 , in SHR rats 465.4 ± 27.05 cells/ mm^2 ($p = 0.1$).

After performing an Iba1/CD68 double immunofluorescence reaction, it was observed that in all brain regions examined, the majority of cells visualized contained Iba1 protein, evenly distributed in the bodies and processes (Fig. 2; green fluorescence). The morphology of these cells in each examined area corresponded to that described in the immunohistochemical reaction to the Iba1 protein for light microscopy. When the preparations were analyzed under low magnification, the CD68 protein appeared to be completely absent from these cells. However, when analyzed under high magnification, CD68 was detected in the cytoplasm of some cells as local clusters (Fig. 2B; the yellow color is the result of colocalization of green and red signals). The size, the number and the distribution of CD68 clusters in the cytoplasm varied greatly between individual microglial cells, but no dependence of these parameters on cell localization was found. Also, there was no increase in the content and/or change in the distribution of CD68 protein in spontaneously hypertensive rats compared to control group rats in any of the brain regions studied.

In addition to microglia containing large amounts of Iba1 and local accumulations of CD68 in the cytoplasm, all

analyzed brain regions showed the presence of single cells with high CD68 content (Fig. 2B; *arrowhead*). The CD68 protein was detected in the cytoplasm of these cells as fine granular structures that gave the cytoplasm a granular appearance (Fig. 2B; *red fluorescence*). The Iba1 protein within the cytoplasm of such cells was present in small amounts (as dot inclusions) or undetectable amounts. Cells high in CD68 were present in the brain of both normotensive and spontaneously hypertensive animals, and were found in all areas studied. They differed a lot from typical microglia in morphological aspect, being oval or elongated in shape, with no branching processes and occurred in most cases perivascularly, rarely within the parenchyma.

DISCUSSION

The study now discussed provides morphological evidence for chronic microglia activation in different rat brain regions in the setting of AH development. Statistical analysis revealed a tendency for the number of microglia in the brain to increase in SHR rats compared to the control group. However, it has not been possible to demonstrate statistically significant differences in the analyzed indicators given the material available, which may be due to insufficient sample size. There is also a marked scattering of indicators among the animals in the control group. This may be due to the fact that WKY rat strain, widely used as a control for the SHR line, has a number of features related to the neural tissue condition. For example, in a recent study we observed that, unlike in Wistar rats, signs of Kolmer Iba1⁺ cell activation can be observed in the brain of WKY rats, and supraependymal CD68⁺ and Iba1⁺ rounded cells are present in the cerebral ventricular cavity. This is indicative of a hemato-liquor barrier damage and activation of monocyte-macrophage cells in WKY rats [11]. Together with our findings in this paper, this raises questions about the adequacy of using WKY rats as a control group in neurobiological studies.

It has previously been reported that SHR rats show a moderate state of microglia activation in the medulla oblongata [5]. Expression of the metabotropic purinergic receptor P2Y₁₂ and fractalkine receptor CX₃CR1 genes was observed to be reduced in SHR rats compared to normotensive WKY rats, which correlated with the phenotypic signs of activation, such as lower microglia cell density in the medulla oblongata and shorter microglial processes [5]. In addition, hypertrophy of microglia was shown in the deep cortical layers of 35-week-old SHR rats, indicating its activation [12]. Microglia activation in this study was further confirmed using flow cytometry, which showed a significant increase in CD11b expression in the brain microglia of SHR rats. In addition to this evidence of microglia activation in several brain regions in spontaneously hypertensive rats, we obtained evidence of microglia activation in the cortex, striatum, white matter and subfornical organ of SHR rats compared to WKY rats of the same age. Interestingly, the most pronounced morphological signs of activation were exhibited by microglia within the subfornical organ. We noted earlier that normally microglia in this area is in a pre-activated state, which may be due to the absence of a blood-brain barrier here [13]. From the perspective of these data, it seems logical that under the influence of additional stimulation associated with arterial hypertension, microglia of the subfornical organ more readily switch to an activated state compared to microglia in other brain regions, where microglia are normally represented by an inactive (ramified) form.

The role of microglia activation in AH, depending on localization, is still an open question. It has been shown that targeted 'silencing' of microglia effectively reduces blood pressure

and neuroinflammation in mice with experimental hypertension. Conversely, adoptive transfer of activated microglia would predispose recipients to hypertensive stimulants. Taken together, these results indicate that microglia are a key cellular element in the neurogenic regulation of hypertension [14]. Further research into the contribution of microglia and neuroinflammation (mediated by the latter) to the pathogenesis of AH may help identify new molecular targets for targeted therapies for this disease.

The fact that microglia are activated in the setting of AH may have important therapeutic implications. For example, chronic AH has been found to be a risk factor for Alzheimer's disease, the most common neurodegenerative disease, which currently cannot be prevented or treated effectively. Neuroinflammation caused by glial cells is thought to be one possible mechanism linking hypertension and an increased risk of developing Alzheimer's disease [15]. Moreover, the available experimental evidence suggests that glia activation and neuroinflammation can be reversed by the use of different classes of antihypertensive drugs. These studies suggest that antihypertensives may be effective in Alzheimer's disease not only because of their ability to affect blood pressure, but also because of their anti-inflammatory effects [15].

Microglia activation is known to be accompanied by an increase in phagocytic activity of these cells. Phagocytosis, carried out by microglia, is critical for the normal functioning of the central nervous system at all stages of its development. During embryonic and early postnatal development, microglia clean the developing brain of apoptotic neurons and oligodendrocytes through phagocytosis. In the adult brain, microglia will normally phagocytize fragments of dying cells as well as inactive synapses, contributing to the regulation of synaptic plasticity and the maintenance of neural tissue homeostasis. During ageing, microglia will phagocytize the remains of dying neurons and collapsing synapses. The phagocytic activity of microglia is increased when pathology develops: in diseases such as Alzheimer's or multiple sclerosis, microglia can phagocytose not only dying neurons, but also β -amyloid and myelin [16, 17].

One of the marker proteins for judging the phagocytic activity of cells is the transmembrane receptor protein CD68. It is localized in the lysosomal and endosomal membranes of monocytic-macrophage cells and microglia. CD68 increases dramatically in inflammatory conditions, so CD68 has traditionally been considered a marker of activated microglia [18]. Based on these findings as well as morphological evidence of microglia activation in different brain regions in spontaneously hypertensive SHR rats, we expected to see an increased content of CD68 protein in microglia in SHR rats compared to control group. Unexpectedly, we found no such increase in any of the brain regions studied. This suggests that activation of microglia against the background of AH is probably not associated with an increase in phagocytic activity of these cells, and may have a regulatory (secretory) nature.

An interesting finding in our research was the discovery of a population of CD68-immunopositive cells with very low levels of Iba1 protein. The detection of Iba1⁻/CD68⁺ cells in the human brain has previously been reported by other authors [19]. They noted that lesions in the deep subcortical structures of the brain result in an increase in microglia containing CD68, a transformation of branched microglia into amoeboid microglia and a loss of Iba1 expression. According to our quantitative assessment, Iba1⁻/CD68⁺ cells account for about 32.5% of total microglia in deep subcortical brain lesions [19]. It has also been noted that in Alzheimer's disease, the development of dementia is positively correlated with CD68 levels and negatively correlated with Iba1 levels, and that different microglia populations expressing these two proteins can coexist in the

brain [20]. Whether the Iba1-/CD68+ cells detected by us and other authors are a new type of microglial cells or a special population of macrophages needs further investigation.

CONCLUSIONS

The development of chronic AH in SHR rats involves activation of microglia in the cerebral cortex, striatum, subcortical white

matter and subfornical organ. The subfornical organ microglia in normotensive rats is in a pre-activated state. Activation of microglia in the organ increases with the development of AH. Activation of microglia in AH is not accompanied by an increase in phagocytic activity of these cells. Microglia is involved in the development of neuroinflammation in AH and may therefore be a potential target for targeted pharmacotherapy for this disease.

References

1. NCD Risk Factor Collaboration (NCD-RisC). Worldwide trends in hypertension prevalence and progress in treatment and control from 1990 to 2019: a pooled analysis of 1201 population-representative studies with 104 million participants. *Lancet*. 2021; 398 (10304): 957–980. DOI: 10.1016/S0140-6736(21)01330-1.
2. Erina AM, Rotar OP, Solntsev VN, Shalnova SA, Deev AD, Baranova EI, et al. Epidemiology of arterial hypertension in Russian Federation — importance of choice of criteria of diagnosis. *Kardiologiya*. 2019; 59 (6): 5–11. DOI: 10.18087/cardio.2019.6.2595
3. Ma J, Li Y, Yang X, Liu K, Zhang X, Zuo X, et al. Signaling pathways in vascular function and hypertension: molecular mechanisms and therapeutic interventions. *Signal Transduct Target Ther*. 2023; 8 (1): 168. DOI: 10.1038/s41392-023-01430-7.
4. Meissner A. Hypertension and the brain: a risk factor for more than heart disease. *Cerebrovasc Dis*. 2016; 42 (3–4): 255–62. DOI: 10.1159/000446082.
5. Cohen EM, Mohammed S, Kavurma M, Nedoboy PE, Cartland S, Farnham MMJ, Pilowsky PM. Microglia in the RVLM of SHR have reduced P2Y12R and CX3CR1 expression, shorter processes, and lower cell density. *Auton Neurosci*. 2019; 216: 9–16. DOI: 10.1016/j.autneu.2018.12.002.
6. Doris PA. Genetics of hypertension: an assessment of progress in the spontaneously hypertensive rat. *Physiol genomics*. 2017; 49 (11): 601–17. DOI: 10.1152/physiolgenomics.00065.2017.
7. Pravenec M, Kurtz TW. Recent advances in genetics of the spontaneously hypertensive rat. *Curr Hypertens Rep*. 2010; 12 (1): 5–9. DOI: 10.1007/s11906-009-0083-9.
8. Leong XF, Ng CY, Jaarin K. Animal Models in Cardiovascular Research: Hypertension and Atherosclerosis. *Biomed Res Int*. 2015; 2015: 528757. DOI: 10.1155/2015/528757.
9. Korzhevskii DE, Sukhorukova EG, Kirik OV, Grigorev IP. Immunohistochemical demonstration of specific antigens in the human brain fixed in zinc-ethanol-formaldehyde. *Eur J Histochem*. 2015; 59 (3): 2530. DOI: 10.4081/ejh.2015.2530.
10. Crowe AR, Yue W. Semi-quantitative Determination of Protein Expression Using Immunohistochemistry Staining and Analysis: An Integrated Protocol. *Bio-protocol*. 2019; 9 (24): e3465. DOI: 10.21769/BioProtoc.3465.
11. Kirik OV, Korzhevskij DEh. Marker makrofagov ED1(CD68) v kletkax golovnogo mozga krys. V sbornike: Materialy IV mezhdunarodnoj nauchnoj konferencii «Sovremennyye problemy nevrobiologii»; 18-20 maya 2023 g.; Yaroslavl': FGBOU VO YaGMU Minzdrava Rossii, 2023; 85 c. Russian.
12. Kaiser D, Weise G, Möller K, Scheibe J, Pösel C, Baasch S, et al. Spontaneous white matter damage, cognitive decline and neuroinflammation in middle-aged hypertensive rats: an animal model of early-stage cerebral small vessel disease. *Acta Neuropathol Commun*. 2014; 2: 169. DOI: 10.1186/s40478-014-0169-8.
13. Guselnikova VV, Razenkova VA, Sufieva DA, Korzhevskii DE. Microglia and putative macrophages of the subfornical organ: structural and functional features. *Bulletin of RSMU*. 2022; (2): 50–7. DOI: 10.24075/brsmu.2022.020.
14. Shen XZ, Li Y, Li L, Shah KH, Bernstein KE, Lyden P, Shi P. Microglia participate in neurogenic regulation of hypertension. *Hypertension*. 2015; 66 (2): 309–16. DOI: 10.1161/HYPERTENSIONAHA.115.05333.
15. Bajwa E, Klegeris A. Neuroinflammation as a mechanism linking hypertension with the increased risk of Alzheimer's disease. *Neural Regeneration Research*. 2022; 17 (11): 2342–6. DOI: 10.4103/1673-5374.336869.
16. Galloway DA, Phillips AEM, Owen DRJ, Moore CS. Phagocytosis in the Brain: Homeostasis and Disease. *Front Immunol*. 2019; 10: 790. DOI: 10.3389/fimmu.2019.00790.
17. Gabandé-Rodríguez E, Keane L, Capasso M. Microglial phagocytosis in aging and Alzheimer's disease. *J Neurosci Res*. 2020; 98 (2): 284–98. DOI: 10.1002/jnr.24419.
18. Jurga AM, Paleczna M, Kuter KZ. Overview of General and Discriminating Markers of Differential Microglia Phenotypes. *Front Cell Neurosci*. 2020; 14: 198. DOI: 10.3389/fncel.2020.00198.
19. Waller R, Baxter L, Fillingham DJ, Coelho S, Pozo JM, Mozumder M, et al. Iba-1-/CD68+ microglia are a prominent feature of age-associated deep subcortical white matter lesions. *PLoS One*. 2019; 14 (1): e0210888. DOI: 10.1371/journal.pone.0210888.
20. Minett T, Classey J, Matthews FE, Fahrenhold M, Taga M, Brayne C, et al. MRC CFAS. Microglial immunophenotype in dementia with Alzheimer's pathology. *J Neuroinflammation*. 2016; 13 (1): 135. DOI: 10.1186/s12974-016-0601-z.

Литература

1. NCD Risk Factor Collaboration (NCD-RisC). Worldwide trends in hypertension prevalence and progress in treatment and control from 1990 to 2019: a pooled analysis of 1201 population-representative studies with 104 million participants. *Lancet*. 2021; 398 (10304): 957–980. DOI: 10.1016/S0140-6736(21)01330-1.
2. Erina AM, Rotar OP, Solntsev VN, Shalnova SA, Deev AD, Baranova EI, et al. Epidemiology of arterial hypertension in Russian Federation — importance of choice of criteria of diagnosis. *Kardiologiya*. 2019; 59 (6): 5–11. DOI: 10.18087/cardio.2019.6.2595
3. Ma J, Li Y, Yang X, Liu K, Zhang X, Zuo X, et al. Signaling pathways in vascular function and hypertension: molecular mechanisms and therapeutic interventions. *Signal Transduct Target Ther*. 2023; 8 (1): 168. DOI: 10.1038/s41392-023-01430-7.
4. Meissner A. Hypertension and the brain: a risk factor for more than heart disease. *Cerebrovasc Dis*. 2016; 42 (3–4): 255–62. DOI: 10.1159/000446082.
5. Cohen EM, Mohammed S, Kavurma M, Nedoboy PE, Cartland S, Farnham MMJ, Pilowsky PM. Microglia in the RVLM of SHR have reduced P2Y12R and CX3CR1 expression, shorter processes, and lower cell density. *Auton Neurosci*. 2019; 216: 9–16. DOI: 10.1016/j.autneu.2018.12.002.
6. Doris PA. Genetics of hypertension: an assessment of progress in the spontaneously hypertensive rat. *Physiol genomics*. 2017; 49 (11): 601–17. DOI: 10.1152/physiolgenomics.00065.2017.
7. Pravenec M, Kurtz TW. Recent advances in genetics of the spontaneously hypertensive rat. *Curr Hypertens Rep*. 2010; 12 (1): 5–9. DOI: 10.1007/s11906-009-0083-9.
8. Leong XF, Ng CY, Jaarin K. Animal Models in Cardiovascular Research: Hypertension and Atherosclerosis. *Biomed Res Int*.

- 2015; 2015: 528757. DOI: 10.1155/2015/528757.
9. Korzhevskii DE, Sukhorukova EG, Kirik OV, Grigorev IP. Immunohistochemical demonstration of specific antigens in the human brain fixed in zinc-ethanol-formaldehyde. *Eur J Histochem*. 2015; 59 (3): 2530. DOI: 10.4081/ejh.2015.2530.
 10. Crowe AR, Yue W. Semi-quantitative Determination of Protein Expression Using Immunohistochemistry Staining and Analysis: An Integrated Protocol. *Bio-protocol*. 2019; 9 (24): e3465. DOI: 10.21769/BioProtoc.3465.
 11. Кирик О. В., Коржевский Д. Э. Маркер макрофагов ED1(CD68) в клетках головного мозга крысы. В сборнике: Материалы IV международной научной конференции «Современные проблемы нейробиологии»; 18–20 мая 2023 г.; Ярославль: ФГБОУ ВО ЯГМУ Минздрава России, 2023; 85 с.
 12. Kaiser D, Weise G, Möller K, Scheibe J, Pösel C, Baasch S, et al. Spontaneous white matter damage, cognitive decline and neuroinflammation in middle-aged hypertensive rats: an animal model of early-stage cerebral small vessel disease. *Acta Neuropathol Commun*. 2014; 2: 169. DOI: 10.1186/s40478-014-0169-8.
 13. Guselnikova VV, Razenkova VA, Sufieva DA, Korzhevskii DE. Microglia and putative macrophages of the subfornical organ: structural and functional features. *Bulletin of RSMU*. 2022; (2): 50–7. DOI: 10.24075/brsmu.2022.020.
 14. Shen XZ, Li Y, Li L, Shah KH, Bernstein KE, Lyden P, Shi P. Microglia participate in neurogenic regulation of hypertension. *Hypertension*. 2015; 66 (2): 309–16. DOI: 10.1161/HYPERTENSIONAHA.115.05333.
 15. Bajwa E, Klegeris A. Neuroinflammation as a mechanism linking hypertension with the increased risk of Alzheimer's disease. *Neural Regeneration Research*. 2022; 17 (11): 2342–6. DOI: 10.4103/1673-5374.336869.
 16. Galloway DA, Phillips AEM, Owen DRJ, Moore CS. Phagocytosis in the Brain: Homeostasis and Disease. *Front Immunol*. 2019; 10: 790. DOI: 10.3389/fimmu.2019.00790.
 17. Gabandé-Rodríguez E, Keane L, Capasso M. Microglial phagocytosis in aging and Alzheimer's disease. *J Neurosci Res*. 2020; 98 (2): 284–98. DOI: 10.1002/jnr.24419.
 18. Jurga AM, Paleczna M, Kuter KZ. Overview of General and Discriminating Markers of Differential Microglia Phenotypes. *Front Cell Neurosci*. 2020; 14: 198. DOI: 10.3389/fncel.2020.00198.
 19. Waller R, Baxter L, Fillingham DJ, Coelho S, Pozo JM, Mozumder M, et al. Iba-1-/CD68+ microglia are a prominent feature of age-associated deep subcortical white matter lesions. *PLoS One*. 2019; 14 (1): e0210888. DOI: 10.1371/journal.pone.0210888.
 20. Minett T, Classey J, Matthews FE, Fahrenhold M, Taga M, Brayne C, et al. MRC CFAS. Microglial immunophenotype in dementia with Alzheimer's pathology. *J Neuroinflammation*. 2016; 13 (1): 135. DOI: 10.1186/s12974-016-0601-z.

MORPHOLOGICAL PECULIARITIES OF REGENERATION OF ORAL MUCOSA ASSOCIATED WITH USE OF POLYMERIC PIEZOELECTRIC MEMBRANES

Koniaeva AD¹✉, Varakuta EYu¹, Leiman AE¹, Rafiev DO¹, Bolbasov EN², Stankevich KS³

¹ Human anatomy department, General medicine faculty, Siberian State Medical University, Tomsk, Russia

² National Research Tomsk Polytechnic University, Tomsk, Russia

³ Chemistry and biochemistry faculty, Montana State University, Bozeman, MT, USA

Wound defects of the oral mucosa are a common pathology the treatment of which often involves synthetic membranes. Development of varieties of such membranes is an ongoing process. This study aimed to register morphological features of the oral mucosa regeneration process in the presence of one of the varieties, the polymer piezoelectric membranes. The study involved 45 Wistar rats divided into 3 groups: 1) animals with an open wound defect; 2) animals with a wound defect covered with a copper-coated polymer membrane; 3) intact animals. The samples for morphometric study were collected on the 3rd, 7th and 12th days. On the 3rd day, rats of group 1 had the specific area of granulation tissue 1.4 times greater than that in group 2 ($p = 0.033$). In group 1 rats, endotheliocytes expressed more VEGF than in the animals of group 2. In group 2, the defect was ultimately completely covered with the epithelial layer, which was not the case in group 1. On the 7th day, the epithelium in rats of group 2 was twice as thick as the layer registered in group 1 ($p = 0.019$). Granulation tissue was replaced by loose fibrous connective tissue. In group 1, the specific area of inflammatory infiltration was greater than that of loose fibrous connective tissue, and the VEGF expression level was lower than in group 2. On the 12th day, the predominant tissue in group 2 was the loose fibrous connective tissue, the VEGF expression level equaled that of group 3, and peripheral nerves began to grow. In group 1, the specific area of dense fibrous tissue was 3.9 times greater than that in group 2 ($p = 0.012$), the epithelium had pathological changes and the VEGF expression was below control values. Thus, a polymer piezoelectric membrane had a positive effect on the post-wound restoration of the oral mucosa tissues.

Keywords: regeneration, wound defect, scaffolds, piezoelectrics, oral mucosa, inflammation

Funding: the study was supported by the Russian Foundation for Basic Research under research project №23-25-00346.

Author contribution: Koniaeva AD, Varakuta EYu, Bolbasov EN, Stankevich KS — study concept and design; Koniaeva AD, Leiman AE — collection and processing of the material; Koniaeva AD, Varakuta EYu, Rafiev DO — text authoring; Koniaeva AD, Varakuta EYu, Rafiev DO, Bolbasov EN, and Stankevich KS — text editing.

Compliance with ethical standards: the study was approved by the Ethics Committee of the Siberian State Medical University (Minutes № 7693/1 of August 26, 2019). All manipulations with the animals were done as prescribed by the Directive 2010/63/EU of the European Parliament of September 22, 2010 "On the protection of animals used for scientific purposes", and the Declaration of Helsinki.

✉ **Correspondence should be addressed:** Anastasiia D. Koniaeva
Moskovsky Trakt, 2, Tomsk, 634034, Russia; asyakonya95@gmail.com

Received: 18.05.2023 **Accepted:** 02.06.2023 **Published online:** 19.06.2023

DOI: 10.24075/brsmu.2023.020

МОРФОЛОГИЧЕСКИЕ ОСОБЕННОСТИ РЕГЕНЕРАЦИИ СЛИЗИСТОЙ ОБОЛОЧКИ ПОЛОСТИ РТА ПРИ ПРИМЕНЕНИИ ПОЛИМЕРНЫХ ПЬЕЗОЭЛЕКТРИЧЕСКИХ МЕМБРАН

А. Д. Коняева¹✉, Е. Ю. Варакута¹, А. Е. Лейман¹, Д. О. Рафиев¹, Е. Н. Больбасов², К. С. Станкевич³

¹ Сибирский государственный медицинский университет, Томск, Россия

² Томский политехнический университет, Томск, Россия

³ Государственный университет штата Монтана, Бозмен, Монтана, США

Раневые дефекты слизистой оболочки рта являются распространенной патологией, для лечения которой разрабатывают покровные мембраны. Целью исследования было изучить морфологические особенности регенерации слизистой оболочки рта при применении полимерных пьезоэлектрических мембран. Исследование проведено на 45 крысах Wistar, разделенных на группы: 1) животные с открытым раневым дефектом; 2) животные с раневым дефектом, перекрытым полимерной мембраной с медным напылением; 3) интактные животные. Забор материала для морфометрического исследования проводили на 3-и, 7-е и 12-е сутки. На 3-и сутки в группе 1 удельная площадь грануляционной ткани была в 1,4 раза больше, чем в группе 2 ($p = 0,033$). Эндотелиоциты ее сосудов экспрессировали VEGF в большей степени в группе 2. В группе 2 происходило полное перекрытие дефекта эпителиальным пластом в отличие от группы 1. На 7-е сутки в группе 2 эпителий был в 2 раза толще, чем в группе 1 ($p = 0,019$). Грануляционная ткань замещалась рыхлой волокнистой соединительной тканью. В группе 1 преобладала удельная площадь воспалительной инфильтрации над рыхлой волокнистой соединительной тканью, экспрессия VEGF была ниже, чем в группе 2. На 12-е сутки в группе 2 преобладала рыхлая волокнистая соединительная ткань, экспрессия VEGF не отличалась от группы 3, отмечалось прорастание периферических нервов. В группе 1 удельная площадь плотной волокнистой ткани была в 3,9 раз больше, чем в группе 2 ($p = 0.012$), в эпителии имелись патологические изменения, а экспрессия VEGF была ниже контрольных значений. Таким образом, использование полимерной пьезоэлектрической мембраны благоприятно влияло на восстановление тканей слизистой оболочки полости рта в области раневого дефекта.

Ключевые слова: регенерация, раневой дефект, скаффолды, пьезоэлектрики, слизистая оболочка полости рта, воспаление

Финансирование: исследование выполнено при финансовой поддержке РФФ в рамках научного проекта №23-25-00346.

Вклад авторов: А. Д. Коняева, Е. Ю. Варакута, Е. Н. Больбасов, К. С. Станкевич — концепция и дизайн исследования; А. Д. Коняева, А. Е. Лейман — сбор и обработка материала; А. Д. Коняева, Е. Ю. Варакута, Д. О. Рафиев — написание текста; А. Д. Коняева, Е. Ю. Варакута, Д. О. Рафиев, Е. Н. Больбасов, К. С. Станкевич — редактирование текста.

Соблюдение этических стандартов: исследование одобрено этическим комитетом Сибирского государственного медицинского университета (№ 7693/1 от 26 августа 2019 г.). Все манипуляции с животными проводили в соответствии с директивой Европейского Парламента № 2010/63/EU от 22.09.2010 «О защите животных, используемых для научных целей» и Хельсинской декларацией.

✉ **Для корреспонденции:** Анастасия Денисовна Коняева
Московский тракт, д. 2, г. Томск, 634034, Россия; asyakonya95@gmail.com

Статья получена: 18.05.2023 **Статья принята к печати:** 02.06.2023 **Опубликована онлайн:** 19.06.2023

DOI: 10.24075/vrgmu.2023.020

Regeneration of a wound defect is a complex process that involves interaction of epithelium, trophic apparatus, fibroblasts, and inflammatory infiltration [1]. Healing includes stages of inflammation, regeneration and reorganization; at each of these stages, the mentioned interacting components have their own morphological scar features [2]. Primary intention healing requires the fastest possible transition from the stage of inflammation to the regeneration stage. Secondary intention healing, which results in a scar, typically has the inflammatory stage dominating the process [3].

The current approach to management of the oral mucosa wound defects implies use of covering materials that protect the wound surface from re-traumatization, which adds urgency to the task of developing new wound dressings that will not only protect the wound but also reduce the severity of inflammation and accelerate regeneration [4].

The polymer piezoelectric membrane tested in the context of this study was made in the Laboratory of Hybrid Materials of the National Research Tomsk Polytechnic University. In addition to piezoelectric properties, it was modified with copper ions, which have proven antimicrobial and anti-inflammatory properties [5].

The purpose of this study was to explore morphological features of regeneration of oral mucosa with an experimental wound covered with polymer piezoelectric membranes.

METHODS

The experiment involved 45 male Wistar rats bred in the vivarium of the Central Research Laboratory of the Siberian State Medical University. The animals were kept under standard vivarium conditions; their rations were limited for a day post surgery. The rats were divided into three groups: group 1, experimental ($n = 15$), in which the animals had the wound defect left open as prescribed by the standard oral cavity wound treatment protocol; group 2, experimental ($n = 15$), where the wound defect was covered with a copper-modified polymer membrane based on vinylidene fluoride with tetrafluoroethylene; group 3, control ($n = 15$), comprised of rats with intact mucosa. The animals were kept under standard vivarium conditions.

Before wound infliction, the animals received 0.3 mg Zoletil intramuscularly that induced narcosis. After sanitizing the surgical field with a 2% chlorhexidine solution, we excised a 7–4 mm buccal mucosa flap. Next, a polymer membrane was stitched onto the resulting wound with simple interrupted sutures along the edge.

The animals were withdrawn from the experiment through hypoxia in a CO₂ chamber on the 3rd, 7th, and 12th days of the study. After withdrawal, we excised buccal mucosa at the wound defect site.

Preparation of histological specimens followed the generally accepted routine; the slides were examined in the Observer D1 light microscope (Karl Zeuss; Germany) with the AxioCam ICc5 camera (Karl Zeuss; Germany). For the purpose, after deparaffinization, the sections were stained with hematoxylin-eosin as per the standard procedure.

For immunohistochemistry, we deparaffinized the previously prepared serial paraffin sections 4–6 μm thick and then stained them with rabbit recombinant polyclonal VEGF antibodies and IgG isotype S-100 (Abcam; USA). The intensity of immunohistochemical staining was assessed on a four-point scale: 0 — no staining, 1 — weak staining, 2 — moderate staining, 3 — strong staining, 4 — very strong staining.

The calculation formula was as follows:

$$\text{Histochemical index (H-score)} = \sum P(i) \times i,$$

where i is the intensity of staining in points from 0 to 4, $P(i)$ — percentage of differently stained cells (by intensity of staining).

We did the counting in three cohorts of 100 cells in different fields of view (lens $\times 40$).

To examine the samples with an electron microscope, we put them in a 2.5% glutaraldehyde solution on the 0.2 M cacodylate buffer (1:9) for fixation and then postfixed the samples in a 1% OsO₄ solution in a refrigerator for 4 hours. The next steps involved dehydration and pouring into a mixture of epon and araldite M.

Ultrathin slides were prepared in the LKB-5 ultratome (BROMMA; Sweden), counterstained with uranyl acetate and lead citrate, and examined using a JEM-1400 CX electron microscope (JEOL; Japan).

Morphometry was performed based on the classical methods of stereometry. We established the thickness of the epithelial layer, the quantitative density of fibroblasts, the specific area of loose and dense fibrous connective tissue, that of granulation tissue and inflammatory infiltration. The software used for the purpose was the Axio Vision imaging system (Karl Zeuss; Germany) and ImageJ, version 1.52u (National Institute of Public Health; USA).

Ultrathin slides allowed us to study ultrastructure of the cells of epithelial layer, trophic apparatus, and fibroblasts.

The data were processed with Statistica 10.0 (IBM; USA). To verify distribution in the statistical hypotheses, we used the Kolmogorov–Smirnov test. The results were processed with the help of methods of descriptive and nonparametric statistics. The studied parameters were described as a median and quartiles, $M (Q_1; Q_3)$. Comparing independent samples, we used the Kruskal-Wallis test with a median test, for paired comparisons — Wilcoxon test. The differences were considered significant at $p < 0.05$.

RESULTS

On the 3rd day of the study, we registered marginal epithelialization of the wound in experimental group 1 was observed, while in group 2 the defect was completely covered by the epithelium, and there were acantholytic blisters there (Fig. 1A).

At the ultrastructural level, samples from both groups had elongated width-wise basal cells, and it was not possible to identify the apical-basal polarity. In group 2, there were signs of high proliferative activity, and some cells were undergoing mitosis (Fig. 1B).

We discovered a regeneration area filled with granulation tissue with numerous thin-walled vessels (Fig. 1C). The specific area of granulation tissue in the experimental group 2 was 1.4 times higher than in the experimental group 1, the difference being significant ($p = 0.033$) (see Table). There was an extensive zone of inflammatory cell infiltration separating healthy tissues from the wound defect; in group 2, it was 1.4 times smaller than in group 1, this difference being significant, too ($p = 0.017$). The said zone consisted of neutrophils, macrophages, plasma cells, lymphocytes, and eosinophils (see Table) (Fig. 1D).

Quantitatively, there were significantly more fibroblasts per 1 mm² of the section in group 2 ($p = 0.035$) (see Table). In addition, separate bundles of connective tissue fibers were found in the animals of this group (Fig. 1A).

We discovered newly formed thin-walled granulation tissue vessels in the area of the wound defect; their endotheliocytes actively expressed VEGF (Fig. 1E), and the calculated H-score in group 2 was 1.4 and 4.7 times higher (significant difference) than in groups 1 and 3 ($p = 0.029$, $p = 0.019$) (see Table).

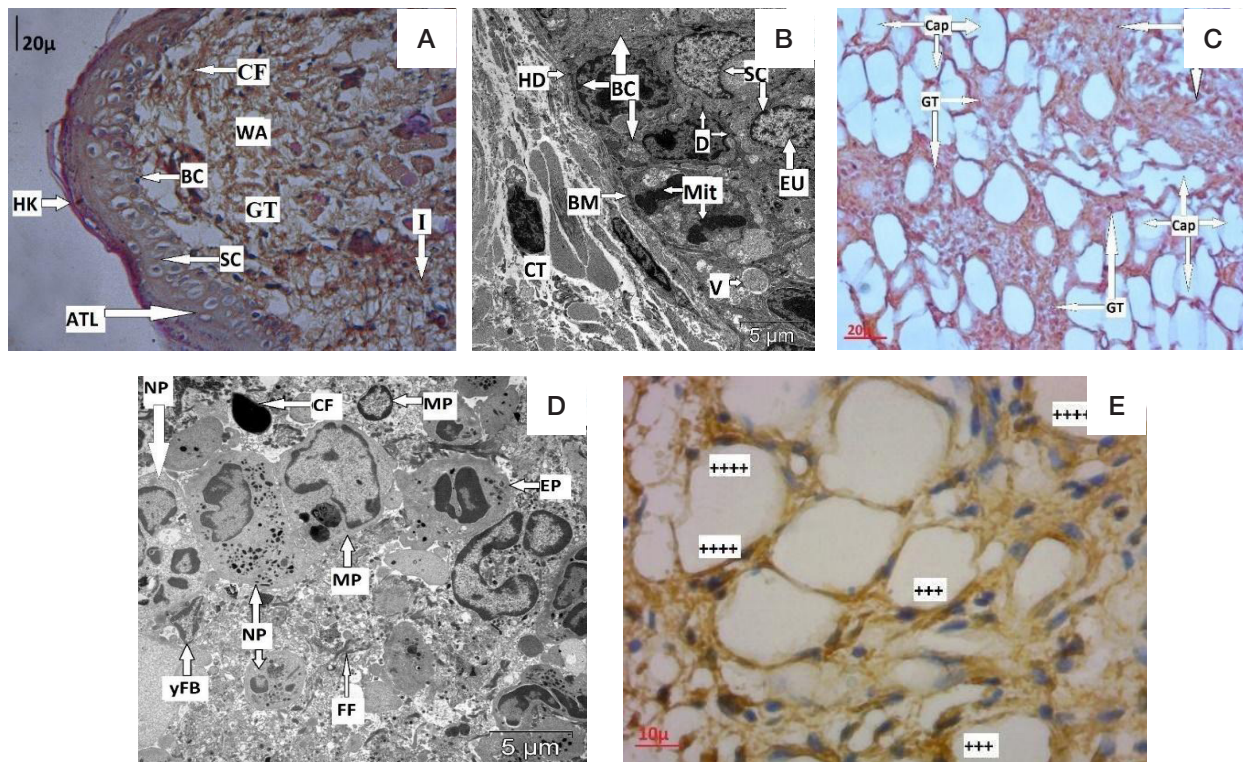


Fig. 1. Rat's buccal mucosa after infliction of the experimental wound defect, 3rd day of the study. **A.** Newly formed thin epithelial layer in the area of the wound defect and underlying granulation tissue. Pathological changes (acantholysis). Experimental group 2, 3rd day of the study (staining: hematoxylin, eosin; magnification: 400). **B.** Basal layer cells with signs of intense proliferation and mitotic figures. Experimental group 2, 3rd day of the study (TEM; magnification: 5000). **C.** New vessels in granulation tissue. Histological picture seen in both experimental groups. Experimental group 2, 3rd day of the study (staining: hematoxylin, eosin; magnification: 400). **D.** Cellular infiltration in the area of the wound defect. Histological picture seen in both experimental groups. Experimental group 1, 3rd day of the study (TEM; magnification: 5000). **E.** Expression of VEGF in the endotheliocytes of granulation tissue; nuclei stained with hematoxylin. Experimental group 2, 3rd day of the study (magnification: 900)

Endothelial lining and basement membrane of the granulation tissue capillaries were thin, and the interendothelial spaces were enlarged. The endotheliocytes were poor in organelles. In group 2, we identified a large number of micropinocytic vesicles and numerous microvilli in the endotheliocytes near the luminal edge of the vessels.

On the 7th day of the study, epithelium completely covered the wound defect in both experimental groups. The thickness of the epithelial layer in group 1 was significantly lower than that in groups 3 and 2 (see Table); there were clear active acantholytic processes (Fig. 2A).

In group 2, epithelium had less pronounced pathological changes than in group 1. The surface began to assume a typical relief with papillae, yet there still were spots of acanthosis and acantholysis. The epithelium was 2.3 times less thick than in the control group (significant difference, $p = 0.023$) but twice as thick as in group 1, where the animals had no membranes covering the defect (significant difference, $p = 0.019$) (see Table). Basal cells gradually assumed the typical shape elongated height-wise and apical-basal polarity, and there appeared hemidesmosomes restoring contacts with the basement membrane.

In both experimental groups, spots of loose fibrous connective tissue were identified in the lamina propria of buccal mucosa by the wound. In group 2, the specific area thereof was 4.5 times greater (significant difference, $p = 0.041$) than in group 1, but 2.6 times smaller than in the control group (significant difference, $p = 0.034$).

In the experimental group 2, the quantitative density of fibroblasts was 1.35 times higher than in the experimental group 1 ($p = 0.041$). Also, the prevailing type of fibroblasts in group 2 were the large differentiated branched fibroblasts

with high synthetic activity. Their plasma membrane sprouted numerous outgrowths. Bundles of connective tissue fibers in different planes were found around the cells (Fig. 2B). As for group 1, there still prevailed young fibroblasts with ultrastructure practically unchanged since the 3rd day of the experiment.

The newly formed vessels in group 2 had the VEGF expression 1.7 and 3.6 times higher than in group 1 and in the control group, respectively (significant difference, $p = 0.022$ and $p = 0.015$) (see table).

At the ultrastructural level, endotheliocytes in group 1 still showed signs of transcapillary metabolism disorders, which was not registered in the experimental group 2 (Fig. 2B), where the basement membrane of the vessels became continuous and uniform in thickness.

In both experimental groups, we discovered peripheral nerves near blood vessels by the wound defect's limits, the dendrons thereof having single edematous mitochondria with destruction of cristae. As shown on Fig. 2D, perineural and endoneural space were edematous (Fig. 2D).

On the 12th day of the study, the animals of group 2 had the epithelial layer as thick as it originally was, while in group 1 that layer was significantly thinner than when the mucosa was intact (see Table). There were no pathological processes registered in the epithelium in group 2, and the underlying connective tissue protruded into the epithelium forming pronounced papillae with microvasculature vessels (Fig. 3A). In group 1, on the contrary, we saw signs of acantholysis, which, at the ultrastructural level, caused appearance of vacuoles in the intercellular space and, with cells proliferating, acanthosis in the spinous layer (Fig. 3B).

On the 12th day of the study, granulation tissue was replaced with young loose fibrous connective tissue in both

Table. Morphological indicators of changes in the oral mucosa during regeneration of a wound defect, M (Q₁:Q₃)

	Epithelium thickness, μ	Numerical density of fibroblasts, c.u.	Specific area of granulation tissue, %	Specific area of loose connective tissue, %	Specific area of fibrous connective tissue, %	Specific area of inflammation infiltration, %	VEGF
Control	203.9 (200.2; 204.4)	380.0 (376.0; 391.7)	–	92.3 (87.2; 95.4)	–	7.7 (5.2; 9.5)	80.0 (75.0; 85.0)
Day 3							
Group 1	–	3782.0* (3721.0; 3849.5)	43.4 (39.4; 47.9)*	–	–	56.6 (50.3; 60.9)*	275.0 (265.0; 290.0)*
Group 2	20.3 (19.1; 22.1)*	5378.5** (5346.2; 5465.7)	60.8 (58.5; 62.6)**	–	–	39.2 (37.3; 41.4)**	375.0 (370.0; 380.0)**
Day 7							
Group 1	44.5 (43.2; 6.1)*	4530.5* (4472.5; 4579.7)	38.9 (35.8; 41.8)*	7.8 (6.3; 9.1)*	–	52.8 (49.9; 56.6)*	165.0 (155.0; 175.0)*
Group 2	87.8 (85.7; 89.5)**	6136.0*# (6126.0; 6145.0)*	41.6 (40.5; 43.5)*	35.1 (33.9; 35.9)**	–	23.3 (21.9; 24.1)**	275.0 (362.5; 282.5)**
Day 12							
Group 1	107.3 (106.2; 69.8)*	2746.5* (2639.0; 2906.0)	–	60.4 (52.5; 73.0)*	23.0 (14.3; 27.8)*	15.4 (11.4; 18.7)*	55.0 (55.0; 60.0)*
Group 2	184.6 (183.4; 1856.0)#	397.5# (395.0; 402.0)	–	92.7 (92.5; 93.9)#	5.9 (5.5; 6.3)**	1.4 (1.2; 1.9)**	120.0 (125.0; 135.0)**

Note: * — significant differences compared to the control group ($p < 0,05$); # — significant differences compared to group 1 ($p < 0,05$).

experimental groups (Fig. 3A). However, the specific area of this tissues reached the control value thresholds only in the experimental group 2. In group 1, we found interstitial edema between connective tissue fibers, and there were cicatricial foci based on the dense fibrous connective tissue (Fig. 3B). Table below shows the values; the maximum specific area of such connective tissue was registered in the experimental group 1.

The quantitative density of fibroblasts in group 2 equaled the respective control value; it was 6.9 times smaller than in group 1 (significant difference, $p = 0.032$). The predominant cells in group 2 were fibrocytes, mature and functionally inactive. There was no extracellular edema around them, but the clearly organized collagen fibers were easily identifiable. At the considered time point, the predominant cells in group 1 were still the branched cells with developed synthesis organelles and dispersed chromatin.

In the experimental group 2 we registered mature, well-formed microvasculature vessels with no signs of sludge, stasis, and thrombosis. The vessels were surrounded with structured connective tissue fibers; there was no perivascular edema. The basement membrane was continuous, of uniform thickness. The quantity of organelles was sufficient, they had a typical structure. There was an active transcapillary exchange under way. In group 1, the capillary basement membrane was thin; we registered few microvilli and micropinocytic vesicles at endotheliocytes, with clearly seen perivascular edema.

Compared to the indicators recorded on the 7th day, expression of the VEGF decreased in both experimental groups. In the experimental group 1, the VEGF H-score was 1.45 times smaller than the control values ($p = 0.026$) (Fig. 3C, D).

Peripheral nerves with unmyelinated nerve fibers in wound defect area were registered only in the experimental group 2 (Fig. 3D). Despite this, immunohistochemistry did not reveal expression of the S-100 marker, which the indicated the nerves began to restore (Fig. 3E).

DISCUSSION

With this study, we have demonstrated the key morphological aspects of the wounded oral mucosa tissue regeneration under a copper-modified polymer piezoelectric membrane.

On the 3rd day of the experiment, in group 2, where the wound was covered with the membrane, the wound was fully covered with a thin layer of epithelium, while in group 1, the animals of which had no membrane on their wounds, only marginal epithelization was observed. The process of epithelialization translated into changes at the ultrastructural level that enabled migration of epithelial cells from the wound's edges to its center [6]. Rørth reported preservation of single desmosomal contacts in his works and explained their presence by the need for coordinated collective migration of the epithelium [7].

Basal layer cells were proliferating intensively only in the experimental group 2. In group 1, we have not detected ultrastructural signs of high proliferative activity; lack of such signs on the part of the basal layer cells may be explained by the migrating cells' inability to undergo mitosis before the wound defect is completely covered by the epithelium layer caused by the decreased content of G1/S-phase cyclins and higher activity of cyclin-dependent kinase [8].

For the first three days, at the first stage of wound healing, inflammatory reaction was the predominant one. It was aimed at fencing healthy tissue from the defect (with its necrotic tissue), microorganisms and elements of primary contamination, as well as removal of these pathological products, elimination of the consequences of damage, activation of cytokines and growth factors [9]. In this connection, the specific area of inflammatory infiltration increased in both experimental groups.

In parallel with the inflammatory response there appeared new granulation tissue pierced with many vessels. In the experimental group 2, with the wound dressed, the ratio of the specific area of granulation tissue and inflammatory infiltration shifted towards the first component thereof, while in group 1, where the animals had no cover on the defects, the ratio prevalence was the opposite, which indicated predominance of inflammatory processes over regenerative ones.

The development of granulation tissue ensured rejection of the dead substrate, created a barrier preventing the spread of microorganisms, and formed the basis for new connective tissue developing at subsequent stages of wound regeneration [10].

Neovascularization was the basic mechanism of wound healing [11]. Capillaries were forming actively in the granulation tissue in

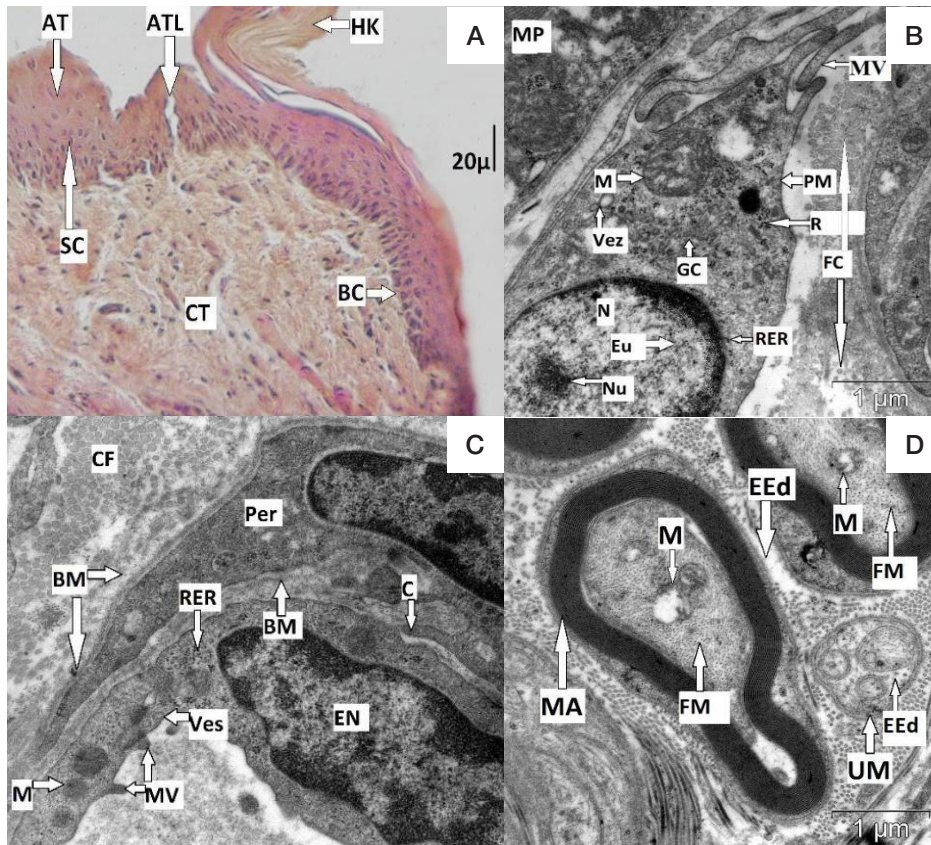


Fig. 2. CRat's buccal mucosa after infliction of the experimental wound defect, 7th day of the study. **A.** Pathological changes in the epithelium, wound defect in the process of regeneration: unevenly thick epithelial layer, thick spinous layer, acantholysis. Experimental group 1, 7th day of the study (staining: hematoxylin, eosin; magnification: 400). **B.** Differentiated fibroblast surrounded by connective tissue fibers, wound defect area. Experimental group 2, 7th day of the study (TEM; magnification: 20000). **C.** Interdigitation between an endothelial cell and a capillary pericyte, wound defect site. Experimental group 2 (TEM; magnification: 20,000). **D.** Peripheral nerve with myelinated and unmyelinated fibers, showing signs of perineural and endoneural edema. Experimental group 2, 7th day of the study (TEM; magnification: 20000).

both experimental groups. Neoangiogenesis and inflammatory response stimulated endothelium and the inflammatory infiltrate cells to express pro-angiogenic molecules — vascular endothelial growth factor (VEGF) and chemokines needed for capillary growth. Previously, researchers have noted that VEGF in the area of a wound defect undergoing regeneration supported the inflammatory response and increased vascular permeability, which contributed to the swelling of the surrounding tissues [12]. In our study, the expression of VEGF was increasing in both experimental groups, especially in group 2, which signaled of a more intense vascularization in the absence of exposure to aggressive factors present in the oral cavity.

On the 7th day of the study, proliferation became the dominant process, with fibroblasts responsible for collagen synthesis and reduction of the wound area playing the key role therein [13]. Fibroblasts secreted an extracellular matrix replacing the fibrin matrix [14], which boosted the synthesis, as registered at the ultrastructural level in the experimental group 2. Their presence in the wound defect area was connected with a significant increase of the specific area of loose fibrous connective tissue in comparison with experimental group 1, where, according to the TEM data, young fibroblasts with low synthetic activity mainly appeared.

On the 7th day of the experiment, the specific area of granulation tissue decreased, and the newly formed vessels underwent changes at the ultrastructural level, as evidenced by the results of immunohistochemistry. The expression VEGF decreased in group 1 significantly more than in group 2, which subsequently hindered blood supply in the wound defect area [15].

The characteristic features of the proliferation stage were differentiation of epithelial cells and thickening of layers of the

epithelium. At the ultrastructural level, in group 2, the apical-basal polarity of the basal layer, desmosomal contacts between cells, and hemidesmosomes with the basement membrane were restoring. We have also seen signs of acceleration of proliferation. In both experimental groups, there were registered pathological changes in the form of acanthosis and acantholysis; morphologically, they manifested as tissue detritus in the intercellular space and thickening of the spinous layer. These pathological features were more pronounced in group 2.

Cicatricial reorganization was the next stage of wound regeneration; it occurred on the 12th day of the study. In contrast with the experimental group 1, in group 2 the specific area of loose fibrous connective tissue was greater than that of scar tissue, and the predominant cells there were the synthetically inactive fibrocytes.

In both experimental groups the number of microvasculature vessels decreased on the 12th day. Previous reports link this regression to selective apoptosis happening against the background of the increasing production of antiangiogenic factors and decreasing expression of proangiogenic factors, such as VEGF [12]. As a confirmation of these findings, in the experimental group 1 we observed that VEGF expression was significantly lower than peculiar to intact mucosa. This signaled of poor blood supply at the wound defect site, which is one of the main causes of cicatricial deformity [16]. In group 2, the expression of vascular markers was higher than the control values.

Using an electron microscope, on the 12th day of the study we saw peripheral nerves with unmyelinated nerve fibers in the experimental group 2; while such were not found in group 1, there, along the edges of the wound defect, we discovered peripheral nerves with signs of perineural and endoneural edema

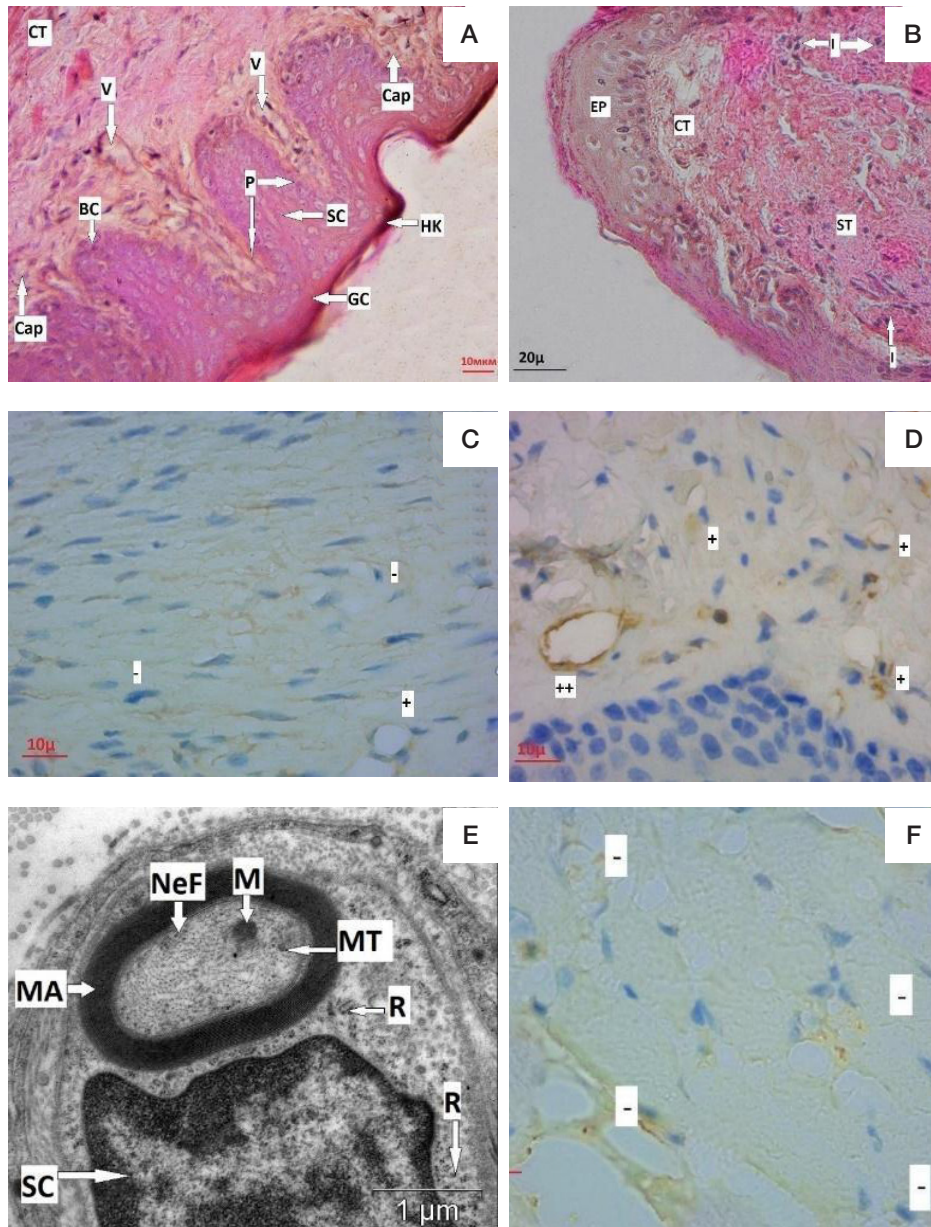


Fig. 3. Rat's buccal mucosa after infliction of the experimental wound defect, 12th day of the study. **A.** Restored mucosa. Experimental group 2, 12th day of the study (staining: hematoxylin, eosin; magnification: 400). **B.** Cicatricial tissue, wound defect site. Experimental group 1, 12th day of the study (staining: hematoxylin, eosin; magnification: 400). **D, C.** Expression of VEGF in the endotheliocytes of granulation tissue; nuclei stained with hematoxylin. **C.** Experimental group 1, 12th day of the study (magnification: 900). **D.** Experimental group 2, 12th day of the study (magnification: 900). **E.** Peripheral nerve with myelin fibers showing no signs of perineural and endoneural edema, wound defect area. Experimental group 2 (magnification: 20000). **F.** Absence of S-100 expression in the mucosa's lamina propria, nuclei staining with hematoxylin. Histological picture seen in both experimental groups. Experimental group 1, 12th day of the study (magnification: 900). WA — wound defect area; CT — loose fibrous connective tissue; GT — granulation tissue; ST — dense fibrous connective tissue; I — infiltration; V — venule; Cap — capillary; EP — epithelium; BM — basement membrane; BC — basal cells; SC — acanthocytes; GC — surface layer cells; HK — stratum corneum; ATL — acantholysis; AT — acanthosis; P — papillae; D — desmosomes; HD — hemidesmosomes; Va — expansion of intercellular space; PM — plasma membrane; EU — euchromatin; N — core; Nu — nucleolus; RER — granular endoplasmic reticulum; R — polysomes; M — mitochondrion; GC — Golgi complex; MV — outgrowths of plasmolemma; Vez — vesicles; C — intercellular contact; Mit — mitosis; yFB — young fibroblast; MP — macrophage; NP — neutrophil; EP — eosinophil; FC — connective tissue fibers; EN — endotheliocyte; Per — pericyte; FF — fragments of connective tissue fibers; CF — destructively altered cells; CF — collagen fibers; PN — peripheral nerve; MA — myelinated nerve fiber; UM — unmyelinated nerve fiber; PEEd — perineural space edema; EEd — edema of the endoneural space; FM — neurofilaments and microtubules; ++++ — very strong staining; +++ — strong staining; ++ — moderate staining; + — weak staining; — — no staining

the axons of which had mitochondria with destroyed cristae. The tests for expression of protein of the S-100 peripheral nerves returned negative in both groups, which indicated the nerve fibers began to grow into the wound defect area.

In the experimental group 2, where the wounds were covered with membranes, complete restoration the epithelium (both thickness and number of layers) occurred because it was protected from microorganisms. When the integrity of the epithelial layer was violated, microorganisms penetrated to the bottom of the open wound defect and excreted exotoxins

that affected the wound both from the inside and the outside, causing apoptosis of epithelial cells and disrupting their proliferation and migration, such course of events associated with collective regulation of the bacterial gene expression in the biofilm, which reinforced their resistance and ability to colonize [17]. In addition, metabolic products of microorganisms boosted production of pro-inflammatory mediators in the epitheliocytes through toll-like receptors [18]. As a result, in group 1 we saw epithelium growing thinner and losing layers, while acanthosis and acantholysis, the pathological changes, persisted.

CONCLUSIONS

The polymer membrane helped form an epithelial layer completely covering the wound defect on the 3rd day of the study and ensured absence of pathological changes on the 12th day thereof. In the group that had no such membrane, epithelization of the wound occurred only on the 7th day, and pathological changes (acanthus and acantholysis) were seen on the 12th day.

The membrane boosted replacement of granulation tissue with loose fibrous connective tissue and decreased the severity of inflammatory infiltration and cicatricial changes. In the group without membranes, by the end of the study, the wound defect

was mainly filled with dense fibrous connective tissue, and there was a pronounced inflammatory infiltration observed.

The polymer membrane boosted neoangiogenesis, which translated into a more intense expression of the VEGF (compared to the group without the membrane) registered at each time point of the study.

Overall, we have shown that use of a polymer piezoelectric membrane had a positive effect on the restoration of the oral mucosa tissues in the wound defect area, which manifested as an accelerated restoration of the epithelium, trophic apparatus and connective tissue component. Further, this helps optimize the process of treatment of wounds of this localization and improve quality of life of the patients.

References

- Hakkinen L, Koivisto L, Heino J, Larjava H. Cell and molecular biology of wound Healing. In: A. Vishwakarma, P. Sharpe, S. Shi, M. Ramalingam, editors. Stem cell biology and tissue engineering in dental sciences. Amsterdam, Boston, Heidelberg, London, New York: Elsevier, Academic Press, 2015; p. 669–90.
- Ridiandries A, Tan JTM, Bursill CA. The role of chemokines in wound healing. *Int J Mol Sci*. 2018; 19 (10): 3217. DOI: 10.3390/ijms19103217.
- Ozgok Kangal MK, Regan JP. Wound Healing. In: StatPearls [Internet]. Treasure Island (FL): StatPearls Publishing, 2023. PMID: 30571027. Available from: <https://www.ncbi.nlm.nih.gov/books/NBK535406/>.
- Zeng Q, Qi X, Shi G, Zhang M, Haick H. Wound dressing: from nanomaterials to diagnostic dressings and healing evaluations. *ACS Nano*. 2022; 16 (2): 1708–33. DOI: 10.1021/acsnano.1c08411.
- Badaraev A, Koniaeva A, Krikova SA, Shesterikov E, Bolbasov E, Nemoykina AL, et al. Piezoelectric polymer membranes with thin antibacterial coating for the regeneration of oral mucosa. *Applied Surface Science*. 2020; 504: 144068. DOI: 0.1016/j.apsusc.2019.144068.
- Marconi GD, Fonticoli L, Rajan TS, Pierdomenico SD, Trubiani O, Pizzicannella J, et al. Epithelial-mesenchymal transition (EMT): The type-2 EMT in wound healing, tissue regeneration and organ fibrosis. *Cells*. 2021; 10 (7): 1587. DOI: 10.3390/cells10071587.
- Rørth P. Collective cell migration. Annual review of cell and developmental biology. 2009; 25: 407–29. DOI: 10.1146/annurev.cellbio.042308.113231.
- Wehrhan F, Schultze-Mosgau S, Schliephake H. Salient features of the oral mucosa. In: Hom DB, Hebda PA, Gosain AK, Friedman CD, editors. Essential tissue healing of the face and neck. Shelton (CT): People's Medical Publishing House. BC Decker Inc., 2009; p. 83–99.
- Rodrigues M, Kosaric N, Bonham CA, Gurtner GC. Wound healing: a cellular perspective. *Physiol Rev*. 2019; 99 (1): 665–706. DOI: 10.1152/physrev.00067.2017.
- Velnar T, Bailey T, Smrkolj V. The wound healing process: an overview of the cellular and molecular mechanisms. *Journal of international medical researches*. 2009; 37 (5): 1528–42. DOI: 10.1177/147323000903700531.
- Veith AP, Henderson K, Spencer A, Sligar AD, Baker AB. Therapeutic strategies for enhancing angiogenesis in wound healing. *Adv Drug Deliv Rev*. 2019; 146: 97–125. DOI: 10.1016/j.addr.2018.09.010.
- Koniaeva AD, Varakuta EY, Leiman AE, Bolbasov E, Stankevich K. Restoration of the microvasculature and hemodynamics in the oral mucosa wound defects area with and without a piezoelectric polymer membrane. *Clinical and experimental morphology*. 2022; 11: 56–66. DOI: 10.31088/CEM2022.11.3.56-66.
- Jiang D, Christ S, Correa-Gallegos D, Ramesh P, Kalgudde Gopal S, et al. Injury triggers fascia fibroblast collective cell migration to drive scar formation through N-cadherin. *Nat Commun*. 2020; 11 (1): 5653. DOI: 10.1038/s41467-020-19425-1.
- Rognoni E, Pisco AO, Hiratsuka T, Sipilä KH, Belmonte JM, Mobasser SA, et al. Fibroblast state switching orchestrates dermal maturation and wound healing. *Mol Syst Biol*. 2018; 14 (8): e8174. DOI: 10.15252/msb.20178174.
- Bao P, Kodra A, Tomic-Canic M, Golinko MS, Ehrlich HP, Brem H. The role of vascular endothelial growth factor in wound healing. *J Surg Res*. 2009; 153 (2): 347–58. DOI: 10.1016/j.jss.2008.04.023.
- Pardali E, Goumans MJ, ten Dijke P. Signaling by members of the TGF-beta family in vascular morphogenesis and disease. *Trends Cell Biol*. 2010; 20 (9): 556–67. DOI: 10.1016/j.tcb.2010.06.006.
- Waasdorp M, Krom BP, Bikker FJ, van Zuijlen PPM, Niessen FB, Gibbs S. The bigger picture: why oral mucosa heals better than skin. *Biomolecules*. 2021; 11 (8): 1165. DOI: 10.3390/biom11081165.
- Smith P, Martinez C. Wound healing in the oral mucosa. In: Cham LA, editor. Oral mucosa in health and disease: a concise handbook. Bergmeier-Switzerland: Springer Int. Publ. AG, 2018; p. 77–91.

Литература

- Hakkinen L, Koivisto L, Heino J, Larjava H. Cell and molecular biology of wound Healing. In: A. Vishwakarma, P. Sharpe, S. Shi, M. Ramalingam, editors. Stem cell biology and tissue engineering in dental sciences. Amsterdam, Boston, Heidelberg, London, New York: Elsevier, Academic Press, 2015; p. 669–90.
- Ridiandries A, Tan JTM, Bursill CA. The role of chemokines in wound healing. *Int J Mol Sci*. 2018; 19 (10): 3217. DOI: 10.3390/ijms19103217.
- Ozgok Kangal MK, Regan JP. Wound Healing. In: StatPearls [Internet]. Treasure Island (FL): StatPearls Publishing, 2023. PMID: 30571027. Available from: <https://www.ncbi.nlm.nih.gov/books/NBK535406/>.
- Zeng Q, Qi X, Shi G, Zhang M, Haick H. Wound dressing: from nanomaterials to diagnostic dressings and healing evaluations. *ACS Nano*. 2022; 16 (2): 1708–33. DOI: 10.1021/acsnano.1c08411.
- Badaraev A, Koniaeva A, Krikova SA, Shesterikov E, Bolbasov E, Nemoykina AL, et al. Piezoelectric polymer membranes with thin antibacterial coating for the regeneration of oral mucosa. *Applied Surface Science*. 2020; 504: 144068. DOI: 0.1016/j.apsusc.2019.144068.
- Marconi GD, Fonticoli L, Rajan TS, Pierdomenico SD, Trubiani O, Pizzicannella J, et al. Epithelial-mesenchymal transition (EMT): The type-2 EMT in wound healing, tissue regeneration and organ fibrosis. *Cells*. 2021; 10 (7): 1587. DOI: 10.3390/cells10071587.
- Rørth P. Collective cell migration. Annual review of cell and developmental biology. 2009; 25: 407–29. DOI: 10.1146/annurev.

- cellbio.042308.113231.
8. Wehrhan F, Schultze-Mosgau S, Schliephake H. Salient features of the oral mucosa. In: Hom DB, Hebda PA, Gosain AK, Friedman CD, editors. *Essential tissue healing of the face and neck*. Shelton (CT): People's Medical Publishing House. BC Decker Inc., 2009; p. 83–99.
 9. Rodrigues M, Kosaric N, Bonham CA, Gurtner GC. Wound healing: a cellular perspective. *Physiol Rev*. 2019; 99 (1): 665–706. DOI: 10.1152/physrev.00067.2017.
 10. Velnar T, Bailey T, Smrkolj V. The wound healing process: an overview of the cellular and molecular mechanisms. *Journal of international medical researches*. 2009; 37 (5): 1528–42. DOI: 10.1177/147323000903700531.
 11. Veith AP, Henderson K, Spencer A, Sligar AD, Baker AB. Therapeutic strategies for enhancing angiogenesis in wound healing. *Adv Drug Deliv Rev*. 2019; 146: 97–125. DOI: 10.1016/j.addr.2018.09.010.
 12. Konjaeva AD, Varakuta EY, Leiman AE, Bolbasov E, Stankevich K. Restoration of the microvasculature and hemodynamics in the oral mucosa wound defects area with and without a piezoelectric polymer membrane. *Clinical and experimental morphology*. 2022; 11: 56–66. DOI: 10.31088/CEM2022.11.3.56-66.
 13. Jiang D, Christ S, Correa-Gallegos D, Ramesh P, Kalgudde Gopal S, et al. Injury triggers fascia fibroblast collective cell migration to drive scar formation through N-cadherin. *Nat Commun*. 2020; 11 (1): 5653. DOI: 10.1038/s41467-020-19425-1.
 14. Rognoni E, Pisco AO, Hiratsuka T, Sipilä KH, Belmonte JM, Mobasser SA, et al. Fibroblast state switching orchestrates dermal maturation and wound healing. *Mol Syst Biol*. 2018; 14 (8): e8174. DOI: 10.15252/msb.20178174.
 15. Bao P, Kodra A, Tomic-Canic M, Golinko MS, Ehrlich HP, Brem H. The role of vascular endothelial growth factor in wound healing. *J Surg Res*. 2009; 153 (2): 347–58. DOI: 10.1016/j.jss.2008.04.023.
 16. Pardali E, Goumans MJ, ten Dijke P. Signaling by members of the TGF-beta family in vascular morphogenesis and disease. *Trends Cell Biol*. 2010; 20 (9): 556–67. DOI: 10.1016/j.tcb.2010.06.006.
 17. Waasdorp M, Krom BP, Bikker FJ, van Zuijlen PPM, Niessen FB, Gibbs S. The bigger picture: why oral mucosa heals better than skin. *Biomolecules*. 2021; 11 (8): 1165. DOI: 10.3390/biom11081165.
 18. Smith P, Martinez C. Wound healing in the oral mucosa. In: Cham LA, editor. *Oral mucosa in health and disease: a concise handbook*. Bergmeier–Switzerland: Springer Int. Publ. AG, 2018; p. 77–91.